

IDENTIFYING DRIZZLE WITHIN MARINE STRATUS WITH W-
BAND RADAR REFLECTIVITY PROFILES

By

Wang, Jingyun

A thesis submitted to the Department of Atmospheric Science and the
Graduate School of the University of Wyoming in fulfillment of the
requirements for the degree of

MASTER OF SCIENCE

IN

ATMOSPHERIC SCIENCE

Laramie, Wyoming

December, 2002

Identifying Drizzle Within Marine Stratus with W-Band Radar Reflectivity profiles

Wang, Jingyun

M.S. thesis

Department of Atmospheric Science, University of Wyoming

December 2002

1 Abstract

Radar reflectivity characteristics of drizzly and drizzle-free warm marine stratus are studied, based on data collected off the Oregon coast with the Wyoming KingAir (UWKA) and the 95 GHz (3mm) Wyoming Cloud Radar (WCR) in 1999 (CS99). Here a drizzle case is defined as one where cloud probes measure drops exceeding 50 μm in size during at least 2 seconds (200 m). The observed drop size distribution (DSD) is compared to a Lognormal Model. The latter is used to diagnose the reflectivity properties of drizzly and drizzle-free marine stratus, assuming Rayleigh scattering.

The reflectivity for drizzly cases, whether calculated from the DSD or measured by the WCR, is generally larger than that for drizzle-free cases. The separation of the reflectivity probability density functions for drizzle and drizzle-free cases is large enough, especially in the lower half of the marine stratus, to determine drizzle presence from reflectivity data alone. This has been demonstrated before, and specific reflectivity values have been suggested in the literature as a threshold for drizzle in marine stratus.

The present study demonstrates that the threshold reflectivity for drizzle is strongly dependent on height within the stratus. The height is normalized between cloud base and cloud top, and statistical methods are applied to obtain an empirical threshold radar reflectivity profile

based on two data sources, in-situ DSDs and WCR measurements. Three flights with a combined length of xx km over marine stratus yield the following threshold profile:

$$Z_t (mm^6 m^{-3}) = 0.046\phi^{1.413}$$

where ϕ is the normalized cloud altitude in warm marine stratus and Z_t is the threshold radar reflectivity factor.

This relationship allows the exclusion of drizzly cases, with the purpose of estimating liquid water content (LWC, in $g m^{-3}$) from reflectivity. A strong relationship,

$$Z(mm^{-6} m^3) = 0.044LWC^{1.34}$$

is derived for drizzle-free marine stratus. This suggests that in the absence of drizzle, which dominates the reflectivity but is insignificant in terms of water mass, variations in reflectivity are largely due to variations in drop number concentration rather than to variations in drop size.

ACKNOWLEDGEMENTS

First of all I would like to express my high appreciation for my graduate advisors, Prof. Gabor Vali and Dr. Bart Geerts for their careful academic guidance and instructions on my graduate study, thesis research and thesis writing. My thanks also extend to graduate committee members, Dr. Jefferson Snider and Prof. Janet Constantinides for their valuable suggestions.

I also want to thank my families and many friends for their encouragement and support.

This work has been supported by the Office of Naval research, grant #DODONR4810.

Table of Contents

ACKNOWLEDGEMENTS	iii	
Table of Contents	iv	
List of Figures	vi	
List of Tables	ix	
Chapter 1	Introduction	1
1.1	Introduction	1
1.2	In-situ instruments and Wyoming Cloud Radar (WCR)	5
1.3	Definition of drizzle	8
1.4	Case studies	9
1.5	Normalized cloud altitude	11
1.6	Division of cloud layers	13
1.7	Outline	13
Chapter 2	Drop size distribution	14
2.1	Background	14
2.2	Drop size distribution in CS99	16
2.3	Lognormal approximation of measured droplet spectra	21
2.4	Radar reflectivity calculated from lognormal DSDs for drizzle-free and drizzly marine stratus	36
2.5	Cloud liquid water content calculated from the lognormal DSDs for drizzle-free and drizzly cases	40
2.6	Discussion	46
2.7	Conclusions	49
Chapter 3	Threshold reflectivity for drizzle	51
3.1	Introduction	51
3.2	Statistical methods	52
3.3	Threshold reflectivity for drizzle based on in-situ measurements	54
3.4	Spatial correlation analysis	60
3.5	Threshold reflectivity for drizzle based on WCR measurements	63
3.6	Relation between calculated reflectivity and WCR reflectivity	69
3.7	Threshold reflectivity applied to WCR measurements	74
Chapter 4	Relationship between LWC and WCR reflectivity	78
4.1	Background	78
4.2	Relationship between LWC and WCR second gate reflectivity	79

Identifying Drizzle Within Marine Stratus with W-Band Radar Reflectivity profiles

Chapter 5	Discussion	87
Chapter 6	Conclusion	89
References	91

List of Figures

Fig. 1.1	Satellite photos with approximate UWKA flight locations for three flights in CS99	9
Fig. 1.2	In situ drizzle probabilities as a function of WCR reflectivity values	10
Fig. 1.3	Profiles of LWC for three flights	12
Fig. 2.1	Example of two lognormal DSDs, the combination of which may be representative of marine stratus.....	15
Fig. 2.2	In-situ DSD for the Aug 09 th flight at various normalized cloud altitudes.....	18
Fig. 2.3	As Fig. 2.2 but for Aug 16 th	19
Fig. 2.4	As Fig. 2.2 but for Aug 17 th	21
Fig. 2.5	Profiles of the lognormal median radius r_0 (μm) for cloud droplets (FSSP measurements) for Aug 09 th flight.....	23
Fig. 2.6	FSSP-measured (dots) and lognormal (curve) DSDs for the drizzle-free cases on the Aug 09 th flight.....	25
Fig. 2.7	As Fig. 2.6 but for drizzle cases on Aug 09 th	26
Fig. 2.8	As Fig. 2.5 but for Aug 16 th	27
Fig. 2.9	As Fig. 2.6 but for Aug 16 th	28
Fig. 2.10	As Fig. 2.7 but for Aug 16 th	30
Fig. 2.11	As Fig. 2.5 but for Aug 17 th	31
Fig. 2.12	As Fig. 2.6 but for Aug 17 th	32
Fig. 2.13	As Fig. 2.7 but for Aug 17 th	34
Fig. 2.14	Radar reflectivity profiles calculated from the lognormal DSDs for drizzle-free (stars) and drizzly (triangles) patches of marine stratus for the Aug 09 th flight.....	37
Fig. 2.15	As Fig. 2.14 but for Aug 16 th	38
Fig. 2.16	As Fig. 2.14 but for Aug 17 th	39
Fig. 2.17	The LWC profile for drizzle-free cases for the Aug 09 th flight	41
Fig. 2.18	As Fig. 2.17 but for Aug 16 th	42
Fig. 2.19	As Fig. 2.17 but for Aug 17 th	43
Fig. 2.20	The comparison between lognormal model calculated LWC (solid line) and in-situ LWC measured by PVM (dots) for the Aug 09 th flight	44

Fig. 2.21	As Fig. 2.20 but for Aug 16 th flight with LWC measured by JW Hot-wire	45
Fig. 2.22	As Fig. 2.20 but for Aug 17 th flight	46
Fig. 2.23	DSDs for drizzle-free cases on Aug 16 th at $\phi = 0.5$	48
Fig. 2.24	Cloud droplet and drizzle drop distributions on Aug 17 th at $\phi = 0.5$	48
Fig. 2.25	Same as Fig. 2.21 but on Aug 09 th	48
Fig. 3.1	Application of the crossover and hit rate methods for reflectivity values calculated from FSSP, IDC and 2DC data for Aug 09 th flight	55
Fig. 3.2	As Fig. 3.1 but for Aug 16 th	57
Fig. 3.3	As Fig. 3.1 but for Aug 17 th	58
Fig. 3.4	Threshold reflectivity profile for drizzle based on calculated reflectivity with in-situ measurements	60
Fig. 3.5	Flight traces for which autocorrelation coefficient is calculated for the three flights.....	62
Fig. 3.6	Autocorrelation coefficients calculated for WCR second gate reflectivities for the three flights	62
Fig. 3.7	As Fig 3.1 but based on WCR 2 nd gate measurements for the Aug 09 th flight	64
Fig. 3.8	As Fig 3.1 but based on WCR 2 nd gate measurements for the Aug 16 th flight	66
Fig. 3.9	As Fig 3.1 but based on WCR 2 nd gate measurements for the Aug 17 th flight	67
Fig. 3.10	Threshold reflectivity for drizzle applied to WCR measurements	69
Fig. 3.11	Threshold reflectivity profiles based on in-situ calculated reflectivities and the profiles based on WCR measurements	70
Fig. 3.12	Profiles of in-situ calculated reflectivity (dashed) and WCR reflectivity (solid) for the Aug 09 th flight	71
Fig. 3.13	As Fig 3.12 but for Aug 16 th	72
Fig. 3.14	As Fig 3.12 but for Aug 17 th	73
Fig. 3.15	Profile of threshold reflectivity for drizzle for three flights	75
Fig. 3.16	Threshold reflectivity profile for drizzle on Aug 09 th , Aug 16 th and Aug 17 th in CS99	76
Fig. 3.17	Regression threshold reflectivity profile for drizzle	77
Fig. 4.1	In situ LWC versus WCR second gate reflectivity for all measurements for the three flights.....	80

Fig. 4.2	LWC versus WCR reflectivity for drizzle-free cases	82
Fig. 4.3	As Fig 4.2, but the solid line is the regression curve based on the remaining points	83
Fig. 4.4	The new relationship between LWC and radar reflectivity (Eq. 4.6 with the form as $Z(mm^{-6}m^3) = aLWC^b + c$)	85
Fig. 4.5	Relationship between LWC and radar reflectivity.....	86

List of Tables

Table 1.1	Parameters of the cloud probes on the UWKA during CS99	7
Table 1.2	Altitudes of cloud top and cloud base, used to determine the normalized cloud altitude	12
Table 1.3	Division of cloud layers	13
Table 2.1	Number of 1-s data segments with and without drizzle during the Aug 09 th flight	19
Table 2.2	As table 2.1 but for Aug 16 th	20
Table 2.3	As table 2.1 but for Aug 17 th	21
Table 2.4	Lognormal model parameters for drizzle-free cases for the Aug 09 th flight	23
Table 2.5	Lognormal model parameters for drizzle cases for the Aug 09 th flight	25
Table 2.6	As table 2.4 but for Aug 16 th	27
Table 2.7	As table 2.5 but for Aug 16 th	29
Table 2.8	As table 2.4 but for Aug 17 th	31
Table 2.9	As table 2.5 but for Aug 14 th	33
Table 2.10	Reflectivity factor contribution from drops measured by 1DC and 2DC for the Aug 09 th flight	38
Table 2.11	As table 2.10 but for Aug 16 th	39
Table 2.12	As table 2.10 but for Aug 17 th	40
Table 2.13	Lognormal calculated LWC for drizzle-free case and drizzly case for the Aug 09 th flight	41
Table 2.14	As table 2.13 but for Aug 16 th	42
Table 2.15	As table 2.13 but for Aug 17 th	43
Table 2.16	LWC formed by cloud droplets and by drizzle drops for drizzle cases.....	43
Table 3.1	Contingency table of drizzle based on 2DC measurements and on reflectivity	53
Table 3.2	Calculated threshold reflectivity for drizzle for the Aug 09 th flight	56
Table 3.3	As table 3.2 but for Aug 16 th	57
Table 3.4	As table 3.2 but for Aug 17 th	59
Table 3.5	Threshold reflectivity based on WCR measurements for the Aug 09 th flight	65
Table 3.6	As table 3.5 but for Aug 16 th	66

Identifying Drizzle Within Marine Stratus with W-Band Radar Reflectivity profiles

Table 3.7	As table 3.5 but for Aug 17 th	68
Table 3.8	Median values of reflectivity calculated from probe data and WCR reflectivity for the Aug 09 th flight	71
Table 3.9	As table 3.8 but for Aug 16 th	72
Table 3.10	As table 3.8 but for Aug 17 th	73
Table 3.11	Improved WCR threshold reflectivity	75
Table 4.1	Regression parameters of Eq. $Z(mm^{-6}m^3) = aLWC^b + c$	83

Chapter 1 Introduction

1.1 Introduction

1.1.1 Marine stratus

Marine stratus (or stratocumulus) clouds are ubiquitous, especially over subtropical oceans off west coasts. They have a significant impact on the global radiation balance. They have much higher albedos (30~40%) than the ocean surface (10%) but their top temperatures are only a few degrees lower than that of the ocean surface. Therefore marine stratus substantially increases the reflection of solar radiation while having little effect on the longwave radiation emitted to space. An estimated 4% increase in the spatial extent of marine stratus is sufficient to offset the global warming due to the radiative effects of a doubling of the atmospheric CO₂ concentration (Randall et al. 1984).

In addition, marine stratus is typically capped by a pronounced stable layer resulting from sustained subsidence. The exchanges of heat and moisture between the mixed layer, whose depth varies between 0.5 and 1.5 km, and the overlying troposphere are poorly understood. Both numerical weather prediction (NWP) models and general circulation models (GCM) continue to struggle to correctly simulate the temporal/spatial extent and radiative properties of marine stratus. In essence the challenge lies in the development and maintenance of a mixed layer whose depth exceeds the surface lifting condensation level. This involves both an accurate representation of momentum and moisture fluxes at the air-sea interface, in the mixed layer, and at the mixed-layer inversion, and an accurate simulation of cloud processes such as drizzle growth and evaporation.

1.1.2 Numerical and experimental studies

Both experimental and theoretical methods have been used to study the mixed-layer fluxes and cloud microphysical processes in marine stratus. Not only does the in-situ probing of cloud micro-structure give an opportunity to understand the cloud itself, the measurements also provide strong support to the evaluation and improvement of cloud parameterizations in models.

Several *field experiments* have provided essential information to validate models and to directly study cloud processes:

- To improve the understanding of radiative and physical processes of clouds in the climate system, the **First ISCCP Regional Experiment** (FIRE, ISCCP is the International Satellite Cloud Climatology Project) was carried out off the coast of southern California in summer of 1987, with a focus on marine stratus.
- The **Atlantic Stratocumulus Transition Experiment** (ASTEX) was conducted on 1992 to study marine stratocumulus near the Azores and Madeira Islands in the northeastern Atlantic. Here marine stratus is prevalent as well, although generally visually broken up in stratocumulus clouds.
- Two projects have been conducted off the Oregon coast with the University of Wyoming King Air (UWKA) and the Wyoming Cloud Radar (WCR) to study coastally trapped marine stratus. The first **Coastal Stratus** (CS) experiment was carried out in 1995 (CS95) and the second one in 1999 (CS99) (<http://www-das.uwyo.edu/wcr/projects/cs99/cs99.html>).
- In the summer of 2001, both the microscale and mesoscale characteristics of marine stratus several hundred km off San Diego were studied in the **Dynamics and Chemistry of Marine Stratocumulus** (DYCOMS-II) experiment (<http://www.atmos.ucla.edu/~bstevens/dycoms/>).

Numerical models have been developed to simulate dynamic and thermodynamic processes in marine stratus, including the following:

- Kerstein (1988) separately treats the turbulent deformation and molecular diffusion processes in his model. This model is capable of describing many features of turbulent mixing (Kerstein 1991). Krueger (1993) successfully applied this model to simulate the development of a mixed layer, even under weak shear, and cloud-top entrainment.
- Moeng et al. (1995) used a LES (Large Eddy Simulation) model to investigate the roles of radiative and evaporative feedbacks in stratocumulus entrainment and breakup.
- Ackerman et al. (1995) coupled a higher-order turbulence closure model to a detailed bin-resolving microphysical model. Notwithstanding the complex parameterization of

boundary-layer and microphysical processes, they failed to accurately predict the presence of marine stratus.

- Wyant et al. (1997) adopted a Lagrangian approach (Bretherton and Austin 1995) in a two-dimensional eddy-resolving model. This study nicely captures the transition from the stratocumulus to cumulus.
- Stevens et al. (1998) improved the Regional Atmospheric Modeling System (RAMS) through the incorporation of a new microphysical parameterization scheme. With lognormal base functions to represent cloud and drizzle drop spectra (Clark 1976), the new scheme needs much less computation time than bin-resolving microphysical schemes.

1.1.3 Studying marine stratus with a cloud radar

In-situ probing only provides one-dimensional cloud information, i.e. following the flight track. The airborne fixed-beam WCR allows the 2D measurement of cloud microstructure; however only radar reflectivity, echo velocity, and polarization can be measured, and these are only indirect measures of cloud microstructure. The interpretation of reflectivity is ambiguous because both droplet number concentration and mainly drop size contribute to the signal. The interpretation of echo vertical motion in marine stratus is ambiguous, unless drizzle is absent, because the motion can be due both to fall-out (mainly of the largest droplets) and to vertical air motion. In the presence of rain, the vertical air motion can be retrieved with a vertically-pointing 95 GHz Doppler radar, because drops of ~ 1 mm diameter correspond to the first scattering cross section depression of the Mie regime (Kollias et al. 2002).

In short, the combined use of in-situ cloud data with radar reflectivity data optimizes the description of the cloud microstructure.

Much work has been done on the interpretation of cloud physical parameters from radar reflectivity measurements in the past few years (Sauvageot and Omar 1987; Sassen and Liao, 1996; Frisch et al. 1995; Fox and Illingworth 1997; Babb and Verlinde 1999; Löhnert et al. 2001). Ruled by Rayleigh scattering which is proportional to the 6th moment of particle size, the radar reflectivity can be considered to be the integral of the droplet concentration at all sizes, weighted by the square of the mass of a droplet of given size. In other words, reflectivity is highly dependent on the concentration of large droplets. Drizzle (having a diameter $> 50 \mu\text{m}$, see

below) is prevalent in marine stratus, and may dominate the radar reflectivity. Drizzle can increase the radar return by 10 to 20 dBZ above the echo due to cloud droplets in extensive marine stratocumulus deeper than 200 m (Fox and Illingworth 1997). Typical concentrations of cloud droplets in marine stratus produce a reflectivity of about -18 dBZ, and typical drizzle amounts increase this value to about -5 dBZ, assuming Raleigh scattering (Frisch et al. 1995). Due to its low number concentration, drizzle has a negligible effect on the cloud liquid water content (LWC) or the cloud effective radius. Therefore, *radar reflectivity cannot be used to characterize the LWC nor the radiative properties of marine stratus if drizzle is present, because the radar reflectivity is dominated by drizzle with insignificant LWC*. Both theoretical and empirical relationships between radar reflectivity and other cloud parameters, such as LWC, can be found in literature, at least for drizzle-free stratus (i.e. all droplets have a diameter <50 μm).

Given the sensitivity to large droplets, *radar reflectivity can be used to identify drizzly regions within marine stratus*. Sauvageot and Omar (1987) used -15 dBZ as the lower reflectivity limit to exclude drizzle-sized particles in their study on the relationship between LWC and radar reflectivity. This discrimination value is also adopted in Löhnert et al. (2001) to profile LWC with microwave remote sensing data. The Doppler spectrum is another variable to discriminate cloud droplets from drizzle drops. Threshold downward velocities of 0.7 m/s (Frisch et al. 1995) and 1.0 m/s (Clothiaux et al. 1995, Fox and Illingworth 1997) have been used. Fox and Illingworth (1997) also distinguish clouds with or without drizzle-size drops according to the vertical reflectivity profiles measured by a ground-based cloud radar. They chose those profiles, which have an increasing radar reflectivity with altitude within a cloud, to represent clouds without drizzle. For drizzle cases the highest reflectivity is encountered lower in the marine stratus, because drizzle grows as it falls by collision/coalescence. Fox and Illingworth (1997) then proposed an empirical Z-LWC relationship for drizzle-free stratocumulus clouds. Krasnov and Russchenberg (2002) classified water clouds into three types: cloud without drizzle, cloud with drizzle and drizzly cloud, depending on the data distribution patterns on the Z/α (where α is the radar reflectivity to the lidar extinction) - r_{eff} (effective radius) plane. They studied the relationships between radar reflectivity and r_{eff} (and LWC) corresponding to the three cloud types separately.

1.1.4 Objectives of this research

Based on the above discussion, marine stratus regions containing drizzle-size drops may be isolated by means of the radar reflectivity field. *The primary objective of this thesis is to identify the presence of drizzle-size drops in marine stratus, by means of W-band radar reflectivity.* Data from three flights in CS99 are studied for this purpose. As an extension of the Sauvageot and Omar (1987) study, we aim to demonstrate that the threshold reflectivity for drizzle is sensitive to altitude within the marine stratus. Once we have defined the threshold reflectivity profile for drizzle, we relate cloud characteristics, such as LWC, to reflectivity for drizzle-free marine stratus.

1.2 In-situ instruments and Wyoming Cloud Radar (WCR)

Five cloud probes aboard the UWKA are discussed. Below are the principles and limitations of FSSP, 1DC, 2DC, PVM, and JW hot wire (Table 1.1).

1.2.1 Forward Scattering Spectrometer Probe (FSSP)

An FSSP detects light scattered by a spherical particle that passes through its laser beam. The intensity of the scattered light is proportional to the droplet size. Utilizing a He-Ne laser with a wavelength of 6328 angstroms ($0.6 \mu\text{m}$) as the illumination source and following Mie scatter theory, the spherical particle size can be determined by measuring the intensity of the forward scattered light. FSSP probes need to be calibrated before and after a field experiment. The measurements are corrected for probe dead time and coincidence before further analysis. FSSP measures the concentration of droplets between 3.0 and $45.0 \mu\text{m}$. It has a sample volume of $50 \text{cm}^3/\text{s}$ (with a sampling frequency of 10 Hz) when the aircraft speed is 100 m/s. The FSSP is the most popular instrument for cloud DSDs (drop size distributions). But well-known errors, about 14% in drop size measurements and 25% in total number concentration measurements, may exist, as discussed by Baumgardner et al. (1993).

1.2.2 Optical array probe: OAP-200X (1DC)

The One-Dimensional Optical Array probe uses a He-Ne laser as the illumination source, and a linear array of diodes as optical sensor. When a droplet passes through its laser beam, the droplet diameter is estimated by the length of the queue of diodes that are shaded. A count of the number of single, non-sequential diode shades gives the concentration of cloud droplets. The 1DC probe only gives the number of droplets without information about droplet shape. The rejecting of those particles which pass only partly through the array bounds may yield an underestimation of the droplet concentration. Because of these shortcomings, there are inevitable errors in 1DC measurement. The 1DC probe can measure droplet sizes between $12.5 \mu\text{m}$ and $185.5 \mu\text{m}$. The 1DC probe has a sampling frequency of 10 Hz and a sample volume of $1000 \text{ cm}^3/\text{s}$, assuming an aircraft speed of 100 m/s.

1.2.3 Optical array probe: 2DC

A 2DC optical array probe uses a similar principle as the 1DC but with multi-arrays of diodes as optical sensor. When a particle passes through the 2DC laser beam, a 2D projective shade is recorded. Both the area and the shape of the particle's cross section can be described. Counting shades with different diameters gives a DSD. The 2DC probe can measure droplets from $50 \mu\text{m}$ to those larger than $800 \mu\text{m}$. Usually measurements of the first two bins, especially of the first bin, are less reliable. The concentration of large drops may be underestimated by the 2DC, because it often is quite low, with frequent zero occurrences in the largest bins in a unit sample volume. The 2DC probe has a sampling frequency of 1 Hz and a sample volume of $5000 \text{ cm}^3/\text{s}$, assuming an aircraft speed of 100 m/s.

1.2.4 Particle volume monitor (PVM-100A) and Johnson-Williams (JW) hot-wire probe

The UWKA has two other instruments, the PVM and Hot-wire probes, to measure the LWC. The probes are used to evaluate LWC profiles in marine stratus. LWC can be estimated also by integrating FSSP measurements.

A PVM probe lets droplets pass through its laser beam. Cloud droplets will scatter He-Ne laser light. The amount of light extinction is used to estimate the LWC. The PVM probe will

overestimate the LWC when the cloud water is contained in more numerous but smaller droplets. The probe measurement range is $0.002 \sim 10.0 \text{ g/m}^3$.

A JW hot-wire probe heats one arm of an a/c resistance wire bridge. Droplets cool the heated wire and reduce the resistance. A current is required to maintain bridge balance. The cloud LWC can be calculated as a function of current and the true air speed. When droplets are larger than $30 \mu\text{m}$, they break up on the sensing arm and may be removed by the airflow before totally evaporating. Therefore the JW hot-wire probe, as the PVM probe, will underestimate the LWC if it is mostly contained in large drops. The probe measurement range is $0.0 \sim 3.0 \text{ g/m}^3$.

Table 1.1 Parameters of the cloud probes on the UWKA during CS99

Probe	Variable	Diameter range	Resolution	Temporal resolution	Volume sampling rate
FSSP	Drop size	$3 \sim 45 \mu\text{m}$	$3 \mu\text{m}$	10 Hz	$50 \text{ cm}^3/\text{s}$
1DC	Drop size	$12.5 \sim 185.5 \mu\text{m}$	$12.5 \mu\text{m}$	10 Hz	$1000 \text{ cm}^3/\text{s}$
2DC	Drop size	$25 \sim >800 \mu\text{m}$	$25 \mu\text{m}$	1 Hz	$5000 \text{ cm}^3/\text{s}$
PVM	LWC	$0.002 \sim 10 \text{ g/m}^3$	$.000015 \text{ g/m}^3$	25 Hz	---
JW Hot-wire	LWC	$0.0 \sim 3 \text{ g/m}^3$	$.000015 \text{ g/m}^3$	25 Hz	---

Note: The volume sampling rate assumes an aircraft speed of 100 m/s.

1.2.5 Wyoming Cloud Radar (WCR)

The 95-GHz (3 mm) Wyoming Cloud Radar (<http://www-das.uwyo.edu/wcr/>) is a polarimetric Doppler radar, which has been mounted on the UWKA and other aircraft. The radar beam can be directed in an up or side direction with a reflector plate on the aircraft. The maximum unambiguous range varies between 1 and 6 km, depending on pulse repetition frequency. The first gate measurement is at 60 m from the aircraft but usually is unreliable. Second gate measurements are used in this paper. With a gate space of 30 m or 15 m, the second gate data depict the cloud structure at 90 m or 75 m away from the aircraft. The second measuring gate has a volume of 57 m^3 at 90 m [assuming a 250 ns pulse length and a 0.7 degree circular beam width]. The 57 m^3 volume is 7 orders of magnitude larger than the 2DC probe volume, and 10 orders of magnitude larger than the FSSP volume (Table 1.1). This implies that WCR reflectivity measurements are much more stable, and can be made at higher frequency, than those from in-situ probes.

1.3 Definition of drizzle

The term drizzle represents a special group of droplets whose sizes are larger than cloud droplets but smaller than raindrops. Different drizzle size ranges have been adopted in the literature, depending on the research purpose. Of particular interest here is the size that discriminates between cloud droplets and drizzle drops.

A conventional definition for the range of drizzle sizes is 200 μm to 500 μm in diameter (Houze 1993). This definition is based on the dependence of droplet terminal velocity on droplet size. Generally, the terminal velocity of droplets smaller than 200 μm in diameter is negligible. And drops larger than 500 μm in diameter have a good chance to reach the ground surface and thus are named as raindrops.

Another definition uses a diameter of 50 μm as the lower threshold for drizzle drops (Frisch et al. 1995, Hudson and Yum 1997, Miles et al. 2000). This discrimination between cloud droplets and drizzle drops is based on different droplet growth mechanisms. The condensational mechanism dominates the growth of droplets smaller than 40 μm in diameter. For larger droplets, growth by coalescence dominates (Gerber 1996).

The latter drizzle definition is used in this study, for practical reasons discussed below. Observations in CS99 show that droplets larger than 200 μm in diameter are very rare in marine stratus.

A continuous droplet spectrum can be formed with the in-situ measurements of the FSSP, 1DC and 2DC probes. The FSSP provides the distribution of droplets from 1.5 μm to 46.5 μm . Measurements of 1DC at droplet range from 50 μm to 100 μm compose the second segment of the spectrum. The spectrum of droplets larger than 100 μm is given by 2DC measurements. Two divisions, one at 50 μm (between FSSP and 1DC measurements) and the other at 100 μm (between 1DC and 2DC measurements), exist in this measured droplet spectrum. The first division, 50 μm , is chosen to be the drizzle lower threshold diameter in this study. This probe-based discrimination of cloud droplets from drizzle at 50 μm in diameter has a physical basis also, as it distinguishes between condensation and coalescence as dominant droplet growth mechanisms.

Measurements of FSSP give the cloud DSD. Droplets measured with the 1DC and 2DC are

considered to be drizzle. *When neither the 1DC nor the 2DC probes detect droplets during a given sample period, then the marine stratus traversed during that sample period is considered to be drizzle-free.* The sampling period is set to that of the slowest instrument, i.e. the 2DC probe, i.e. 1 second (~ 100 m). This means that ten 10 Hz FSSP data are cumulated, as well as ten 1DC data. The WCR data have a sampling frequency of ~ 33 Hz. At a range of 90 m to the side of the aircraft, these 33 profiles collected over 100 m are independent, since the beamwidth there is only 1.25 m, less than the profile spacing ($100/33 = 3$ m). Each of the 33 WCR reflectivities in one second will be compared against cloud probe data cumulated during the same second.

Because 1DC measurements were less reliable than 2DC measurements in CS99 (the 1DC probe undersampled droplets), only the 2DC measurements, starting at 2DC bin 2, are used to determine drizzle presence. In what follows, this drizzle presence is referred to as ‘in-situ drizzle’.

1.4 Case studies

The UWKA with WCR examined stratus off the Oregon coast during August 1999 (CS99). Data from three flights are studied in detail, on Aug 09th, Aug 16th and Aug 17th. Drizzle fell heavily on Aug 17th, and was present during the two other flights. A visible satellite image reveals significant mesoscale variations of cloud albedo on these three days near the flight track, especially on Aug 16th (Fig 1.1).

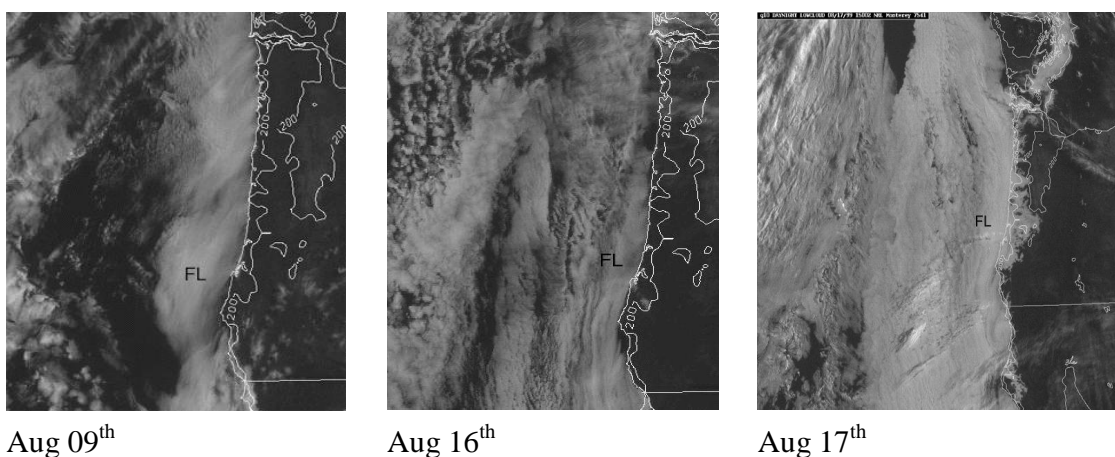


Fig. 1.1 Satellite photos with approximate UWKA flight locations for three flights in CS99. The *FL* denotes the area of flight activity (Vali, 1999). The light lines represent the coast and the 200 m contour.

The first question is whether a clear threshold value of radar reflectivity exists, above which drizzle is present. Certainly, drizzle was more likely and more numerous when the radar equivalent reflectivity, 90 m (or 75 m) to the side of the aircraft, was higher. This reflectivity will be referred to as the ‘sideways reflectivity’.

Fig. 1.2 shows the probability of in situ drizzle (P_Z) for given values of sideways reflectivity Z , calculated as:

$$P_Z = \frac{N_{dz}}{N_Z} \quad (1.1)$$

where N_Z is number of samples of sideways reflectivity value Z , and N_{dz} is the number of these samples with in situ drizzle. Since the WCR has a much higher sampling rate than the 2DC, all sideways reflectivities with in situ drizzle will contribute to the number N_{dz} and N_Z

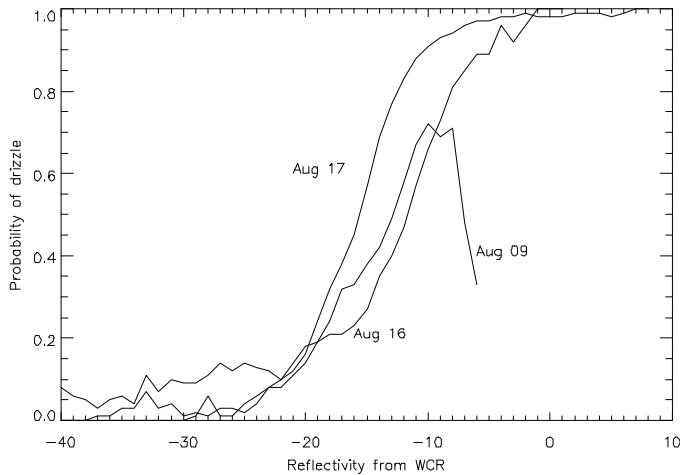


Fig 1.2 In situ drizzle probabilities as a function of WCR reflectivity values.

In situ drizzle probabilities sharply increase in the sideways reflectivity range of -20 dB to -10 dB (Fig 1.2). This implies little uncertainty about the existence and validity of a drizzle reflectivity threshold in marine stratus. This also suggests a possible threshold, based on points of $P = 0.5$, between -16 dBZ and -12 dBZ for whole cloud layer. A strong dependence of this threshold reflectivity for drizzle on cloud altitude is observed for the three CS99 flights. This will be discussed in more detail in Chapter 3.

1.5 Normalized cloud altitude

1.5.1 Definition

To facilitate comparisons, a normalized cloud altitude will be used in this study. Assume that the normalized cloud top is 1.0 and the cloud base is 0.0. Then the normalized cloud altitude ϕ can be calculated as:

$$\phi = \frac{h - h_b}{h_t - h_b} \quad (1.2)$$

where h is the cloud altitude, h_b is the altitude of the cloud base, and h_t is the altitude of the cloud top.

When the WCR points sideways, the radar beam may not be exactly horizontal. A small correction of the altitude of the radar second gate is calculated as:

$$\Delta h = d \times \sin \theta \quad (1.3)$$

where d is the distance between aircraft and radar second gate, and θ is the angle of the radar beam from the horizontal plane.

1.5.2 Altitudes of cloud top and cloud base

An optically relatively uniform horizontal structure is often observed in marine stratus, yet discrete radar echo structures can be seen (Vali et al. 1999). Some of these echo variations are associated with the topography of the top of the marine stratus. In situ LWC estimates are used to determine the altitudes of cloud top and cloud base. The UWKA did several ascents and descents through the cloud layer on Aug 09th, Aug 16th and Aug 17th. From the cloud base, where water vapor first condenses, the LWC increases adiabatically with cloud altitude. Clearly the stratus cloud tops, where the LWC drops off dramatically, are not the same for all aircraft soundings during any given flight (Fig 1.3). The altitudes of cloud top and cloud base based on the three different probes (PVM, JW Hot-wire and FSSP) have similar values. The LWC estimates based on the integration of FSSP bin measurements are a little smaller than those of the two other probes. PVM measurements on Aug. 09th and Aug. 17th and JW hot-wire measurements on Aug. 16th are plotted in Fig. 1.3.

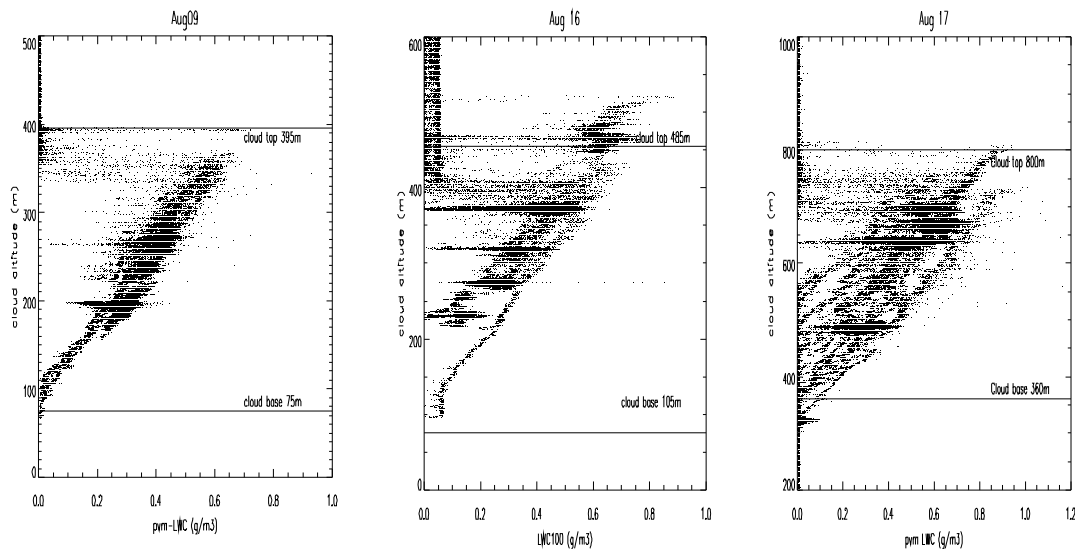


Fig. 1.3 Profiles of LWC from for three flights. These profiles are used to determine the mean cloud top and cloud base, as shown. In each case the measured LWC for the entire flight record is plotted.

The LWC increases with altitude as expected from moist adiabatic processes without precipitation. The altitude from which point LWC begins to increase from near zero values is considered to be cloud base. And the cloud top is located at the altitude with a sudden LWC drop-off. Here the LWC can vary from zero (higher than cloud top) to the largest value of the vertical profile (just below the cloud top) within less than 100 m.

A large LWC range at a given altitude suggests non-uniformities of horizontal cloud structure. In some cases the LWC range begins at zero, as observed on Aug 16th and Aug 17th. This suggests that the stratus cloud was broken on these flights and/or that cloud layers with different altitude ranges may coexist in the flight area. Uncertainty also exists in the choice of cloud base because of the coexistence of different cloud layers (Fig. 1.3). The choice of a single cloud base and top for the three flights of study (Table 1.2) is somewhat subjective, but it enables the generalizations proposed further in this study.

Table 1.2 Altitudes of cloud top and cloud base, used to determine the normalized cloud altitude.

	Aug 09 th	Aug 16 th	Aug 17 th
Altitude of Cloud Top (m)	395	485	800
Altitude of Cloud Base (m)	75	105	360
Depth of Cloud layer (m)	320	380	440

1.6 Division of cloud layers

Many cloud-microphysical properties, such as LWC (Fig. 1.3), and radar reflectivity (Fig 3.12, Fig. 3.13 and Fig 3.14), have a strong altitude dependence in marine stratus. Therefore, it is assumed that the threshold radar reflectivity for drizzle also varies with cloud altitude. To assess this dependency on height within the stratus layer, data are binned in nine cloud layers (Table 1.3). Cloud characteristics will be estimated for each layer separately.

Table 1.3 Division of cloud layers (all altitudes are normalized values)

Cloud altitude	0.9	0.8	0.7	0.6	0.5
Altitude range	0.85~0.95	0.75~0.85	0.65~0.75	0.55~0.65	0.45~0.55
Cloud altitude	0.4	0.3	0.2	0.1	-0.1
Altitude range	0.35~0.45	0.25~0.35	0.15~0.25	0.05~0.15	-0.05~0.05

1.7 Outline

This thesis consists of six chapters. A lognormal model is utilized to simulate the DSD in marine stratus, in Chapter 2. The existence and values of a reflectivity threshold for drizzle are discussed in Chapter 3. With the results of Chapter 3, the relationship between LWC and side-looking WCR second gate echoes for drizzle-free cases (droplets smaller than 50 μ m in diameter) is investigated in Chapter 4. Discussion of this work is done in Chapter 5. Some conclusions and future works are summarized in Chapter 6.

Chapter 2 Marine stratus drop size distribution

2.1 Background

The equivalent radar reflectivity depends on the target size distribution. Most if not all droplets in marine stratus scatter the 95 GHz signal in proportion to the 6th power of their radius (Rayleigh scattering). In other words, an understanding of marine stratus drop size distributions (DSDs) is important to interpret its reflectivity characteristics. Much research on DSDs in clouds has been done in the past years. The two main cloud DSD models reported in the literature are the Gamma model, and the Lognormal model. Observations show that the Lognormal distribution is a good approximation for the DSD in marine stratus (Davidson et al. 1984). The Lognormal DSD model has same number of parameters as the Gamma model (Borovikov 1961; Atlas et al. 1989; White et al. 1991), but it is computationally more convenient. Therefore this study employs the Lognormal model to characterize DSD in marine stratus.

The Lognormal model is expressed in the form

$$n(x) = \frac{N}{\sigma_x r \sqrt{2\pi}} \exp\left(-\frac{(x-x_0)^2}{2\sigma_x^2}\right) \quad (2.1)$$

where $n(x)$ is the number density of droplets with radius of r . It has units of $\#m^{-3}\mu m^{-1}$. Further, x is defined as $x = \ln(r)$, $x_0 = \ln(r_0)$, where r is the droplet radius, and r_0 is the median radius (most likely radius). N is total number of droplets per unit volume ($\#m^{-3}$) and σ_x is the logarithmic width of the distribution. σ_x is the standard variation of $\ln(r)$ to $\ln(r_0)$.

To describe the droplet spectrum with a Lognormal model, values for the parameters N , r_0 and σ_x must be found. For drizzle-free marine stratus, 100 cm^{-3} is a reasonable approximation of N (Frisch et al. 2002) and for drizzle drops larger than $50 \mu \text{ m}$ in diameter, $N = 0.1 \text{ cm}^{-3}$. Frisch et al. (1995) gave σ_x a value of 0.35 for marine stratus. Atmospheric Radiation Measurement (ARM) data suggest a value of σ_x of 0.32 ± 0.09 for continental stratus. Using data from FIRE, Frisch et al. (2002) found σ_x to be 0.34 ± 0.09 for marine stratus.

Two types of marine stratus are discriminated in this study (Section 1.3): in situ drizzle cases

(clouds containing drops $>50 \mu m$) and drizzle-free cases (containing only droplets $<50 \mu m$). A drizzle case is one with at least two consecutive seconds of non-zero 2DC measurements, and a drizzle-free case is one with at least two consecutive seconds of zero 2DC measurements. This implies that a large fraction of the marine stratus is ignored (about 40% for the three CS99 flights), i.e. the edges of drizzle patches, as well as borderline drizzle cases. The distinction between drizzle and drizzle-free cases is important, as it is the guiding concept throughout this thesis.

Two lognormal DSDs are illustrated in Fig 2.1, one with $r_0 = 8\mu m$ (radius) for cloud droplets and another with $r_0 = 30\mu m$ (radius) for drizzle drops. The first DSD is typical of DSDs encountered in drizzle-free marine stratus. The sum of both DSDs is typical for drizzly marine stratus.

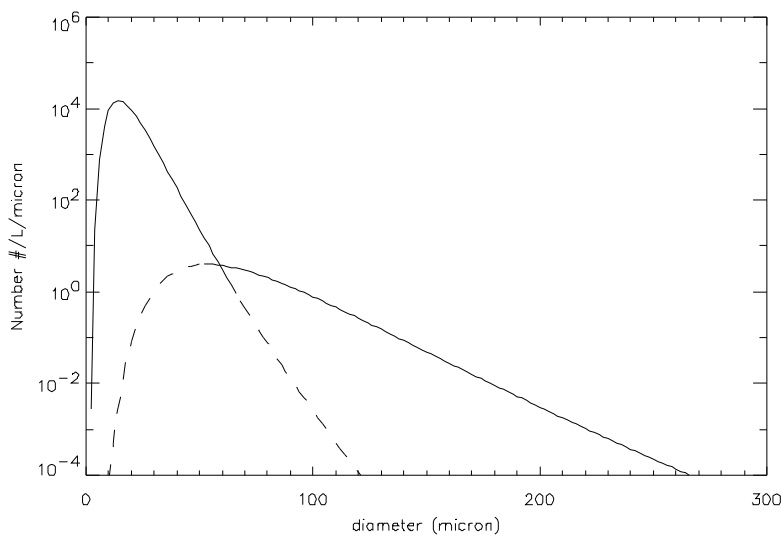


Fig 2.1 Example of two Lognormal DSDs, the combination of which may be representative of marine stratus. The left curve represents a cloud droplet spectrum with $r_0 = 8\mu m$ and $N=100 cm^{-3} \mu m^{-1}$. The right curve simulates the distribution of drizzle drops with $r_0 = 30\mu m$ and $N=0.1 cm^{-3} \mu m^{-1}$. Both spectra use 0.35 as value of σ_x . Since the number concentration of droplets varies by some five orders of magnitude, depending on their size, a logarithmic coordinate is applied in the Y-direction.

2.2 Drop size distribution in CS99

Three in-situ probes, FSSP, 1DC and 2DC, are used to estimate the DSD in CS99 marine stratus. All those instruments measure particle diameter. Thus all particle sizes used in this paper will refer to the diameter, not the radius.

Since the measurement ranges of the three probes form two overlapping regions, not all bin measurements of the 1DC and 2DC probes are used. The fifteen 3- μm bin measurements of FSSP form the first segment of the droplet spectrum, from 1.5 μm to 46.5 μm . 1DC measurements provide data to the second segment of the spectrum. Although the 1DC probe counts the number density of droplets from 12.5 to 185.5 μm , only the concentration of droplets from 50 μm to 100 μm is used. The first three 1DC bins are neglected, and the next four 12.3- μm size bins are used. 2DC measurements provide the DSD information for drops larger than 100 μm . Eleven 2DC bins, beginning at the third bin, are used. These choices are justified also by the well-established fact that optical array probes tend to underestimate the droplet count in their first few bins.

In short, a continuous drop spectrum can be produced by in situ measurements, although the bin width is not constant, and the bin resolution is rather coarse above 50 μm . Such spectrum can be produced by in-situ measurements with a frequency of 1 Hz, which corresponds to a spatial resolution of 100 m (Table 1.1). This is the sampling rate of the 2DC probe. It should be noted that the sample size is important to estimate the DSD. Cloud radar data have shown that the DSD changes over small spatial scales, not only in the vertical but also in the horizontal dimension (Vali et al. 1998). Yet DSDs deduced from insufficient data will produce large departures from the true, continuous spectrum, and large errors in the derived reflectivity result. So there is a trade-off: too large a sampling period ignores too much spatial variability, and too small a sampling period yields incomplete DSDs, especially for drizzle-size drops.

Independent observations have shown that the DSD in marine stratus is highly dependent on altitude within the cloud. Therefore, the DSD is studied in nine layers, between the normalized cloud altitudes 0.05 and 0.95, for each flight.

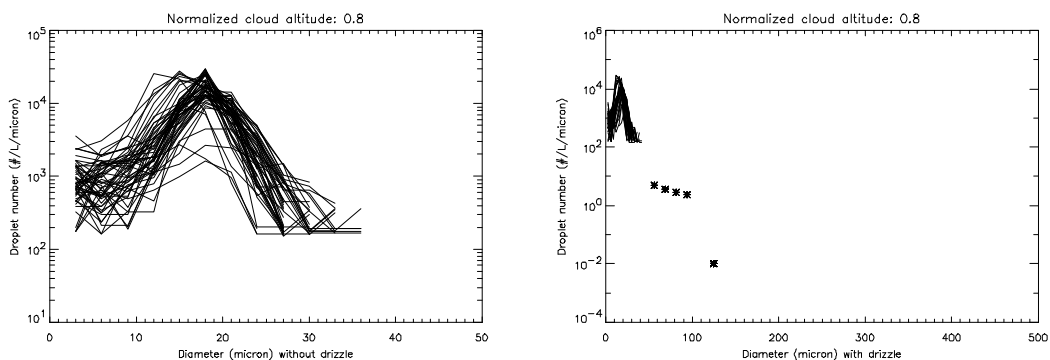
2.2.1 Measurements of FSSP, 1DC, and 2DC

The observed DSDs of drizzly and drizzle-free cases are plotted for four heights on three flights (Fig 2.2, Fig 2.3 and Fig 2.4). The definition of a drizzle-free case is given in Section 1.3. Drizzle-free DSDs are based on FSSP measurements only. In drizzle cases all three probes are used to construct a DSD. The reliability of the 1DC probe, especially in CS99, appears to be somewhat questionable: most instantaneous 1DC measurements do not form a smooth distribution in the four bins between 50 μm to 100 μm , unlike the FSSP data, and unlike the 2DC data in drizzle areas. It is possible that the 1DC probe undersampled the true droplet numbers, yet the amount of undersampling is unknown.

Because of the uncertainty regarding the 1DC probe, 2DC measurements have been used to define in situ drizzle cases (Section 2.1). Those instantaneous samples, for which the sum of the 15 bins of FSSP measurements is less than 5 droplets/ cm^3 , are rejected, i.e. flimsy cloud sections are ignored.

Only a few stars appear at the 1DC range (Fig 2.2-2.4), but the distribution of stars suggests a continuous spectrum between the measurements of the FSSP and 2DC probes, especially on Aug 17th. When the 2DC sample size is small, a smooth curve cannot be obtained at this range either. In this case a star symbol is used to represent 2DC measurements.

2.2.2 Drop size distribution for the Aug 09th flight



Identifying Drizzle Within Marine Stratus with W-Band Radar Reflectivity profiles

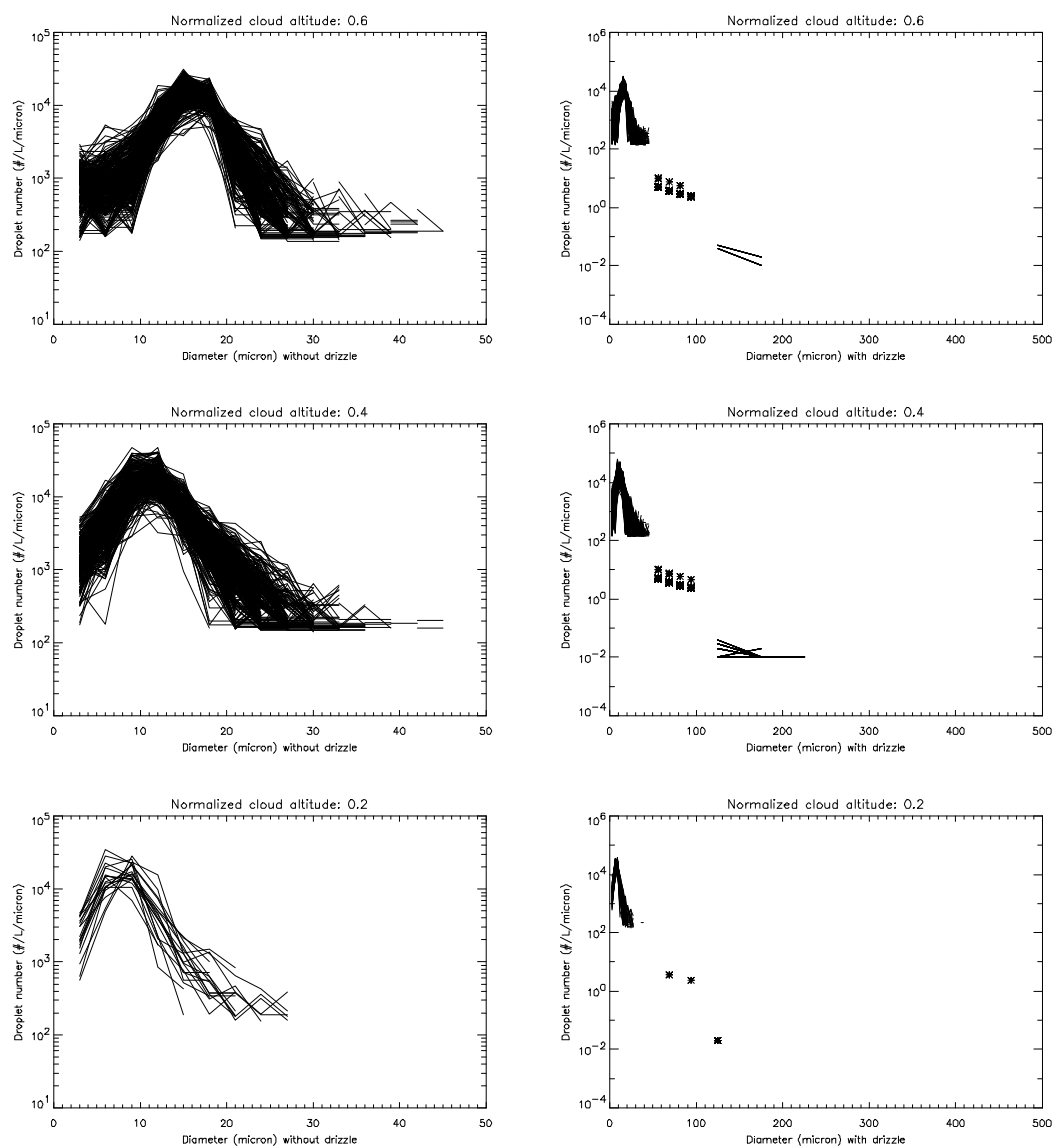


Fig. 2.2 In-situ DSD for the Aug 09th flight at various normalized cloud altitudes. The DSDs for drizzle-free cases (measurements of FSSP) are shown on the left. Not all 10 Hz samples are shown, but rather only 1 in 10. The DSDs for drizzle cases (with measurements of FSSP, 1DC, and 2DC) are shown on the right. Star symbols are used in the DSD curves to illustrate the droplet spectrum shape where the 1DC or 2DC sample sizes are small.

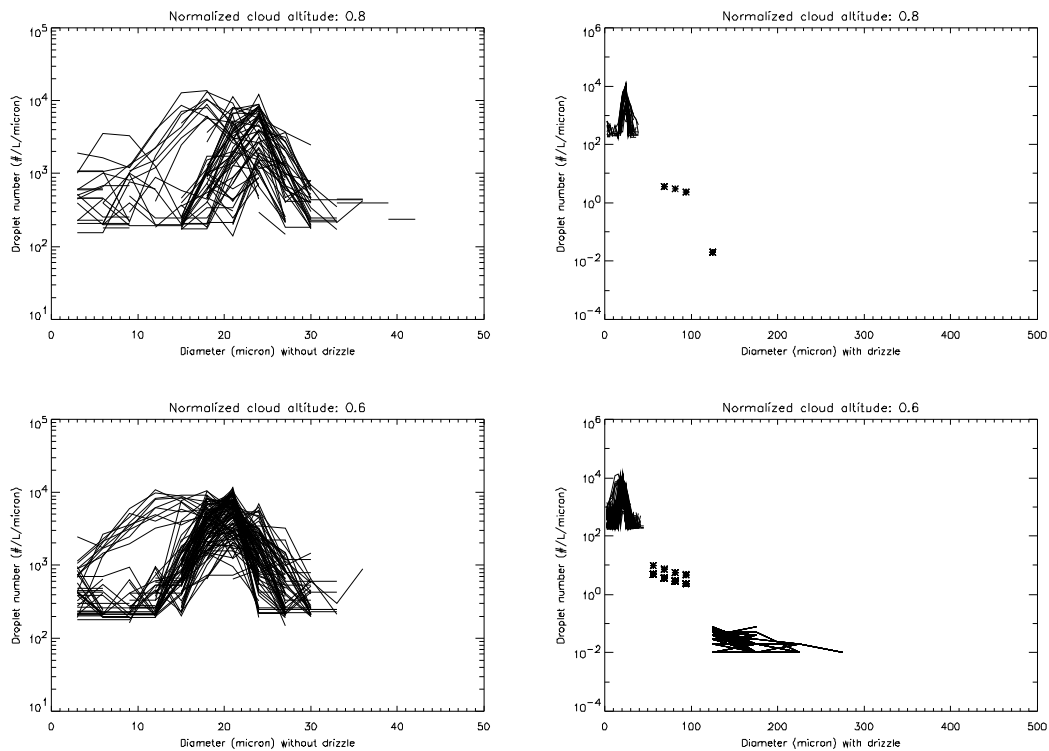
All graphs have a clear peak in the FSSP measurement range. The mode diameter of cloud droplet spectrum increases from cloud base to cloud top. And the spectrum becomes wider with altitude too. The distributions of star symbols, which represent 1DC measurements, suggest a second mode. A third local spectrum peak may be located at 2DC measurement range. No obvious dependence of model radius and spectrum width on altitude is observed for the last two

modes (Fig. 2.2). The sample size increases from cloud top to the lower middle part of cloud, and dwindles again below (Table 2.1). This sample size trend partly matches the general drizzle drop distribution: more drizzle/rain drops are found at low levels of marine stratus (Fox and Illingworth 1997). The small sample size in the lowest levels of the marine stratus deck is due to the limited flight time there.

Table 2.1 Number of 1 second data segments with and without drizzle during the Aug 09th flight, as a function of normalized cloud altitude.

Cloud altitude (ϕ)	0.9	0.8	0.7	0.6	0.5	0.4	0.3	0.2	0.1
drizzle-free	33.2	54.3	84.3	345.3	147.8	348.4	42.3	17.5	17.9
drizzle	0	5.8	43.4	109.4	86.1	315.1	40.5	6.4	0

2.2.3 Drop size distribution for the Aug 16th flight



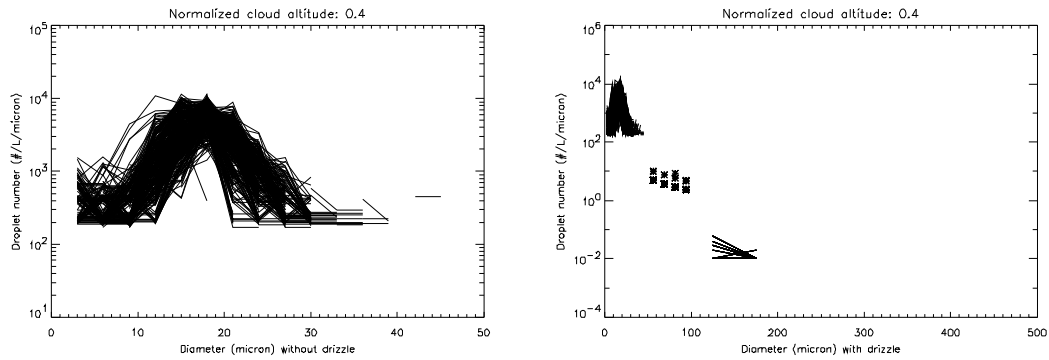


Fig 2.3 As Fig. 2.2, but for the Aug 16th flight.

Table 2.2 As Table 2.1, but for the Aug 16th flight.

Cloud altitude (ϕ)	0.9	0.8	0.7	0.6	0.5	0.4	0.3	0.2	0.1
drizzle-free	40.2	59.8	672.0	103.7	83.0	316.2	14.1	1.7	1.8
drizzle	29.8	8.0	171.4	170.1	75.0	259.9	65.5	3.3	3.2

Two DSD modes are observed in FSSP measurements on Aug 16th (Fig 2.3 e.g. $\phi=0.8$). One group of spectra has median diameters smaller than 15 μ m. This DSD is consistent with the theoretical droplet spectrum calculated with the condensational growth mechanism (Gerber 1996). The larger mode diameter, with median diameters around 20 μ m, corresponds with typical broadening spectra often observed in marine cloud WJY ??? (Warner 1969). The diameters of both spectral peaks, as well as the spectral width, grow from cloud base to cloud top, as does the LWC. The spectrum of larger drops is similar to that of the Aug 09th flight (Fig. 2.2).

2.2.4 Drop size distribution for the Aug 17th flight

Identifying Drizzle Within Marine Stratus with W-Band Radar Reflectivity profiles

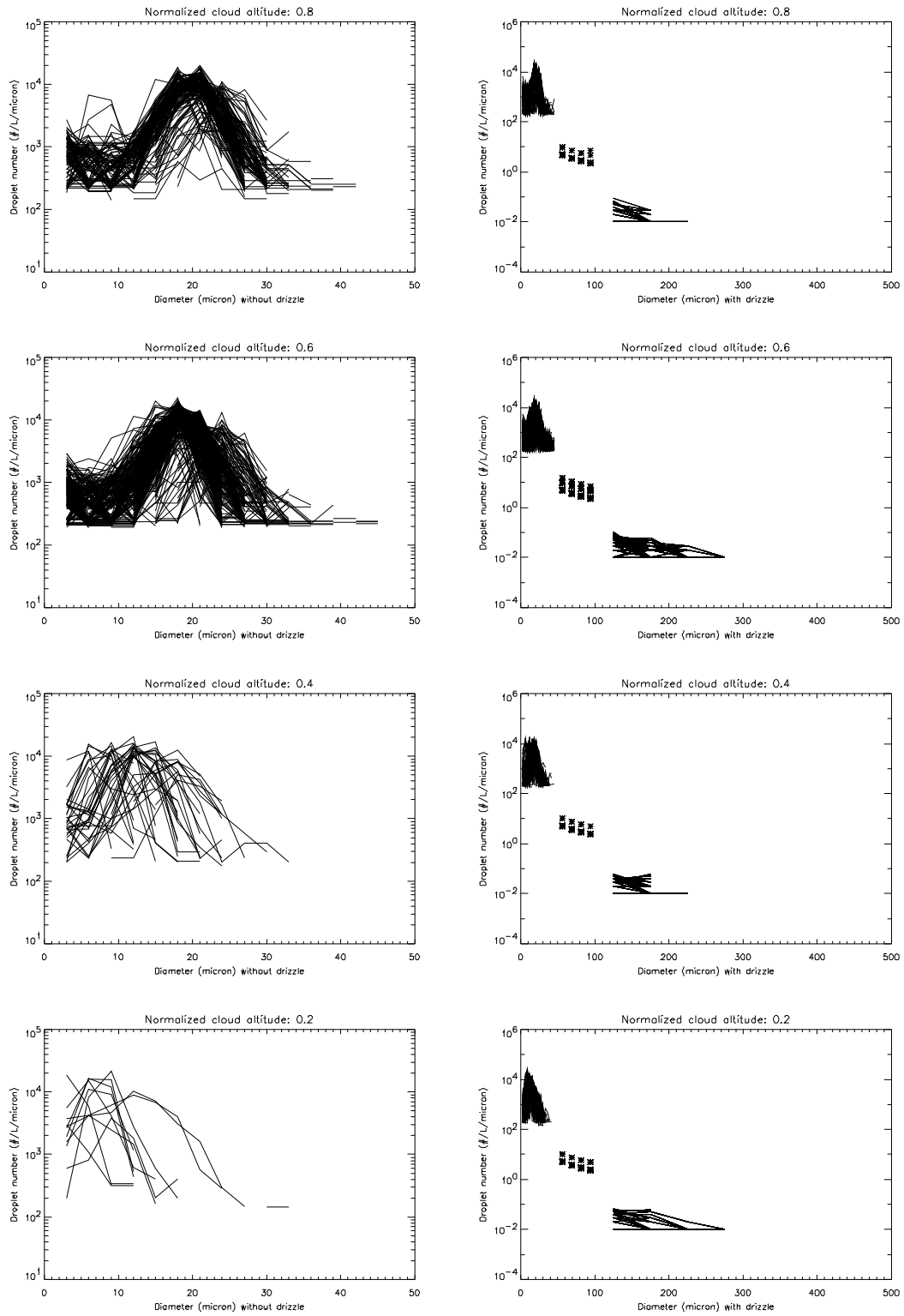


Fig 2.4 As Fig. 2.2, but for the Aug 17th flight.

Table 2.3 As Table 2.1, but for the Aug 17th flight.

Cloud altitude (ϕ)	0.9	0.8	0.7	0.6	0.5	0.4	0.3	0.2	0.1
drizzle-free	33.0	142.6	199.3	313.0	49.4	36.4	30.2	11.1	4.2
Drizzle	15.0	137.1	205.0	686.6	49.2	43.8	983.5	42.3	32.9

Drizzle was widely observed along the Aug 17th flight, at all levels but especially at low levels (Table 2.3). The Aug 17th drizzle-free DSDs display variable mode diameters at each cloud layer. Possibly this implies different broadening phases during the probing period. As was the case for the two other flights, both the center diameter and the spectrum width increase with cloud altitude (Fig 2.4).

2.3 Lognormal approximation of measured droplet spectra

2.3.1 The use of a continuous function to extend in situ measurements

As discussed in Section 2.1, a Lognormal model is adopted to approximate the DSD of both “drizzle-free” and “drizzly” marine stratus in CS99. Such model description is especially useful to extend probe measurements at the right tail of the DSD (the larger drops).

As mentioned before, some bins of the 1DC probe, especially the first few bins including those in the 50-100 μm range, may have underestimated the true droplet count (Section 2.2.1). Also, the 2DC probe samples slowly. Because of the discrete bin sampling, the relatively small probe sample volumes, and the tendency of optical array probes, esp the 1DC probe, to underestimate counts in the smaller bins, a lognormal DSD is more continuous, and integral quantities derived from the lognormal distribution may be estimated more accurately than merely with the observations on which the lognormal DSD is based. In particular, a knowledge of the right tail end of the DSD is essential in this study, because we plan to use radar reflectivity to assess the presence of drizzle, and reflectivity is strongly affected by the few large droplets that may exist in marine stratus.

Drizzle-free cases will be presented by one lognormal DSD, based on FSSP measurements. An assumption is made for drizzle cases: *we assume that the total DSD is the sum of several lognormal DSDs*. This concept is illustrated in Fig 2.1. The concept is not new. Frisch (1995) etc already used it. Now the total DSD is not the sum of two lognormal DSDs (cloud droplets and drizzle droplets), but rather the sum of three lognormal DSDs, because the King Air carried three

instruments. This seems to be a rather arbitrary argument, lacking a cloud-physical basis. The argument does have a basis in terms of droplet growth phases, as will be discussed later.

So we assume a tri-modal DSD for drizzle cases, each with its own median radius and logarithmic width. The first mode, covering FSSP measurements, has a median diameter smaller than $30 \mu\text{ m}$. A secondary mode has a maximum number density corresponding to a size $50 \mu\text{ m}$ – $100 \mu\text{ m}$. And a third local peak exists in the 2DC measurement range.

2.3.2 Method

The lognormal parameters corresponding to drizzle-free cases and drizzle cases are calculated with in-situ probe measurements. A lognormal model can be fitted to each of the 10 Hz FSSP measurements. The resulting lognormal parameters are the averages of the 10 Hz lognormal parameters. Another method to determine the model parameters in the FSSP and drizzle ranges is to add up all counts in each bin, for each cloud level during the entire flight, and then to compute a lognormal model that best fits the cumulative droplets density. The 1DC and 2DC measurements only form a segment of the whole DSD ($50 \mu\text{ m}$ to $100 \mu\text{ m}$ for 1DC and $100 \mu\text{ m}$ to $600 \mu\text{ m}$ for 2DC). The mathematical principle that a minimum of three points is needed to define a curve with three unknown parameters is utilized for the 1DC and 2DC ranges. Of course this implies that the drizzle DSDs are less certain than the cloud droplet DSDs. The total drop number frequency, based on the entire volume sampled for all drizzle events at a given altitude, in each bin is used to retrieve the lognormal model parameters for the modes corresponding to 1DC and 2DC measurements. When only one or two bin measurements exist at 1DC range at a given level, then the 50-100 μm lognormal DSD is interpolated between FSSP and 2DC measurements.

The calculated spectra are shown below, together with observed DSDs, for nine layers on three flights.

2.3.3 Droplet spectra for the Aug 09th flight

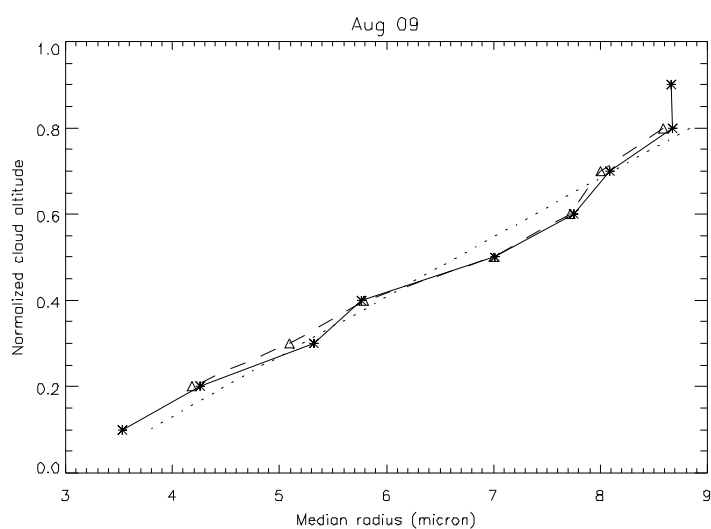
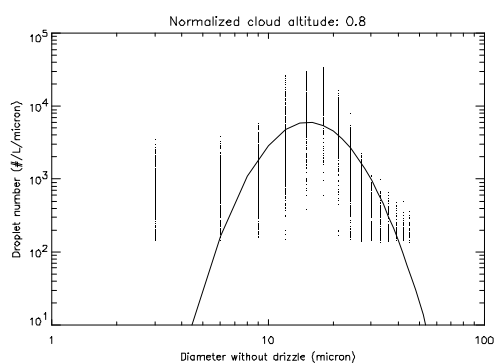
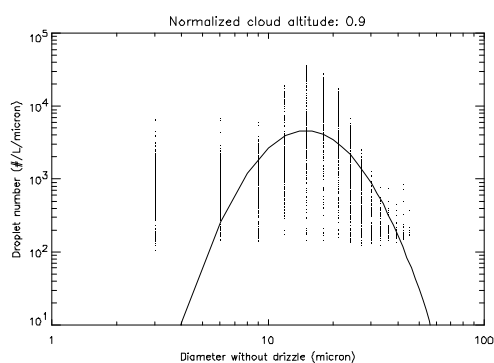


Fig. 2.5 Profiles of the lognormal median radius r_0 (μm) for cloud droplets (FSSP measurements) for Aug 09th flight. The solid line represents median radii for drizzle-free cases. The dashed line represents median radii of the cloud droplets in cases with drizzle. The dotted line is a regression line, based on both cases.

Table 2.4 Lognormal model parameters for drizzle-free cases for the Aug 09th flight.

ϕ	0.9	0.8	0.7	0.6	0.5	0.4	0.3	0.2	0.1
r_0 (μm)	8.66	8.68	8.09	7.76	7.02	5.77	5.32	4.26	3.53
σ_x	0.38	0.35	0.35	0.32	0.32	0.37	0.35	0.36	0.45
N (cm^{-3})	108.0	130.1	127.2	133.9	144.8	150.1	148.3	125.1	66.0
Sample size (#)	332	543	843	3453	1478	3484	423	175	179



Identifying Drizzle Within Marine Stratus with W-Band Radar Reflectivity profiles

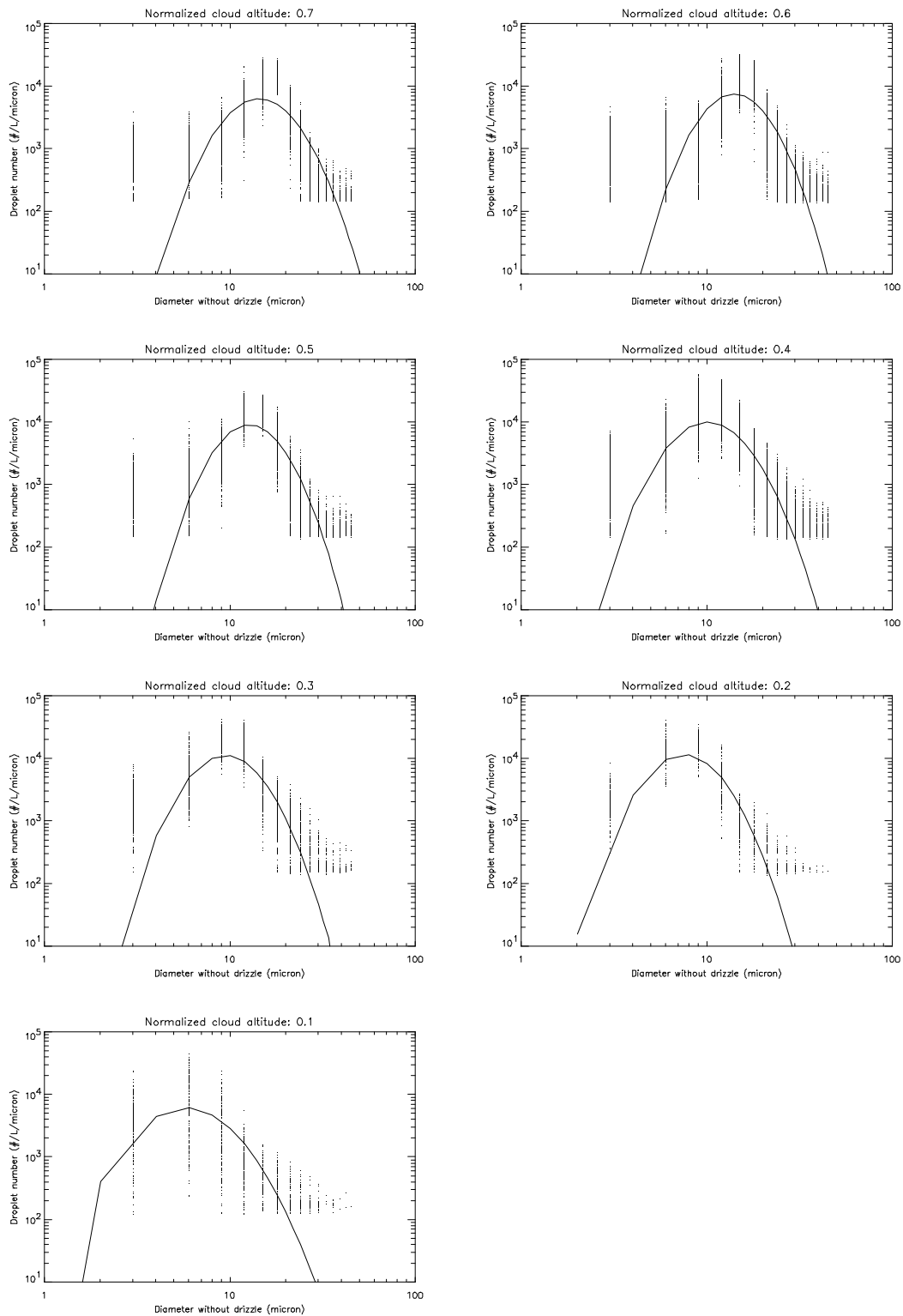
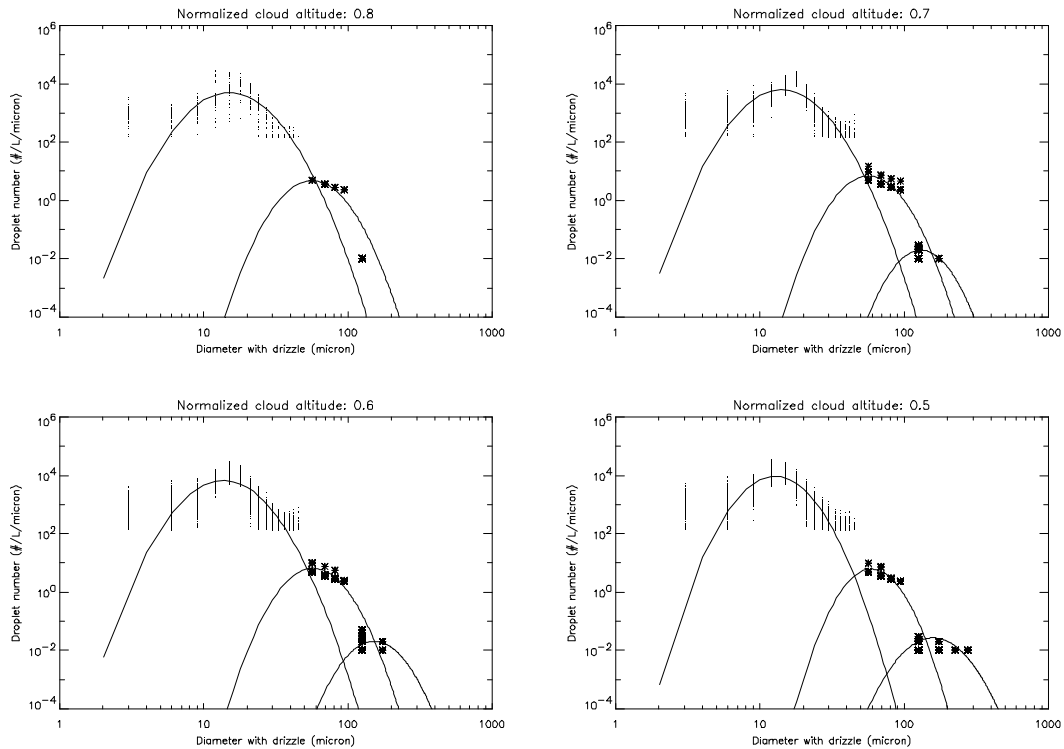


Fig 2.6 FSSP-measured (dots) and lognormal (curve) DSDs for the drizzle-free cases on the Aug 09th flight. The dots are based on 10 Hz measurements. To emphasize the lognormal characteristic of spectra, logarithmic coordinates are applied in both X and Y direction.

Table 2.5 Lognormal model parameters for drizzle cases for the Aug 09th flight.

ϕ	0.9	0.8	0.7	0.6	0.5	0.4	0.3	0.2	0.1
Sample size (#)		58	434	1094	861	3151	405	64	
FSSP measurement range									
r_0 (μm)		8.59	8.00	7.72	7.00	5.79	5.10	4.18	
σ_x		0.37	0.36	0.36	0.32	0.36	0.38	0.32	
N (cm^{-3})		111.8	128.1	133.7	152.7	158.9	160.7	148.4	
1DC measurement range									
r_0 (μm)		30.9	30.8	31.1	31.7	31.1	32.2	34.8	
σ_x		0.3	0.29	0.29	0.26	0.29	0.29	0.25	
N (cm^{-3})		0.10	0.15	0.14	0.12	0.14	0.13	0.07	
2DC measurement range									
r_0 (μm)		--	70.0	82.3	87.3	87.8	77.2	--	
σ_x		--	0.26	0.28	0.31	0.31	0.28	--	
N (dm^{-3})		--	0.87	1.15	1.75	1.22	0.85	--	



Identifying Drizzle Within Marine Stratus with W-Band Radar Reflectivity profiles

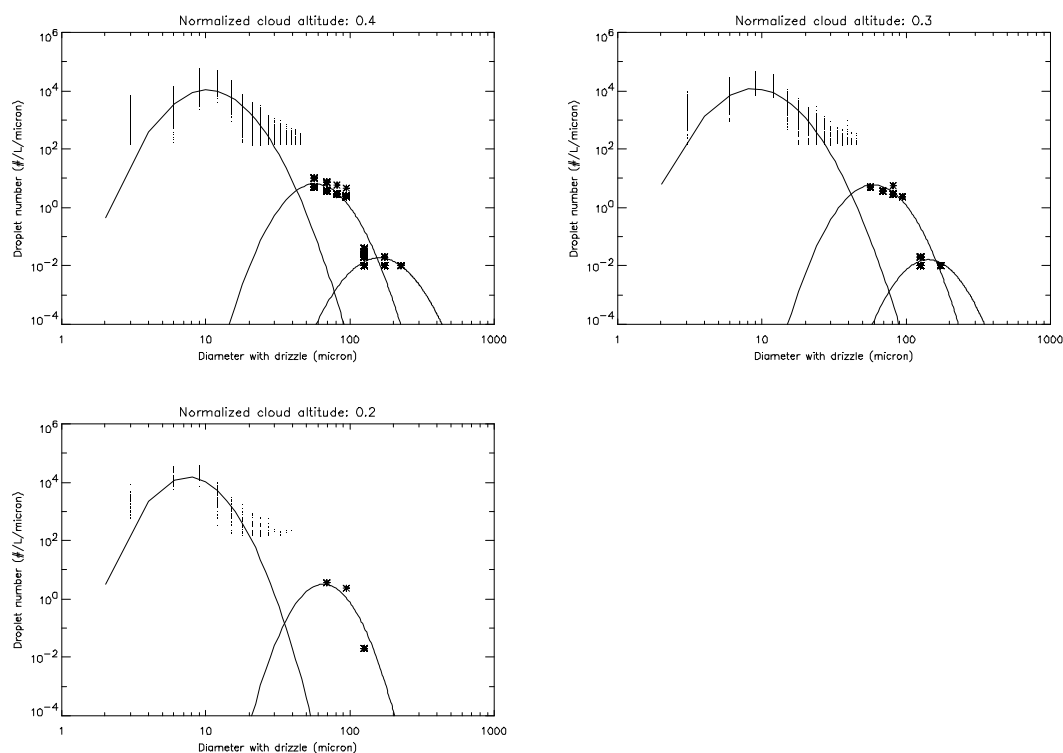


Fig. 2.7 As Fig. 2.6, but for drizzle cases on Aug 09th. Stars represent 1DC and 2DC measurements.

2.3.4 Droplet spectra for the Aug 16th flight

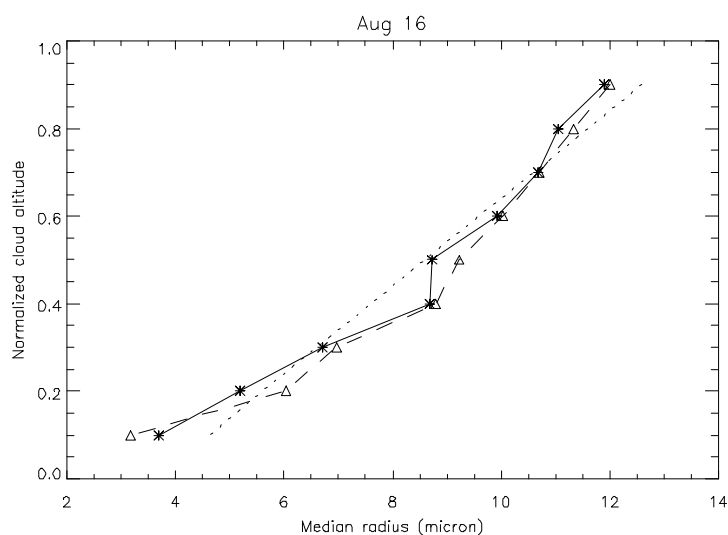
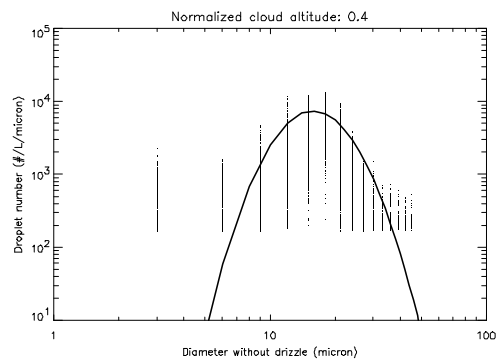
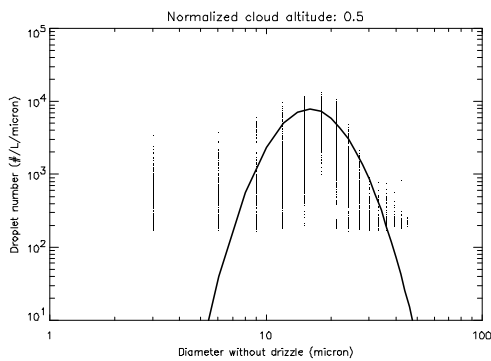
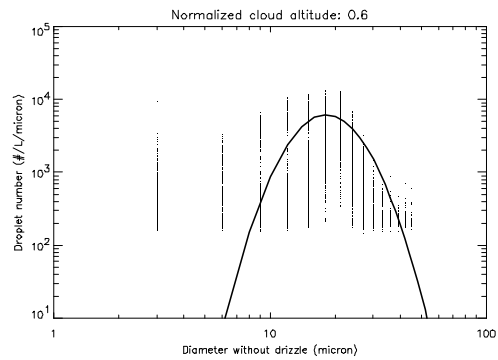
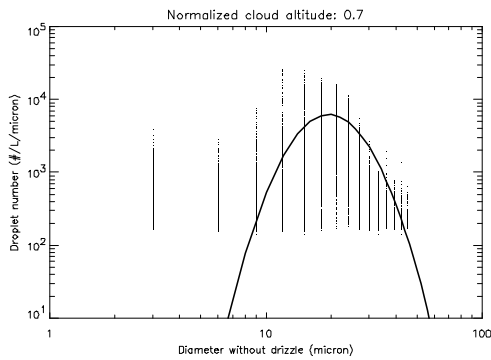
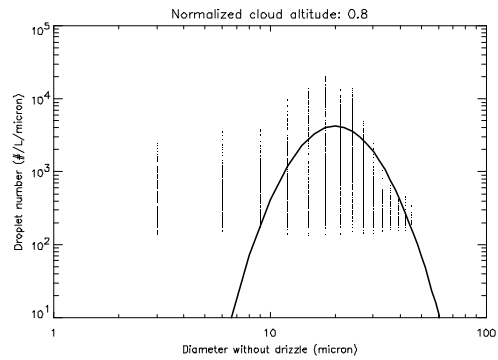
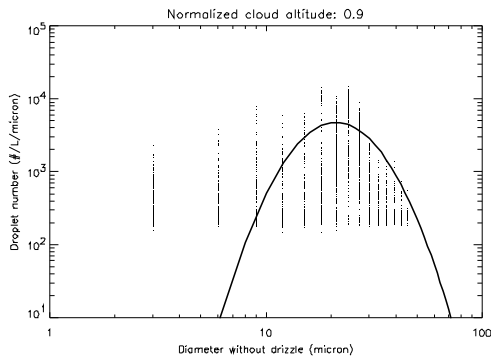


Fig. 2.8 As Fig. 2.5, but for the Aug 16th flight.

Table 2.6 As Table 2.4, but for Aug 16th.

ϕ	0.9	0.8	0.7	0.6	0.5	0.4	0.3	0.2	0.1
r_0 (μm)	11.9	11.1	10.7	9.9	8.7	8.7	6.7	5.2	3.7
σ_x	0.35	0.32	0.30	0.30	0.30	0.31	0.36	0.37	0.31
N (cm^{-3})	46.7	35.6	48.0	44.0	49.1	47.6	37.7	40.0	37.1
Sample size (#)	402	598	6720	1037	830	3162	141	17	18



Identifying Drizzle Within Marine Stratus with W-Band Radar Reflectivity profiles

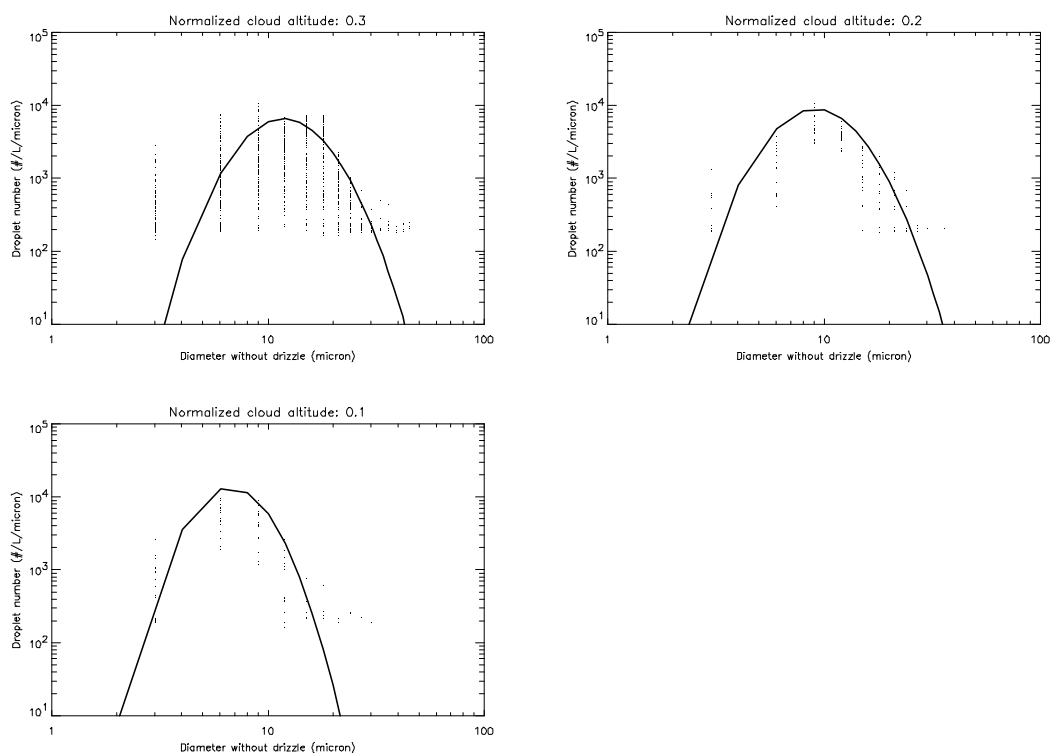
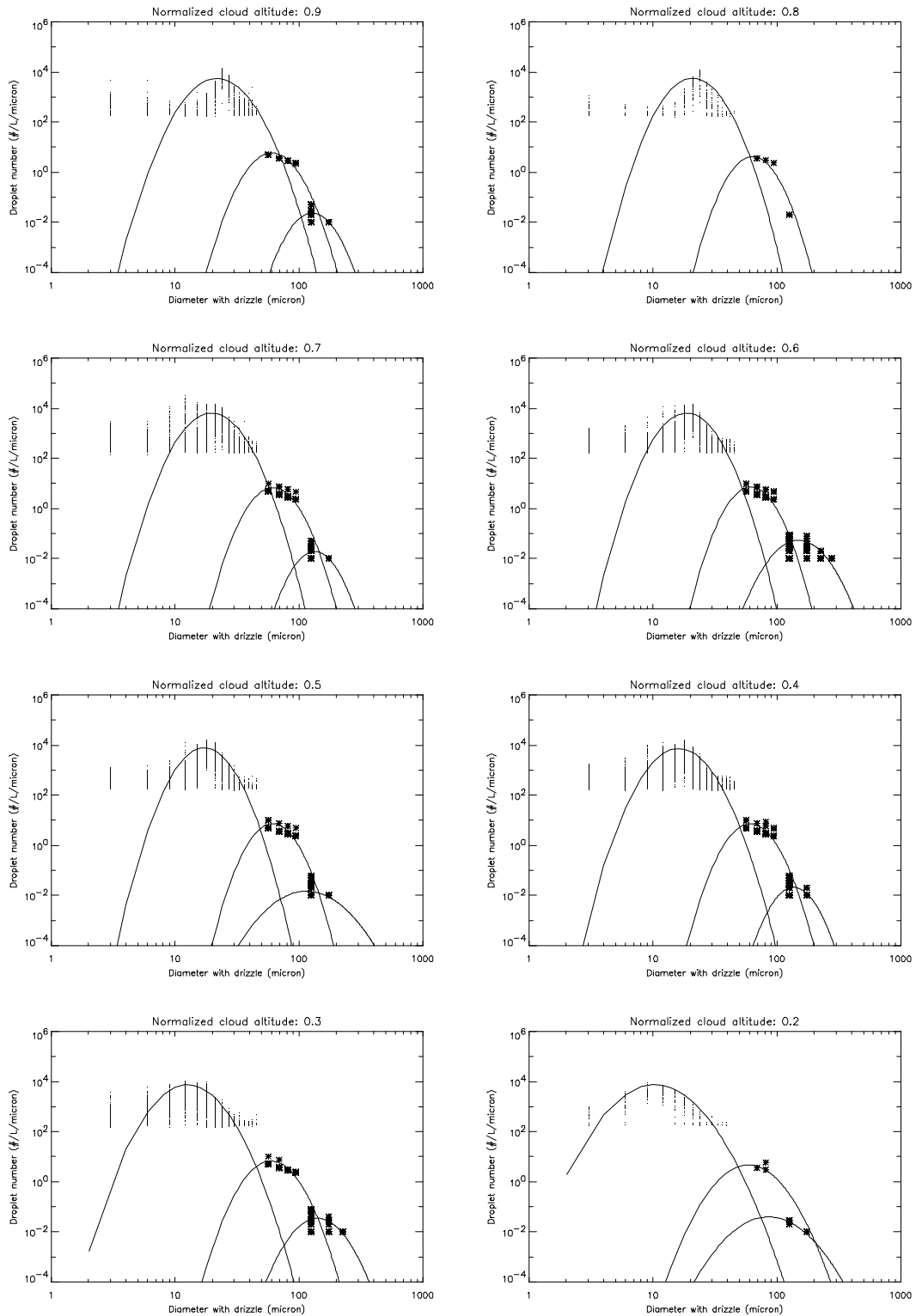


Fig 2.9 As Fig. 2.6, but for the Aug 16th flight

Table 2.7 As Table 2.5, but for Aug 16th.

ϕ	0.9	0.8	0.7	0.6	0.5	0.4	0.3	0.2	0.1
Sample size (#)	298	80	1714	1701	750	2599	655	33	32
FSSP measurement range									
r_0 (μm)	12.0	11.3	10.7	10.0	9.2	8.8	7.0	6.0	3.2
σ_x	0.31	0.28	0.29	0.28	0.27	0.30	0.33	0.40	0.33
N (cm^{-3})	48.8	43.4	48.5	44.3	46.6	46.4	41.6	41.9	32.8
1DC measurement range									
r_0 (μm)	32.3	33.6	32.8	32.6	34.5	32.5	31.8	42.8	34.7
σ_x	0.26	0.24	0.25	0.24	0.24	0.25	0.27	0.33	0.24
N (cm^{-3})	0.12	0.08	0.13	0.14	0.14	0.14	0.14	0.12	0.05
2DC measurement range									
r_0 (μm)	67.8	--	70.6	81.1	67.4	72.1	76.4	50.2	62.2
σ_x	0.24	--	0.23	0.29	0.21	0.23	0.28	0.37	0.26
N (dm^{-3})	0.93	--	0.76	3.09	0.93	0.85	1.79	1.84	1.14

Identifying Drizzle Within Marine Stratus with W-Band Radar Reflectivity profiles



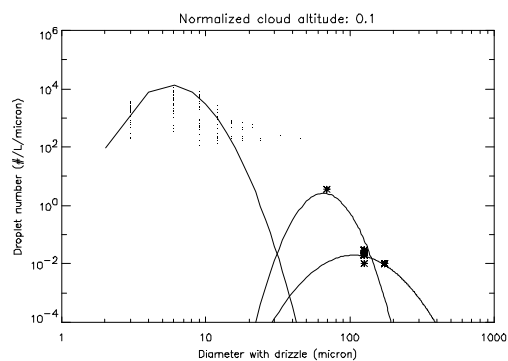


Fig. 2.10 As Fig. 2.7, but for the Aug 16th flight

2.3.5 Droplet spectra for the Aug 17th flight

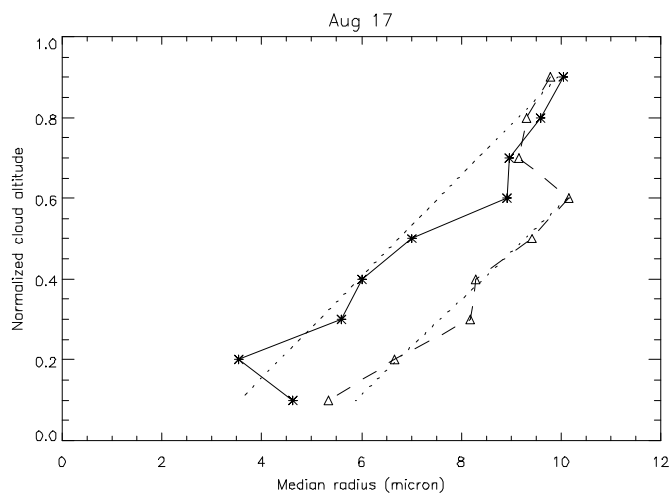
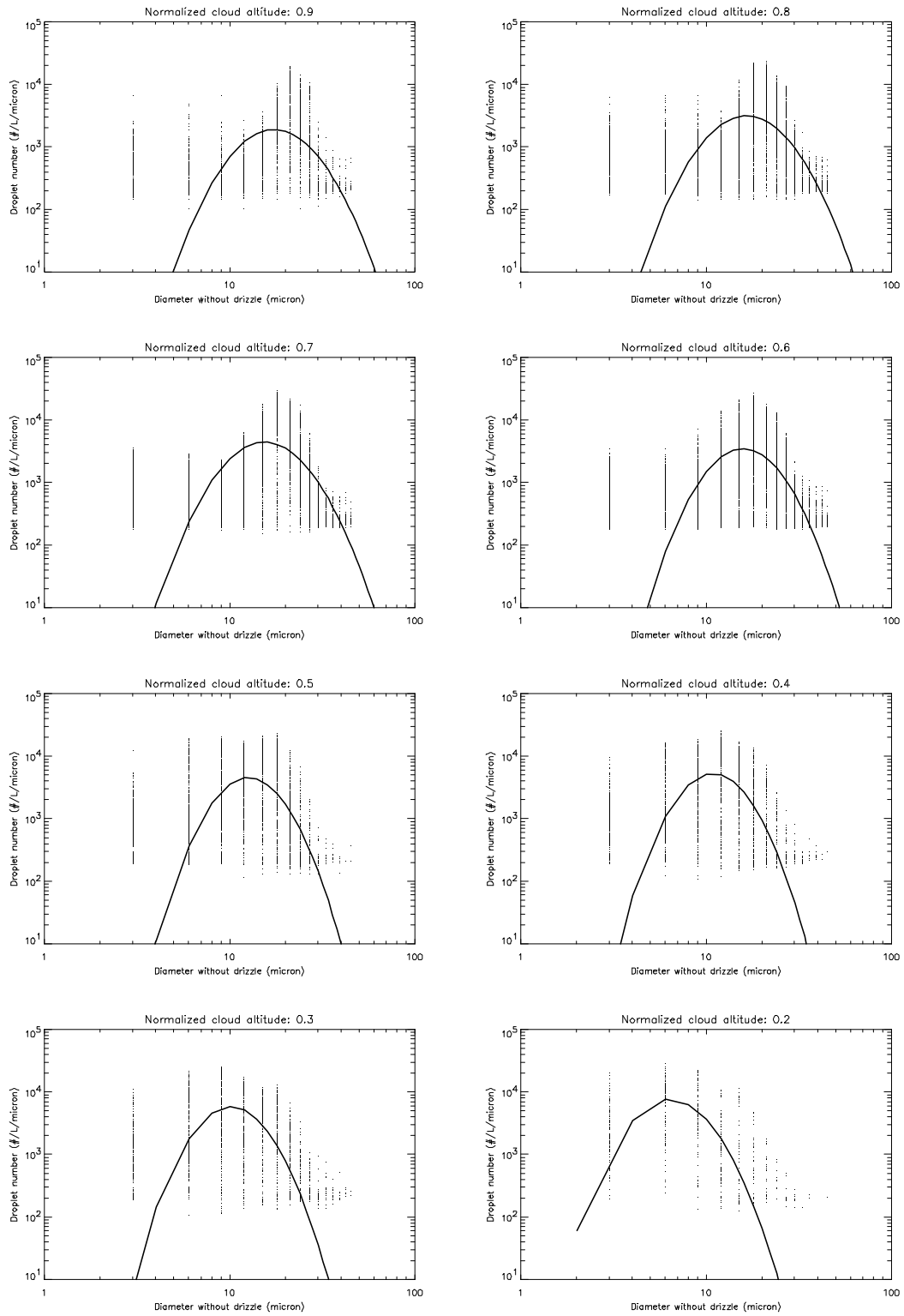


Fig. 2.11 As Fig. 2.5 but for the Aug 17th flight. Two linear estimates are shown, one for drizzle (right dotted line) and one for drizzle-free cases (left dotted line).

Table 2.8 As table 2.4, but for the Aug 17th flight.

ϕ	0.9	0.8	0.7	0.6	0.5	0.4	0.3	0.2	0.1
r_0 (μm)	10.1	9.6	9.0	9.0	7.0	6.0	5.6	3.5	3.6
σ_x (μm)	0.39	0.39	0.39	0.35	0.33	0.33	0.34	0.37	0.46
N (cm^{-3})	48.0	81.4	107.5	77.1	75.5	75.0	79.6	68.6	36.8
Sample size (#)	330	1426	1993	3130	494	364	302	111	42

Identifying Drizzle Within Marine Stratus with W-Band Radar Reflectivity profiles



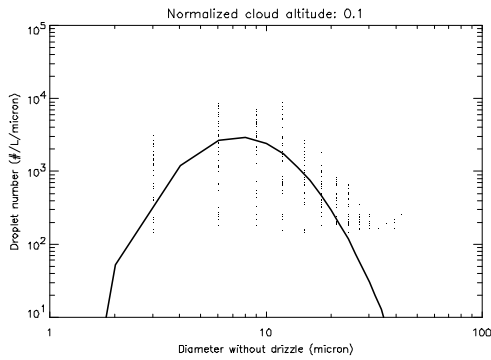
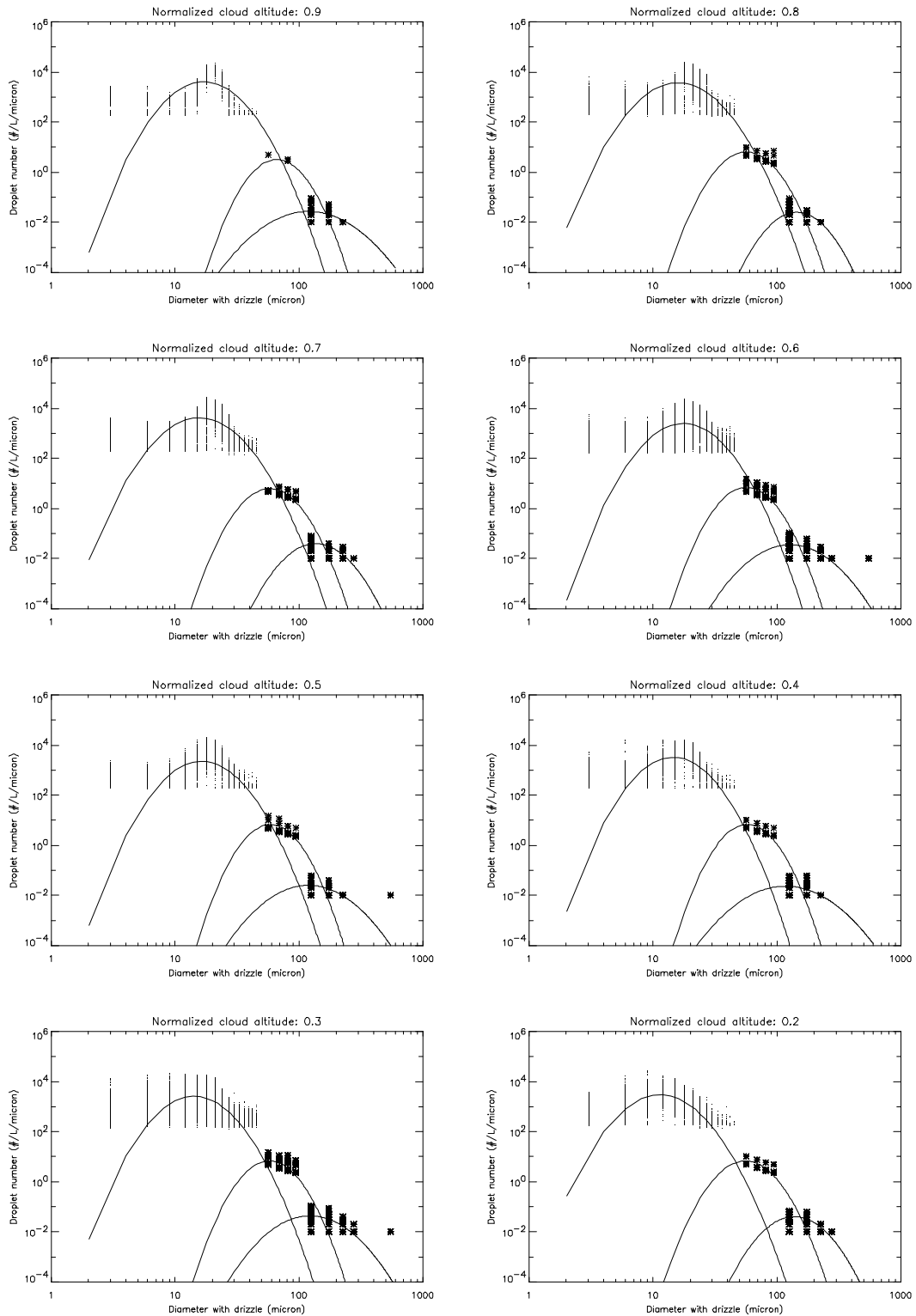


Fig 2.12 As Fig. 2.6 but for the Aug 17th flight.

Table 2.9 As Table 2.5 but for the Aug 17th flight.

ϕ	0.9	0.8	0.7	0.6	0.5	0.4	0.3	0.2	0.1
Sample size (#)	150	1371	2050	6866	492	438	9835	423	329
FSSP measurement range									
r_0 (μm)	9.8	9.3	9.2	10.2	9.4	8.3	8.2	6.7	5.3
σ_x (μm)	0.38	0.40	0.40	0.38	0.38	0.37	0.38	0.40	0.45
N (cm^{-3})	107.1	96.3	106.3	67.4	56.1	71.4	57.1	55.0	52.9
1DC measurement range									
r_0 (μm)	36.0	31.2	31.9	31.0	31.9	31.4	31.5	30.8	31.3
σ_x (μm)	0.34	0.33	0.33	0.33	0.32	0.31	0.33	0.34	0.36
N (cm^{-3})	0.08	0.15	0.15	0.16	0.15	0.15	0.15	0.16	0.17
2DC measurement range									
r_0 (μm)	76.9	80.0	77.3	77.6	73.7	75.5	74.6	78.1	65.6
σ_x (μm)	0.30	0.32	0.35	0.44	0.46	0.30	0.44	0.35	0.36
N (dm^{-3})	2.31	1.54	2.55	2.78	1.95	1.97	3.27	2.62	2.74

Identifying Drizzle Within Marine Stratus with W-Band Radar Reflectivity profiles



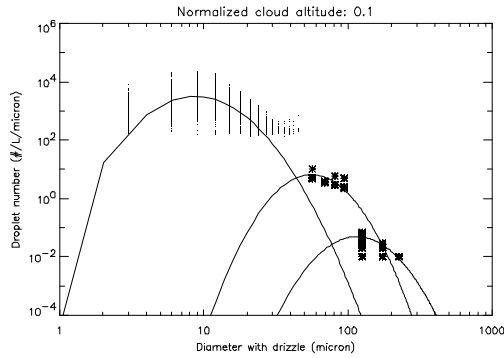


Fig 2.13 As Fig 2.7 but for Aug 17th.

2.3.6 Lognormal DSDs: a summary

A tri-modal lognormal spectrum is applied to simulate DSDs for droplet diameter from $1.5 \mu\text{m}$ to $<800 \mu\text{m}$ in marine stratus. The first mode (corresponding to FSSP measurements) gives good representation at the center of the true DSD but underestimates at the tail areas (Fig. 2.7, Fig. 2.10 and Fig. 2.12). The second mode is designed to coincide with 1DC measurements. And a third mode is inferred when many drops are detected by the 2DC probe.

The median (most likely) radii for drizzle-free case and the first mode of drizzle case linearly increase from cloud base to cloud top, irrespective of the presence of drizzle for flights of Aug 09th and 16th (Fig. 2.5 and Fig. 2.8).

An equation representing the best-fit relation between the median cloud droplet radius r_0 (μm) and the normalized cloud altitude ϕ (dimensionless, ranging from 0 to 1) for Aug 09th flight is:

$$r_0 = 3.05 + 7.24 * \phi \quad (2.2)$$

The intercept and slope of the linear approximation for Aug 16th (Fig 2.8) are larger than those for Aug 09th flight (Fig. 2.5). The best-fit linear equation for Aug 16th is:

$$r_0 = 3.62 + 9.96 * \phi. \quad (2.3)$$

The most likely radii of cloud droplets observed along the Aug 17th flight also increase with height in the cloud, but the radii are some two microns larger if drizzle is present, except in the upper levels of the cloud (Fig 2.11). This suggests that drizzle mainly collects the smaller droplets, resulting in larger median cloud droplet sizes in drizzly patches. Or else the drizzly patches include a number of large cloud droplets, which are growing to become drizzle-size. The

reason why this was not observed on the previous two flights may be related to the fact that heavy drizzle fell on Aug. 17th, i.e. that the collision-coalescence growth process was more vigorous.

The following linear regressions apply to the drizzle-free and drizzle cases, respectively, for Aug 17th flight:

$$r_0 = 2.77 + 7.95 * \phi \quad (2.4)$$

$$r_0 = 4.60 + 8.54 * \phi \quad (2.5)$$

The median radii for the second and third modes of drizzle cases decrease slightly with cloud altitude, unlike the median radius of the first mode. This indicates that more large drops stay at low level in cloud.

Neither the standard deviation σ_x nor total droplet number (N) of all modes displays a clear dependence on cloud altitude (Table 2.4 to Table 2.9). For the flights of Aug 09th and Aug 16th, both σ_x and N for drizzle cases at FSSP range have similar values to the corresponding parameters for drizzle-free cases (Table 2.4 to table 2.7). In other words the cloud DSD is not seriously affected by the formation of drizzle for light drizzle cases. For the Aug 17th flight, at the upper levels, cloud DSDs have similar shapes for both drizzle-free and drizzle cases. But at mid-lower levels on Aug 17th, a wider cloud DSD and a larger median radius is observed for drizzle cases. Regarding drizzle drops (2DC data), more large drops and a wider DSD are recorded for the Aug 17th flight compared to the two other flights. This suggests that the marine stratus for the Aug 17th flight is a case with heavy drizzle.

2.4 Radar reflectivity calculated from lognormal DSDs for drizzle-free and drizzly marine stratus

The radar reflectivity characteristics of marine stratus are investigated based on the best-fitting lognormal DSDs retrieved in Section 2.3. The power returned at 95 GHz (3 mm wavelength) from marine stratus clouds is due to two kinds of scatter modes, Rayleigh scatter and Mie scatter. When the droplet diameter is no larger than about 1/10 of the radar wavelength, the particles will behave as Rayleigh scatterers. Larger particles behave as Mie scatterers.

Virtually all droplets (cloud droplets and drizzle drops) in marine stratus are smaller than

300 μ m in diameter. Therefore, only the Rayleigh scatter mode is used to calculate equivalent radar reflectivity from lognormal DSDs, as follows:

$$Z = \int n(D)D^6 dD \quad (2.6)$$

where Z is the equivalent radar reflectivity factor ($\text{mm}^6 \text{m}^{-3}$), D is particle diameter (mm), and $n(D)$ is number density of droplets with diameter D ($\text{mm}^{-1} \text{m}^{-3}$).

Since the magnitude of Z spans several orders of magnitude, a logarithmic scale is used as $\text{dBZ} = 10 \log_{10} Z$. Usually, dBZ is called *radar reflectivity* while Z is called the *radar reflectivity factor*.

Radar reflectivities for drizzle-free and drizzle cases are calculated assuming the lognormal parameters retrieved for nine layers for three flights. Such reflectivity values should represent the average reflectivity observed by the Wyoming Cloud Radar at a given level in the marine stratus sampled on that day. For drizzle-free cases, the lognormal DSD with parameters given in Tables 2.4, Table 2.6, and Table 2.8, for Aug 09th, 16th and 17th respectively are integrated from 0 μ m to 50 μ m (Eqn 2.6) to obtain the average radar reflectivity for drizzle-free cases. The integration is done in finite differences with a diameter increment of 1 μ m.

For drizzle cases, the radar reflectivity is calculated as the sum of three DSD segments, each of them a truncated lognormal function. The first segment, corresponding to droplets smaller than 50 μ m, uses the lognormal equation derived from FSSP measurements as in the drizzle-free case. The second segment, representing the distribution of drops from 50 μ m to 100 μ m, uses the data of the second lognormal mode. And the third one, forming the drop spectrum at the range from 100 μ m to 600 μ m, is based on the third lognormal equation. The lognormal model parameters corresponding to the three DSD segments for drizzle cases are given in Tables 2.5, Table 2.7, and Table 2.9. Only two lognormal modes are retrieved for some cloud layers, (Table 2.5 and Table 2.7). In that case the second lognormal mode is used to represent DSD for drops from 50 μ m to 600 μ m.

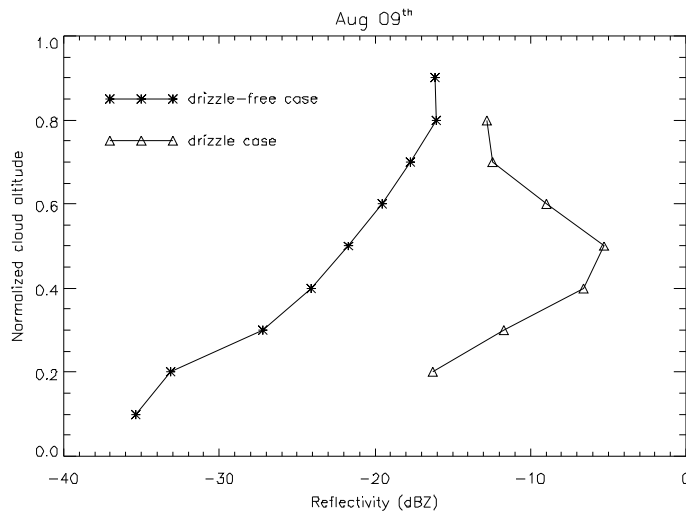


Fig. 2.14 Radar reflectivity profiles calculated from the lognormal DSDs for drizzle-free (stars) and drizzly (triangles) patches of marine stratus for the Aug 09th flight. The lognormal functions, from which the reflectivity profiles are calculated, are shown in Fig 2.6 (drizzle-free cases) and Fig 2.7 (drizzly cases), and the corresponding lognormal parameters are listed in Table 2.4 and Table 2.5, respectively.

Lognormal calculated reflectivities for drizzle-free cases are much smaller than those for drizzle cases, especially in the lower 2/3 of the cloud layer (Fig 2.14). The reflectivity for drizzle-free cases increases with cloud altitude, consistent with the increase of LWC with altitude. But drizzle cases produce a maximum reflectivity at mid-levels, or, more generally, at some level between cloud top and cloud base. The downward increase from the cloud top is due to drizzle, falling and growing by coalescence. The downward decrease below the maximum is due to the dearth of cloud droplets near the cloud base, inhibiting further drizzle growth. Just below the cloud top the reflectivity is partly due to cloud droplets, partly due to embryonic drizzle. Near the cloud base the reflectivity is entirely due to drizzle (see, for instance, Tables 2.9 to 2.11). In the case of Aug 09th the reflectivity in drizzly patches near the cloud base may be underestimated somewhat, due to the short sampling period at this level, and the paucity of drizzle drops.

Since the 1DC probe didn't work very well during CS99, the reflectivity due to droplets measured with the 1DC probe is examined separately (Table 2.10 to Table 2.12). Reflectivity returned only by droplets with diameter from 50 μm to 100 μm (1DC measurements) is compared with reflectivity due to droplets larger than 100 μm in diameter (2DC) in Table 2.10.

Table 2.10 Reflectivity factor contributions from drops measured by 1DC and 2DC for the Aug 09th flight. ($\text{mm}^6 \text{m}^{-3}$)

ϕ	0.9	0.8	0.7	0.6	0.5	0.4	0.3	0.2	0.1
Z-FSSP			0.017	0.015	0.007	0.004	0.002		
Z-1DC			0.017	0.017	0.016	0.017	0.018		
Z-2DC			0.022	0.093	0.275	0.198	0.047		
Z-total			0.056	0.125	0.298	0.219	0.067		

It appears that the impact of the 1DC drop range on the overall calculated reflectivity factor is small compared to the impact of the 2DC drop range, less than $0.02 \text{ mm}^6 \text{m}^{-3}$ for the Aug 09th flight (Table 2.10).

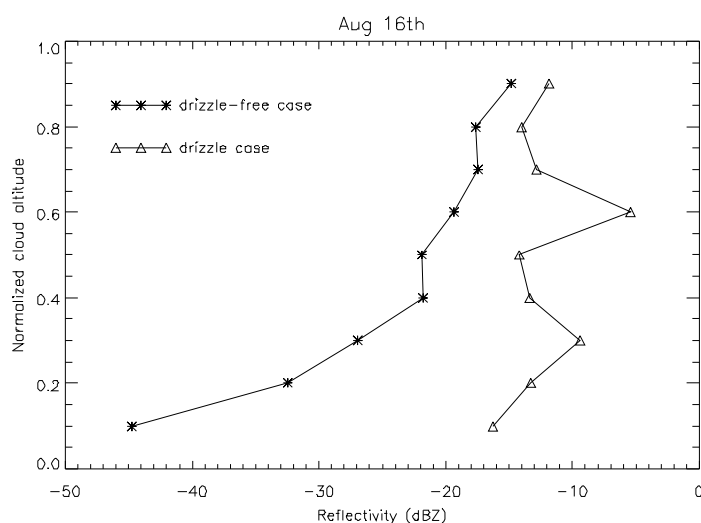


Fig. 2.15 As Fig. 2.14 but for the Aug 16th flight.

The reflectivity profile for drizzle-free cases on the Aug 16th flight again shows a clear dependence on cloud altitude. And the profile for drizzle has several large values in the middle of the cloud; these spikes are entirely due to droplets measured with the 2DC probe. For instance, the lower reflectivity value at $\phi = 0.5$ in Fig 2.15 for the drizzle cases is attributed to a small sample size (Table 2.6).

Table 2.11 As Table 2.10 but for the Aug 16th flight.

ϕ	0.9	0.8	0.7	0.6	0.5	0.4	0.3	0.2	0.1
Z-FSSP	0.032		0.017	0.011	0.006	0.006	0.002	0.002	0.00
Z-1DC	0.016		0.019	0.019	0.019	0.019	0.018	0.023	0.009
Z-2DC	0.016		0.015	0.256	0.012	0.020	0.093	0.022	0.014
Z-total	0.064		0.051	0.286	0.038	0.045	0.113	0.047	0.023

The effects of 1DC measurement on the calculated reflectivity factor for the Aug 16th flight are summarized in Table 2.11. The 1DC measurements are slightly more significant for this flight, as compared to the Aug 9th flight. And the drops measured with the 2DC probe have a smaller impact on the overall reflectivity factor. This means that drops between 50 μ m to 100 μ m are numerous, probably even more numerous than the 1DC measurements suggest.

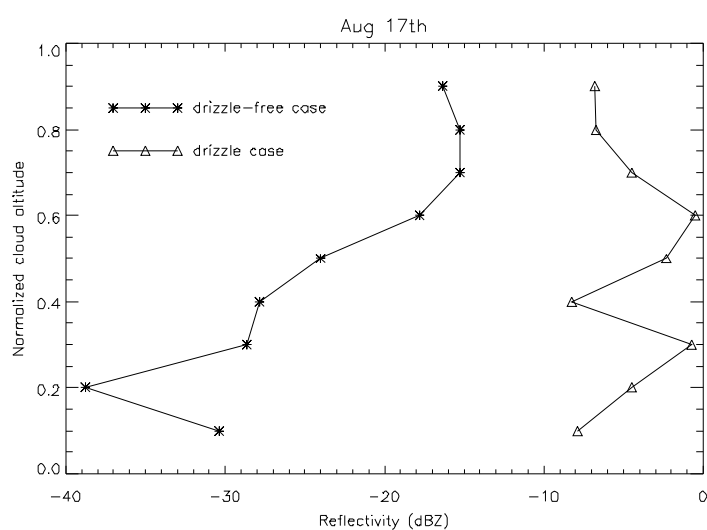


Fig. 2.16 As Fig. 2.14 but for Aug 17th flight

Table 2.12 As Table 2.10 but for the Aug 17th flight.

ϕ	0.9	0.8	0.7	0.6	0.5	0.4	0.3	0.2	0.1
Z-FSSP	0.041	0.033	0.024	0.029	0.018	0.013	0.010	0.004	0.002
Z-1DC	0.014	0.018	0.019	0.019	0.020	0.019	0.019	0.019	0.020
Z-2DC	0.154	0.161	0.303	0.849	0.553	0.118	0.824	0.331	0.141
Z-total	0.209	0.212	0.356	0.897	0.591	0.150	0.853	0.354	0.163

The 2DC measurements indicate higher drizzle abundance on the Aug 17th flight compared to the two other flights. The reflectivity factor is dominated by drizzle (Table 2.12). Because of the presence of large drizzle, cloud droplets have no significant effect on the radar reflectivity factor on Aug 17th.

2.5 Cloud liquid water content calculated from the lognormal DSDs for drizzle-free and drizzly cases

While radar reflectivity is proportional to the sixth moment of droplet diameter, the liquid water content (LWC) (g/m^3) is a function of the third moment. It can be calculated as follows:

$$LWC = \rho_w \frac{4}{3} \pi \int n(r) r^3 dr \quad (2.7)$$

where r (m) is the droplet radius, $n(r)$ is the number density of droplets with radius of r ($\text{m}^{-1}\text{m}^{-3}$), and ρ_w (g/m^3) is the density of water.

The droplet number concentration has a more important effect on LWC than on radar reflectivity. Drizzle drops contribute little to the total cloud LWC, due to their small number density.

The LWC is calculated with the simulated (lognormal) spectra for drizzle-free and drizzle cases in nine layers observed on three flights in CS99. The drizzle-free LWC is calculated with the lognormal spectrum derived from FSSP measurements only (e.g. Table 2.4 for Aug 9th). The LWC in drizzly stratus is calculated with the three truncated lognormal spectra, exactly as was the case for the calculation of reflectivity (Section 2.4): the droplets concentration from 0 μm to 50 μm uses the first mode obtained with FSSP, the segment from 50 μm to 100 μm is based on the mode retrieved from the 1DC probe, and the third segment from 100 μm to 600 μm uses the mode based on 2DC measurements (e.g., Table 2.5 for Aug 9th). Again only one lognormal function is considered in each segment.

Since the lognormal DSD for drizzle-free cases is retrieved from FSSP measurements, the lognormal calculated LWC profile is plotted versus in-situ measured LWC obtained from integrating FSSP data alone (Eq. 2.7). The comparison is shown in Fig 2.17, Fig 2.18 and Fig 2.19.

Table 2.13 Lognormal calculated LWC (g/m^3) for drizzle-free cases (Lc) and drizzly cases (Ld) for the Aug 09th flight.

ϕ	0.9	0.8	0.7	0.6	0.5	0.4	0.3	0.2	0.1
LWC in drizzle-free regions	0.522	0.595	0.4776	0.413	0.332	0.223	0.162	0.073	0.003
LWC in regions with	--	0.533	0.500	0.472	0.374	0.256	0.193	0.084	--

drizzle									
(Ld-Lc)/Lc (100%)	--	-10	5	14	13	15	19	15	--

The difference between LWC corresponding to drizzle-free and drizzle cases is negligibly small for the Aug 9th flight (Table 2.13). At some points, the LWC for the drizzle case is even smaller than the value for the drizzle-free case. This is because the LWC is dominated by cloud droplets and the cloud droplet density for drizzle cases may be smaller than the cloud droplet density for drizzle-free cases.

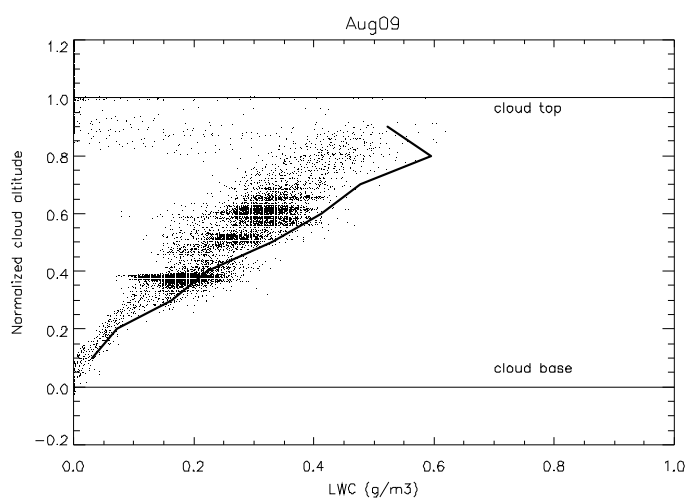


Fig 2.17 The LWC profile for drizzle-free cases for the Aug 09th flight. The solid curve is the LWC calculated from the lognormal function whose parameters are given in Table 2.4. The dots represent the LWC calculated by integrating FSSP measurements at their original sampling frequency (10 Hz).

The lognormal calculated LWC is plotted for Aug 09th flight, for all 9 levels. Good consistency is obtained between calculated LWC with lognormal spectra and that obtained from FSSP (Fig 2.17). The lognormal profile is larger than most of the in-situ measurements. Higher up, the lognormal calculated LWC decreases, due to the variance of the cloud top height.

Table 2.14 As Table 2.13 but for Aug 16th.

ϕ	0.9	0.8	0.7	0.6	0.5	0.4	0.3	0.2	0.1
LWC in drizzle-free regions	0.461	0.292	0.350	0.263	0.203	0.198	0.084	0.043	0.012
LWC in regions with drizzle	0.503	0.360	0.373	0.294	0.235	0.221	0.122	0.099	0.018
(Ld-Lc)/Lc (100%)	9	28	7	12	15	11	44	130	50.

Small differences exist between LWC profiles of drizzle-free and drizzle cases for most layers for Aug 16th flight as well (Table 2.14). A large difference is calculated at an altitude of $\phi = 0.8$ and a much larger difference at $\phi = 0.2$. This can be explained by the difference in total cloud droplet numbers and model radius: 36 cm^{-3} of N and $11.1 \text{ } \mu\text{m}$ of r_o for the drizzle-free cases, and 44 cm^{-3} of N and $11.3 \text{ } \mu\text{m}$ of r_o for the drizzle cases at $\phi = 0.8$; 40 cm^{-3} of N and $5.2 \text{ } \mu\text{m}$ of r_o for the drizzle-free cases, and 42 cm^{-3} of N and $6.0 \text{ } \mu\text{m}$ of r_o for the drizzle cases at $\phi = 0.2$. At low levels drizzly marine stratus holds more liquid water than drizzle-free marine stratus, at least on the 16 Aug flight (Table 2.14). This is due to the small LWC value for drizzle-free cases on this flight.

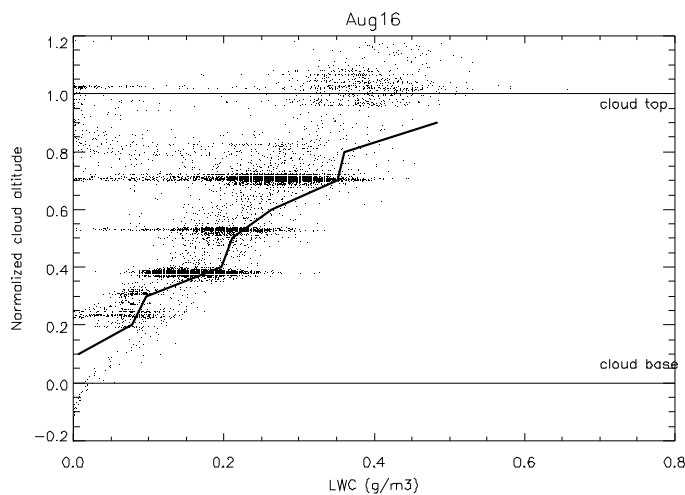


Fig 2.18 As Fig 2.17 but for Aug 16th.

Table 2.15 As Table 2.13 but for the Aug 17th flight.

ϕ	0.9	0.8	0.7	0.6	0.5	0.4	0.3	0.2	0.1
LWC in drizzle-free regions	0.338	0.517	0.578	0.380	0.177	0.111	0.099	0.024	0.019
LWC in regions with drizzle	0.706	0.579	0.613	0.482	0.336	0.303	0.239	0.137	0.082
(Ld-Lc)/Lc (100%)	109	12	6	27	90	173	141	471	332

On the other hand, large differences occur between the lognormal-calculated LWC for drizzle-free and drizzle cases on the Aug 17th flight. This is because the drizzle-free DSD is different from the drizzly DSD at cloud droplet range (Fig 2.7). To examine the contribution of drizzle drops, the LWC values, corresponding to cloud droplets and to drizzle drops, are calculated separately in Table 2.16, which nicely verifies that the drizzle's contribution to the total cloud

LWC is insignificant.

Table 2.16 LWC (g/m^3) formed by cloud droplets (LWC-c) and by drizzle drops (LWC-d) for drizzle case

ϕ	0.9	0.8	0.7	0.6	0.5	0.4	0.3	0.2	0.1
LWC-c	0.705	0.578	0.612	0.481	0.336	0.302	0.238	0.136	0.082
LWC-d	0.0011	0.0006	0.0006	0.0008	0.0007	0.0006	0.0008	0.0007	0.0007

The cloud LWC is primarily due to cloud droplets in marine stratus, even under heavy drizzle.

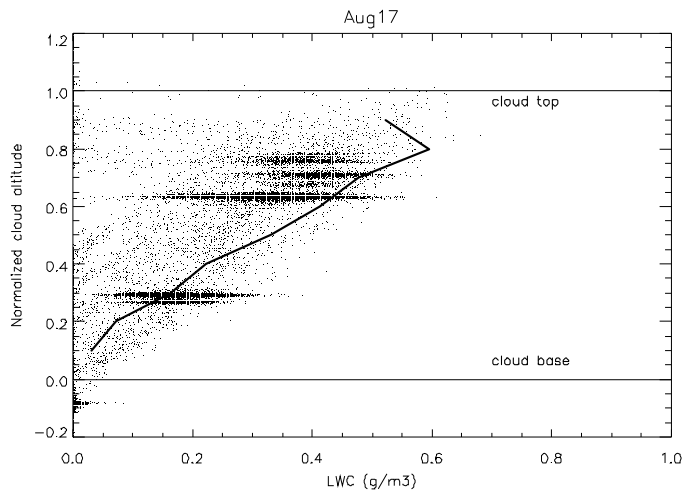


Fig 2.19 As Fig 2.17 but for the Aug 17th flight

Similar to Aug 09th (Fig 2.17) and Aug 16th (Fig 2.18) flights, the LWC profile calculated with a lognormal spectrum of cloud droplets (<50 micron) agrees well with the FSSP-only estimate. At cloud top, the calculated LWC dwindles (Fig 2.19).

To assess the accuracy of the lognormal functions, values of the calculated LWC and in-situ LWC observed by other probes (PVM for flights of Aug 09th and Aug 17th) rather than FSSP are compared for drizzle-free and drizzle cases (Figs 2.20-2.25).

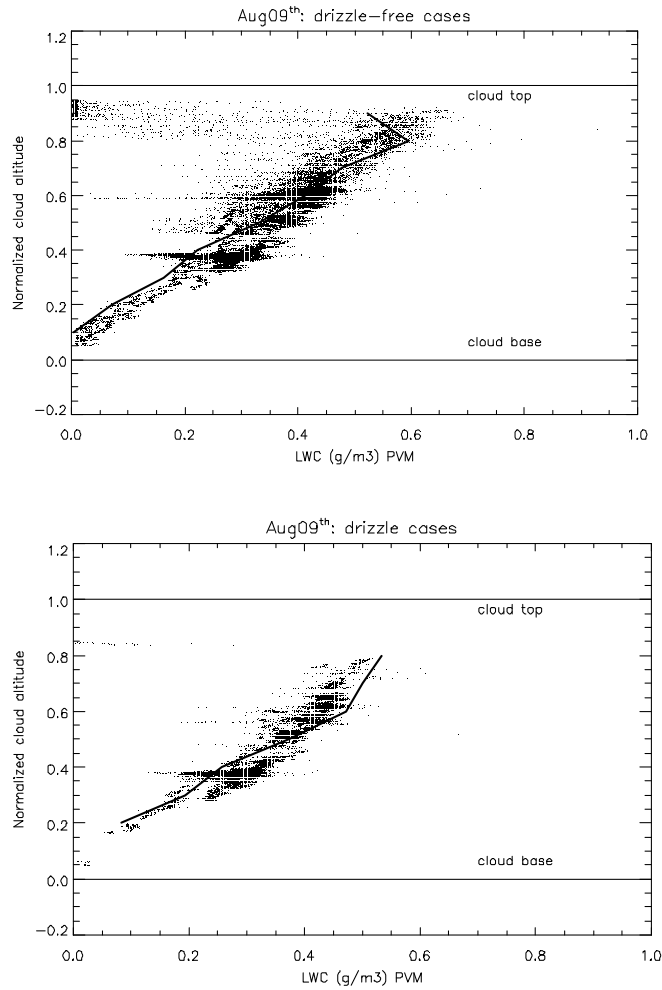


Fig 2.20 Comparison between the LWC calculated from the lognormal function (solid line) and the LWC measured by PVM (dots) for the Aug 09th flight. The upper (lower) plot is for drizzle-free (drizzle) cases. The PVM LWC is plotted at its original sampling frequency (25 Hz).

Identifying Drizzle Within Marine Stratus with W-Band Radar Reflectivity profiles

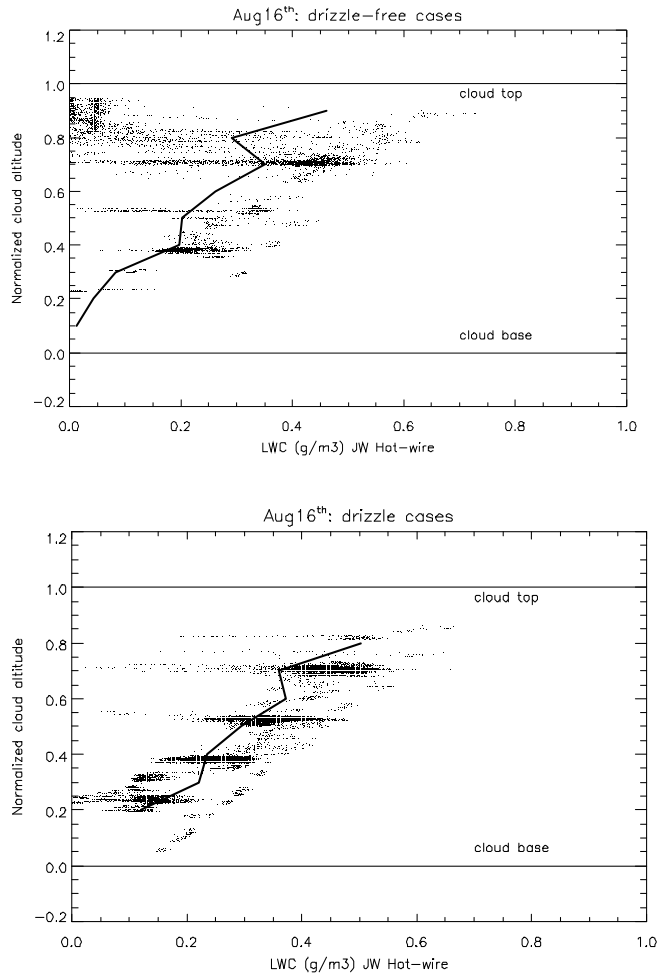
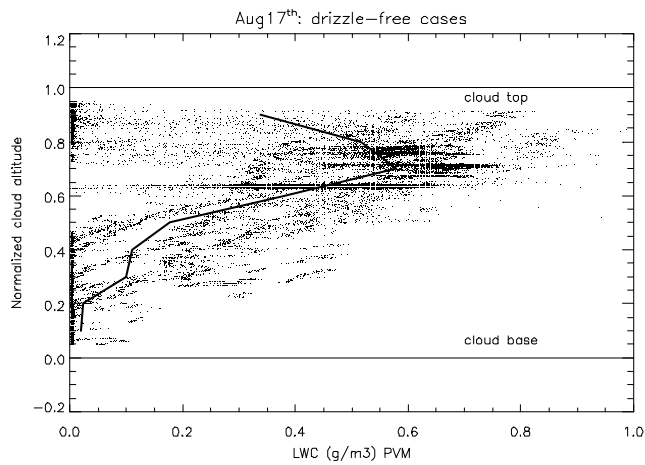


Fig. 2.21 As Fig. 2.20 but for Aug 16th flight. Dots represent in-situ LWC measured with JW hot-wire.



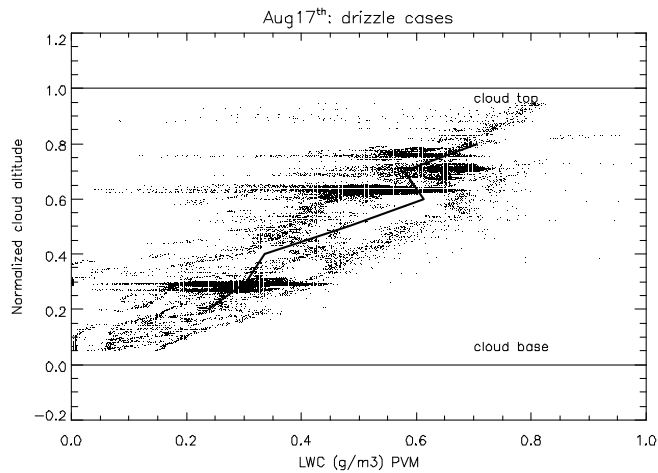


Fig. 2.22 As Fig. 2.20 but for Aug 17th flight.

The LWC calculated from the lognormal model shows good correspondence with the LWC measured with PVM or JW Hot-wire. This confirms the capability of lognormal model to approximate the DSD in marine stratus.

2.6 Discussion

The main purpose of the derivation of a lognormal approximation is to complement in-situ measurements, which do not yield a full DSD because of the short sampling time (1 second or 100 m). Especially the larger, drizzle-size drops are insufficiently sampled, because the 2DC sampling volume is only 0.005 m^3 (Table 1.1). Of course one can increase the sampling period in marine stratus, but then the ability to describe spatial heterogeneity suffers. A mathematical approximation of the DSD can be used to estimate cloud properties such as LWC. It is particularly useful to derive the radar reflectivity, which, in the presence of drizzle in marine stratus, may be dominated by a few drizzle drops. A tri-modal lognormal approximation corresponding to the three in-situ probes (FSSP, 1DC, 2DC) has been contrived for drizzle cases. The first mode describes the cloud DSD, and the last two simulate the drizzle DSD.

Uncertainties exist in the retrieval of the best-matching lognormal model:

All in-situ measurements obtained in the probing period are analyzed to retrieve the model

parameters, yet they represent discrete bin sizes, they typically do not cover the full width of a continuous equation, and not all bins may have non-zero values, especially if the sample volume is small and the droplets are large (i.e. rare). On the other hand, a mathematical approximation such as the lognormal function is continuous, and it can have a broader width than any instantaneous measured spectrum. For instance, the FSSP measures the droplet concentration ranging from $1.5 \mu\text{m}$ to $46.5 \mu\text{m}$, while the lognormal model simulates the DSD from $0.0 \mu\text{m}$ to $50 \mu\text{m}$. However one should be cautious with a mathematical representation that is based on a relatively small number of observations, and one should be especially careful with integrated variables derived from that mathematical representation, such as LWC and especially radar reflectivity. One arbitrary change in droplet numbers in a bin, especially a 2DC bin, can have a dramatic impact on the lognormal function and reflectivity derived from it.

Another uncertainty of the modeled cloud droplet spectrum regards the choice of the total droplet number N . The total droplet number just uses the sum of 15 bin measurements of FSSP. This value includes the number density of droplets from $1.5 \mu\text{m}$ to $46.5 \mu\text{m}$. A lognormal model departs from observations mostly at the tail areas. The concentration of both the smallest and the largest droplets are underestimated by the lognormal spectrum (Fig 2.20). If the model uses the same total droplet number obtained from in-situ measurements, the model will overestimate at the center part but still underestimate at the tail areas. Because the concentration of the smallest droplets is much higher than the concentration of the largest droplets at cloud range, the underestimation mainly occurs at the small droplet end. As a result, the lognormal spectrum based on the total droplet count is slanted towards larger droplets. The radar reflectivity and LWC calculated with a lognormal DSD then may be a little larger compared with corresponding values integrated directly from in-situ measurements (Fig 2.17, Fig 2.18 and Fig. 2.19).

Identifying Drizzle Within Marine Stratus with W-Band Radar Reflectivity profiles

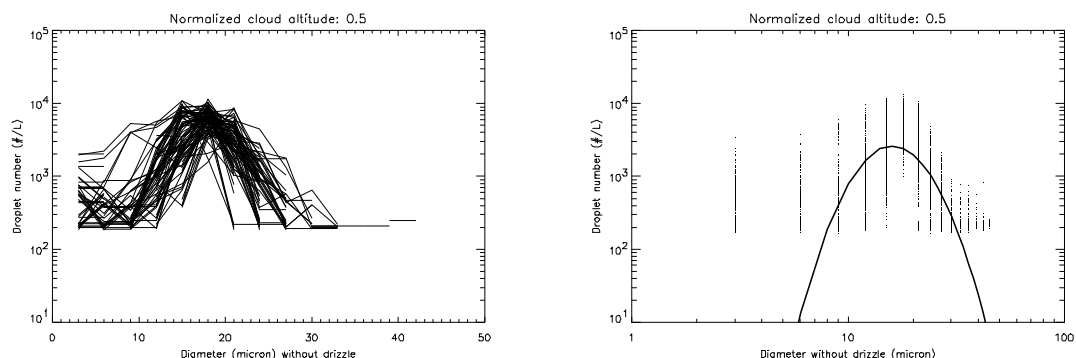


Fig. 2.23 DSDs for drizzle-free cases on Aug 16th at $\phi=0.5$. The left graph represents cloud droplet spectra obtained with FSSP measurements. The right graph is the lognormal DSD (solid curve) that optimally matches all FSSP measurements (dots). The lognormal parameters are given in Table 2.6.

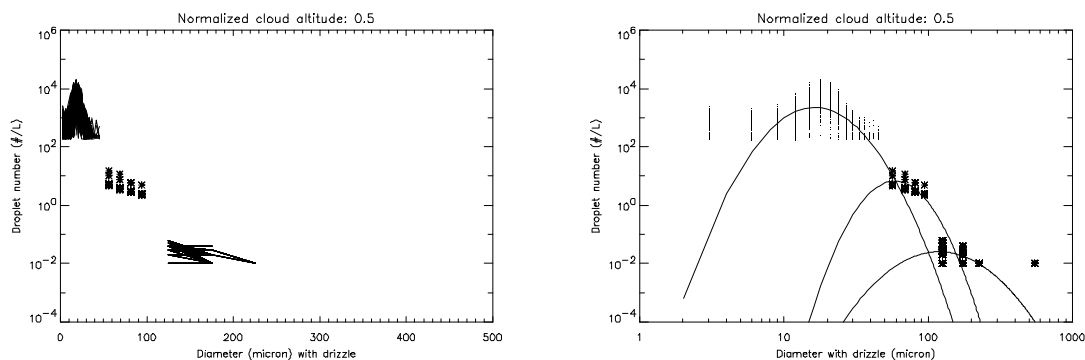


Fig. 2.24 Cloud droplet and drizzle drop distributions on Aug 17th at $\phi=0.5$. The left graph represents droplet spectra derived from the FSSP (left curves), 1DC (stars), and 2DC probes (right curves). The right one shows the lognormal curves (solid curves) that best match the in-situ measurements (dots and stars). The lognormal parameters are given in Table 2.9.

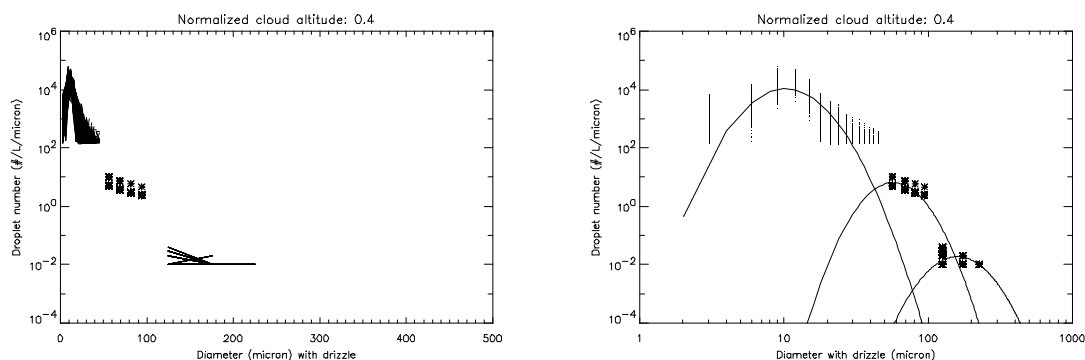


Fig. 2.25 Same as Fig. 2.21 but on Aug 09th. The lognormal parameters are given in Table 2.5.

In most situations, large drizzle is very rare, and the calculated radar reflectivity, based on the lognormal curves, will be larger than that calculated with in-situ measurements directly (Fig. 2.21 and Fig. 2.22). That is because the 2DC probe rarely samples the very few large drizzle drops that do occur, for instance in the much larger radar volume (Table 1.1).

The different dependence of cloud and drizzle DSDs on cloud altitude results in different slopes of radar reflectivity versus cloud altitude for drizzle-free and drizzle cases. In the presence of drizzle, radar reflectivity is rather constant with height, with a slight maximum somewhere between cloud base and top. The reflectivity profiles of drizzle-free marine stratus are rather linear, increasing with height. Since drizzle drops contribute little to the cloud LWC, the underestimation of the concentration of small cloud droplets is the main source of error of the LWC integrated from the lognormal DSD. And since drizzle drops contribute a lot to the radar reflectivity, the uncertainty of drizzle-size drop concentrations is the main source of error of the reflectivity integrated from the lognormal DSD.

Although all those inaccuracies exist in the retrieval of the best-fit lognormal spectra, the lognormal model still is a good tool to diagnose the reflectivity characteristics within marine stratus.

2.7 Conclusions

A lognormal model has been used to simulate the DSD in marine stratus. The lognormal DSDs, derived from cloud probe data, confirm that:

- The vertical profile of the lognormal cloud DSD yields an increase of median diameter and integrated LWC with height in marine stratus. These trends are consistent with observations.
- The cloud lognormal DSD (<50 micron) varies little, irrespective of whether drizzle is present, at least light drizzle (Fig 2.5 and Fig 2.8). But the presence of more numerous, larger cloud droplets, which grow by coalescence, is a prerequisite for heavy drizzle (as on Aug 17th).
- More drizzle drops are observed in the lower parts of marine stratus.
- Drizzle does not contribute significantly to the cloud LWC, even in case of heavy drizzle.

- The LWC calculated with a lognormal DSD corresponds well with that measured by the PVM or JW Hot-wire.
- The radar reflectivity calculated with a lognormal DSD is always larger for drizzle cases than for drizzle-free cases. The reflectivity profile for drizzle-free cases increases linearly with cloud altitude, while the profile for drizzle cases has a maximum value at some level within marine stratus.
- Radar reflectivity profiles based on the lognormal approximations of the drizzle-free and drizzle DSDs are sufficiently distinct to suggest the existence of a height-dependent threshold reflectivity for drizzle.

Chapter 3 **Threshold reflectivity for drizzle**

3.1 Introduction

Much of the improvement of our understanding of cloud and precipitation systems in the last decade or two has resulted from data from radars at wavelengths ranging from 3 mm (W-band or cloud radar) to 30 cm. In-situ measurements, combined with cloud radar reflectivity, extend in-situ probing with the aircraft to the volume sampled by the radar.

The concept of a W-band radar has long been known, but it has been developed specifically for cloud studies only since the mid 1980s (Lhermitte 1987). Hence the identification and explanation of cloud radar echoes in marine stratus are a rather novel activity (Sauvageot and Omar 1987, Sassen and Liao 1996, Fox and Illingworth 1997). Both theoretical and empirical relationships between cloud microphysical parameters and radar reflectivity have been established. The 3 mm radar reflectivity is proportional to the sixth power of droplet size, as long as the cloud particles behave as Rayleigh scatterers. Therefore the reflectivity is very sensitive to large drops. The presence of a few large drops or, in the case of shallow continental stratus, insects, may sharply increase radar reflectivity (Fox and Illingworth 1997). This makes it very difficult to establish a relationship between radar reflectivity and cloud physical parameters such as LWC, effective radius, parameters which depend more on the distribution of small droplets in cloud. Therefore it is not surprising that most effort was focused on the relationships between cloud physical parameters and radar reflectivity for drizzle-free clouds, as will be discussed in Chapter 4.

The radar reflectivity can be used in the first place to determine whether or not stratus clouds contain drizzle-size droplets. Sauvageot and Omar (1987) found that clouds containing drops smaller than $200 \mu\text{m}$ have reflectivity values below -10 dBZ ; and stratus containing drops larger than $200 \mu\text{m}$ have a reflectivity of at least -18 dBZ . A threshold reflectivity of -15 dBZ discriminates well between drizzle-free cases and drizzle cases. This value also was used by Löhnert et al. (2001) to exclude drizzle cases from their study. Fox and Illingworth (1997) also

distinguish clouds with or without drizzle-size drops according to the vertical reflectivity profiles measured by a ground-based cloud radar. They chose those profiles, that have an increasing radar reflectivity with cloud altitude, to represent drizzle-free clouds. The highest reflectivity is encountered closer to the cloud base for drizzle cases (as we also discovered, see Section 2.4). Based on the above discussion, drizzly marine stratus regions may be isolated from drizzle-free regions, using radar reflectivity, or its vertical profile.

Increasing radar reflectivity always corresponds to increasing drizzle probability in CS99 (Fig. 1.1). This figure already hinted at the possibility of the existence of a threshold reflectivity that clearly separates drizzly clouds from drizzle-free clouds. *The main objective of this thesis is to develop and assess a technique to identify drizzle in marine stratus using W-band radar reflectivity.* This work differs from previous work (Sauvageot and Omar 1987, Sassen and Liao 1996, and Fox and Illingworth 1997) in that the dependence of the drizzle threshold reflectivity on altitude in marine stratus is investigated.

The discussion in Chapter 2 suggests distinct reflectivity profiles for drizzle-free (all droplets smaller than $50\mu\text{m}$) and drizzly marine stratus (including both droplets $< 50\mu\text{m}$ and drops $>50\mu\text{m}$) (Figs 2.14-2.16). Indeed, the reflectivity calculated with a lognormal DSD is always larger for drizzle cases than for drizzle-free cases. The difference between the two cases is height-dependent, and becomes smaller towards the top of marine stratus, where cloud droplets are numerous, drizzle becomes rare, and large drizzle is non-existent.

In this Chapter, statistical methods are used to assess the existence and value of a threshold reflectivity for drizzle. A bulk statistical approach is needed because the in-situ measurements are somewhat uncertain over the short sampling period, and because radar measurements are displaced some 90 m to the side of the in-situ measurements (i.e. the aircraft). The uncertainty due to this lateral displacement between radar and in situ data will be assessed separately. Data from the same three CS99 flights, used in Chapter 2 to study marine stratus DSDs, are used for this purpose.

3.2 Statistical methods

Two kinds of statistical methods are performed to assess the existence of a threshold reflectivity discriminating between drizzle cases and drizzle-free cases. To emphasize the

association between in-situ measurement and WCR radar reflectivity, two drizzle threshold estimation data sources are compared: one is based on the equivalent reflectivity calculated with in-situ measurements (Eq. 2.6); the other uses WCR reflectivity. First the statistical techniques are discussed.

3.2.1 Hit rate

A coefficient, the *hit rate*, is calculated to select a threshold reflectivity indicating drizzle presence. In Table 3.1, the *2DC Yes* includes all cases when the 2DC probe detects drizzle drops in the cloud. The *reflectivity Yes* applies when the reflectivity exceeds an assumed threshold reflectivity. This reflectivity can either be that at the WCR second range gate, or the reflectivity calculated from the DSD measured in situ. The values in Table 3.1 are the number of situations satisfying both *2DC Yes/No* and *reflectivity Yes/No*, for example n_{00} counts how many reflectivity measurements are larger than the assumed threshold in the *2DC Yes* group.

Table 3.1 Contingency table of drizzle based on 2DC measurement and on reflectivity.

Drizzle presence	2DC Yes	2DC No	Total
Reflectivity Yes	n_{00}	n_{01}	$n_{0\bullet}$
Reflectivity No	n_{10}	n_{11}	$n_{1\bullet}$
Total	$n_{\bullet 0}$	$n_{\bullet 1}$	n

A series of threshold reflectivity values between -35 and -10 dBZ is assumed. The optimal drizzle threshold reflectivity is the one corresponding to the maximum *hit rate*. The hit rate is defined as:

$$H = \frac{n_{00} + n_{11}}{n} \quad (3.1)$$

3.2.2 Cross point of reflectivity probability distribution

Reflectivity values can be divided into two groups, corresponding to in situ drizzle-free cases and drizzle cases. Since the reflectivity due to cloud droplets is generally less than that due to both cloud droplets and drizzle drops, the two groups of reflectivities are expected to form distinct probability density functions (pdfs). The reflectivity corresponding to the cross point of the two pdfs is then chosen to be the drizzle threshold reflectivity. Again this method can be

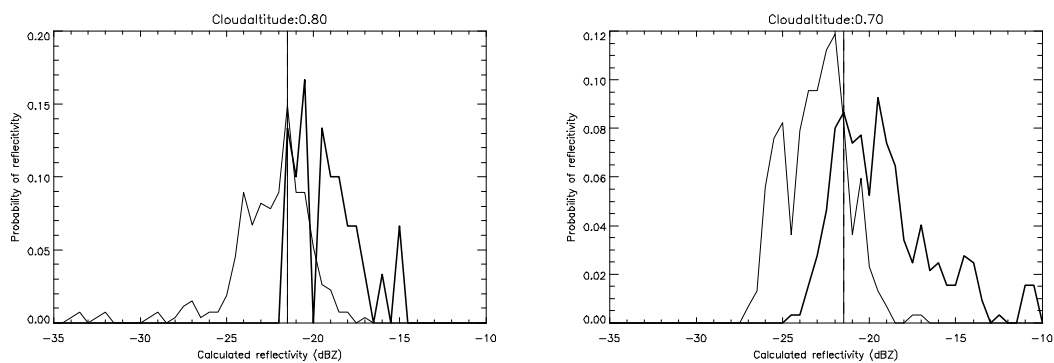
applied both to the WCR-measured reflectivity, to the side of the aircraft, and the reflectivity calculated from in situ DSDs.

3.3 Threshold reflectivity for drizzle based on in-situ measurements

In this section, we focus on in situ measurements, and use the two statistical methods introduced in Section 3.2 to determine a drizzle threshold reflectivity.

In this study, we define drizzle events as a series of at least two seconds (200 m) with drizzle-size drops, as measured by the 2DC probe. The reason, to be expanded on in section 3.4, is that we want to focus on the larger drizzle patches, where the sideways WCR reflectivity is more likely to sample the same drizzle patch. Drizzle-free events are those series of at least two seconds, with non-zero FSSP data and zero 1DC and 2DC data. Radar reflectivities for the two different events are calculated directly based on the observed composite DSDs, using the FSSP, 1DC and 2DC probes.

3.3.1 Calculated threshold reflectivity for the Aug 09th flight



Identifying Drizzle Within Marine Stratus with W-Band Radar Reflectivity profiles

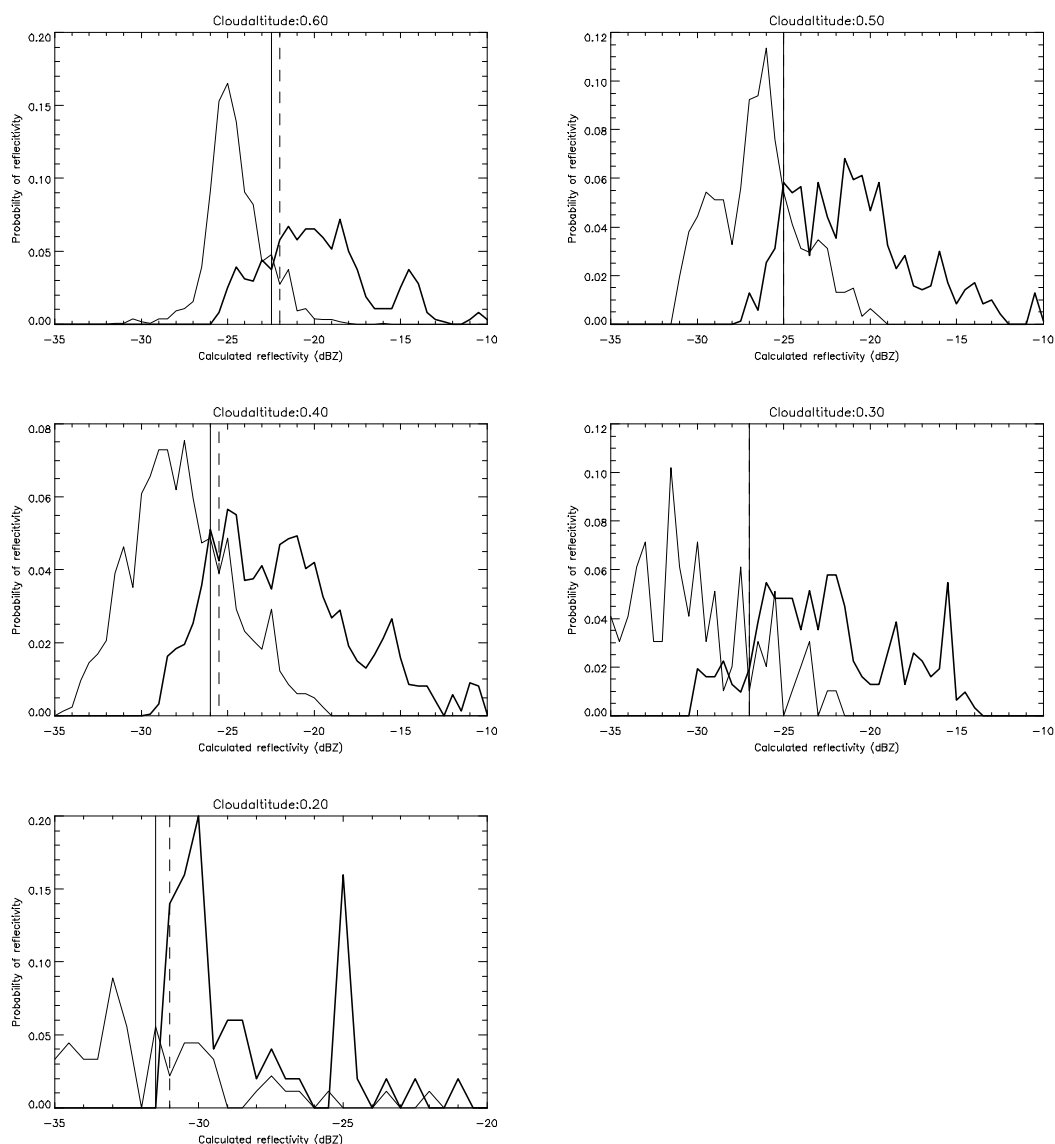
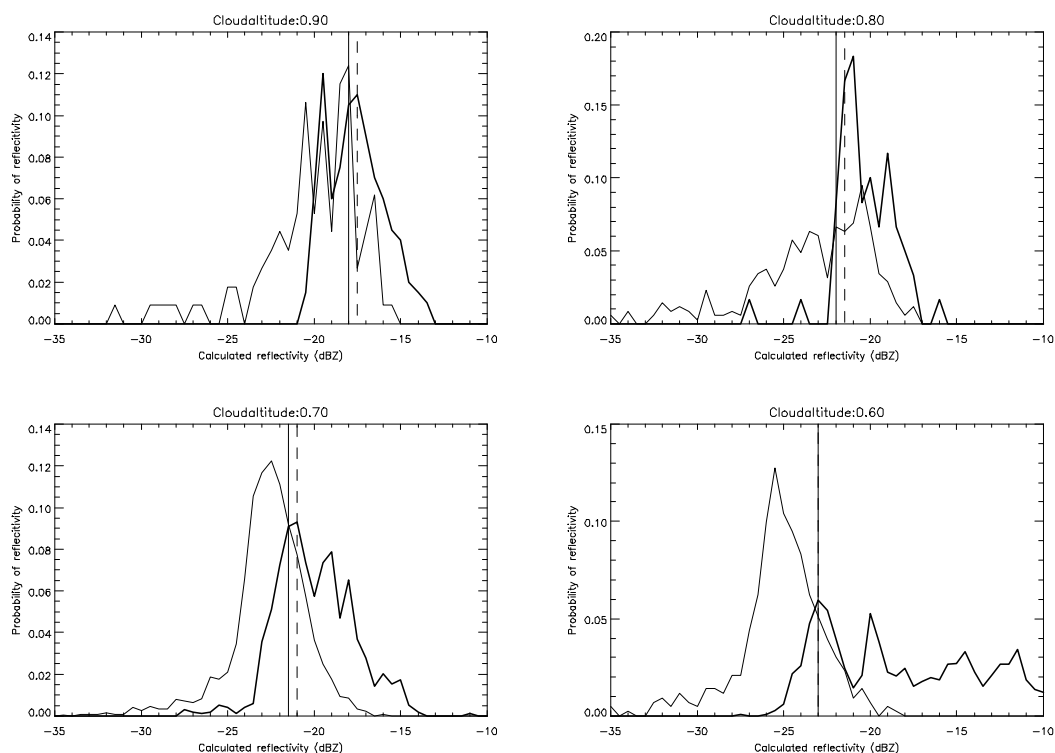


Fig 3.1 Application of the crossover (Section 3.2.2) and hit rate (Section 3.2.1) methods for reflectivity values calculated from FSSP, 1DC and 2DC data. Shown are reflectivity probability distributions for drizzle-free (thin curve) and drizzly (bold curve) events at various cloud altitudes for the Aug 09th flight. The solid vertical lines show the cross value of the two probability curves. The dashed straight line is the threshold reflectivity determined by the hit rate method. Only one solid straight line is displayed when both methods yield the same threshold reflectivity in that layer.

Table 3.2 Calculated threshold reflectivity for drizzle for the Aug 09th flight. Units of meters are adopted to mark the sample size, which is determined as the product of the number of instantaneous events in each data group, times the duration of an event, times the aircraft speed. Thus the sample size represents the cumulative distance of drizzle-free and drizzly patches.

ϕ	Sample size (m)		Threshold Z with hit rate (dB)	Threshold Z with pdf crossover method (dB)	Difference (dB)	Mean value (dB)
	Drizzle-free	Drizzle				
0.9						
0.8	300	2680	-21.5	-21.5	0.0	-21.5
0.7	3260	3030	-21.5	-21.5	0.0	-21.5
0.6	6680	12820	-22.0	-22.0	0.0	-22.0
0.5	7150	6070	-25.0	-25.0	0.0	-25.0
0.4	25630	8220	-25.5	-25.5	0.0	-25.5
0.3	3110	980	-27.0	-27.0	0.0	-27.0
0.2	500	900	-31.0	-31.5	0.5	-31.25
0.1						

3.3.2 Calculated threshold reflectivity for the Aug 16th flight



Identifying Drizzle Within Marine Stratus with W-Band Radar Reflectivity profiles

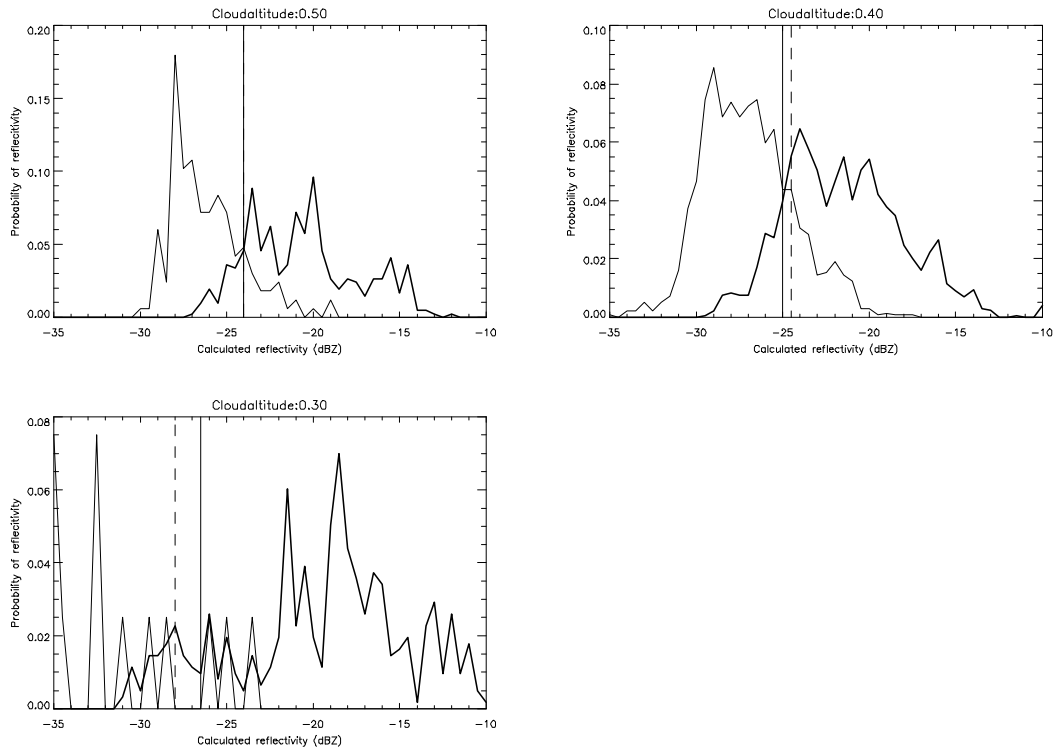


Fig 3.2 As Fig 3.1 but for the Aug 16th flight.

Table 3.3 As Table 3.2 but for the Aug 16th flight

ϕ	Sample size (m)		Threshold Z with hit rate (dB)	Threshold Z with pdf crossover method (dB)	Difference (dB)	Mean value (dB)
	Drizzle-free	Drizzle				
0.9	2000	1130	-17.5	-18.0	0.5	-17.75
0.8	600	3470	-21.5	-22.0	0.5	-21.75
0.7	9780	33670	-21.0	-21.5	0.5	-21.25
0.6	15160	4320	-23.0	-23.0	0.0	-23.0
0.5	4170	1670	-24.0	-24.0	0.0	-24.0
0.4	24410	13690	-24.5	-25.0	0.5	-24.75
0.3	6150	400	-27.0	-27.0	0.0	-27.0
0.2						
0.1						

3.3.3 Calculated threshold reflectivity for the Aug 17th flight

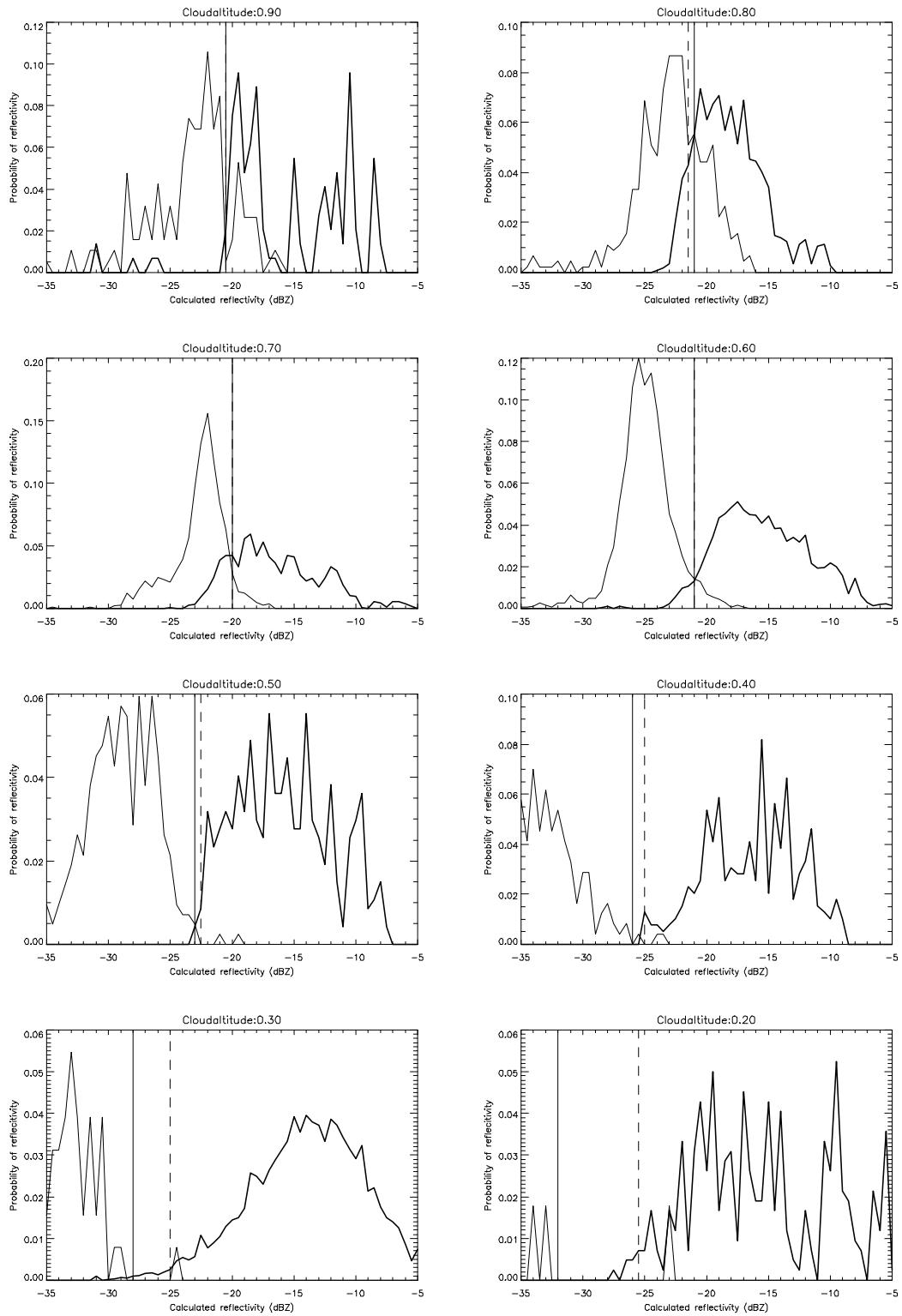


Fig 3.3 As Fig 3.1 but for the Aug 17th flight.

Table 3.4 As Table 3.2 but for the Aug 17th flight.

ϕ	Sample size (m)		Threshold Z with hit rate (dB)	Threshold Z with pdf crossover method (dB)	Difference (dB)	Mean value (dB)
	Drizzle-free	Drizzle				
0.9	1460	1890	-20.5	-20.5	0.0	-20.5
0.8	11450	4510	-21.5	-21.0	0.5	-21.25
0.7	17950	10450	-20.0	-20.0	0.0	-20.0
0.6	65730	20260	-21.0	-21.0	0.0	-21.0
0.5	4700	4200	-22.5	-23.0	0.5	-22.75
0.4	3910	2430	-25.0	-26.0	1.0	-25.5
0.3	98060	1280	-27.0	-27.0	0.0	-27.0
0.2	4200	560	-31.0	-31.0	0.0	-31.0
0.1						

3.3.4 Drizzle reflectivity threshold based on in situ data

Two statistical methods, the hit rate method and the pdf cross-over method, are applied to reflectivity values derived from in situ probes to find a drizzle threshold reflectivity (Figs 3.1-3.3). The two methods yield similar results, with differences of 1dBZ at most (Tables 3.2-3.4). This coincidence confirms the validity of defining a reflectivity threshold for drizzle, and the dependence of this threshold on altitude within marine stratus.

For all three flights the drizzle threshold reflectivity values increase with cloud altitude (Fig 3.4). A distinct gap exists between the reflectivity pdf of drizzle-free events and that of drizzly events at lower levels, especially on Aug 16th and Aug 17th. Therefore it is straightforward to select a drizzle reflectivity threshold in the lower half. But at the upper part of the marine stratus, the pdfs are less separated and the threshold slopes become smaller. This phenomenon can be explained with the lognormal DSD, derived from all in situ measurements in various height bins (Chapter 2). The lognormal-calculated reflectivity for drizzly marine stratus increases with height in the cloud with a much slower rate than that for drizzle-free stratus, and up to some level between cloud base and cloud top, where a maximum reflectivity occurs. The drizzle-free marine stratus has lognormal-calculated reflectivities that increase monotonically with height, approaching reflectivity values typical of drizzly marine stratus near the cloud top (Chapter 2).

In summary, the reflectivity pdfs for drizzle and drizzle-free cases merge near the cloud top, and the drizzle threshold reflectivity is most crisply defined, and least variable from day to day, in the lower half of marine stratus.

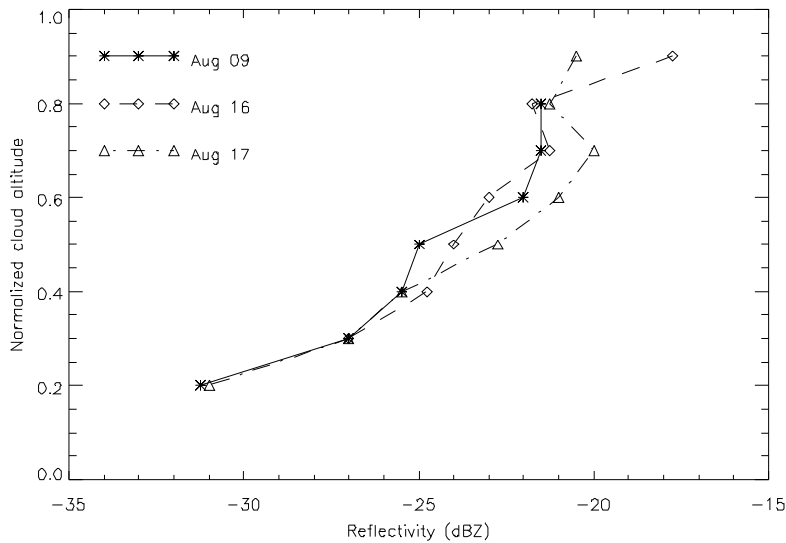


Fig 3.4 Threshold reflectivity profile for drizzle based on calculated reflectivity with in-situ measurements.

3.4 Spatial correlation analysis

In order to assess the two statistical methods discussed in Section 3.2 to discriminate drizzle presence in marine stratus based on WCR measurements, we must first evaluate how representative the laterally-displaced WCR data are for in situ measurements, which are used to define drizzle and drizzle-free cases. The reflectivity at the first reliable gate of the side-looking WCR beam is analyzed. The first gate is 60 meters away from the aircraft but the reflectivity is corrupted by transmitter noise. Therefore we use second-gate measurements. The WCR reflectivity will hereafter refer to the second radar gate only. A distance of 90 m between aircraft and the second gate exists in measurements for the Aug 09th flight. And this distance is 75 m for the Aug 16th and Aug 17th flights.

The advantage of WCR reflectivity data is that they represent a sample volume that is orders of magnitude larger than the in situ probes (Table 1.1). But the drawback is that this reflectivity is displaced by 75-90 m to the side of the DSD sampling probes, which are used to identify drizzle presence. The distance of 90/75 m between in-situ measurements and radar second gate data is a main source of uncertainty in the relationship between WCR reflectivity and in situ

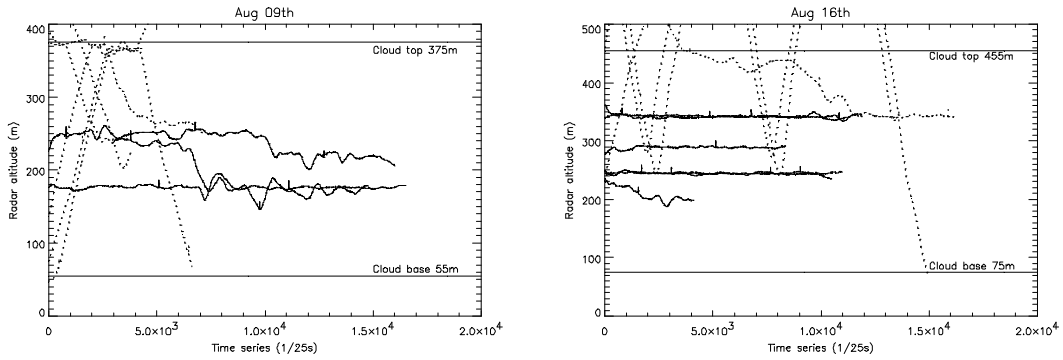
measurements. To evaluate how much uncertainty is introduced by this displacement, we start with a spatial correlation analysis of marine stratus properties.

Through the application of Taylor's hypothesis, the autocorrelation coefficient $Cor(L)$, calculated with a time series of a variable along any level flight leg, can be used to examine the scales of horizontal variability of that variable:

$$Cor(L) = Cor(-L) = \frac{\sum_{k=0}^{N-L-1} (x_k - \bar{x})(x_{k+L} - \bar{x})}{\sum_{k=0}^{N-1} (x_k - \bar{x})^2} \quad (3.2)$$

where N is the sample size, L is the time or space lag, and \bar{x} is the mean of the sample population $x = (x_0, x_1, \dots, x_{N-1})$. The time lag can be converted to a spatial separation.

To examine the *horizontal* coherence of echo structures, only flight legs without a sharp altitude variance are analyzed (Fig 3.5). The variable we use is the second-gate WCR reflectivity. We can of course use all WCR gates and examine spatial coherence along the radar range, sideways from the aircraft, but the echo would have to be corrected for attenuation first, which adds further uncertainty.



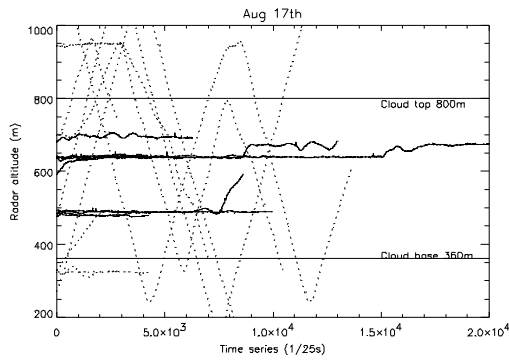


Fig 3.5 Flight traces for which autocorrelation coefficient is calculated for the three flights. Solid lines represent those flight traces where the spatial correlation analysis is applied. Dotted lines are other flight legs, which are omitted because of non-steady flight altitude.

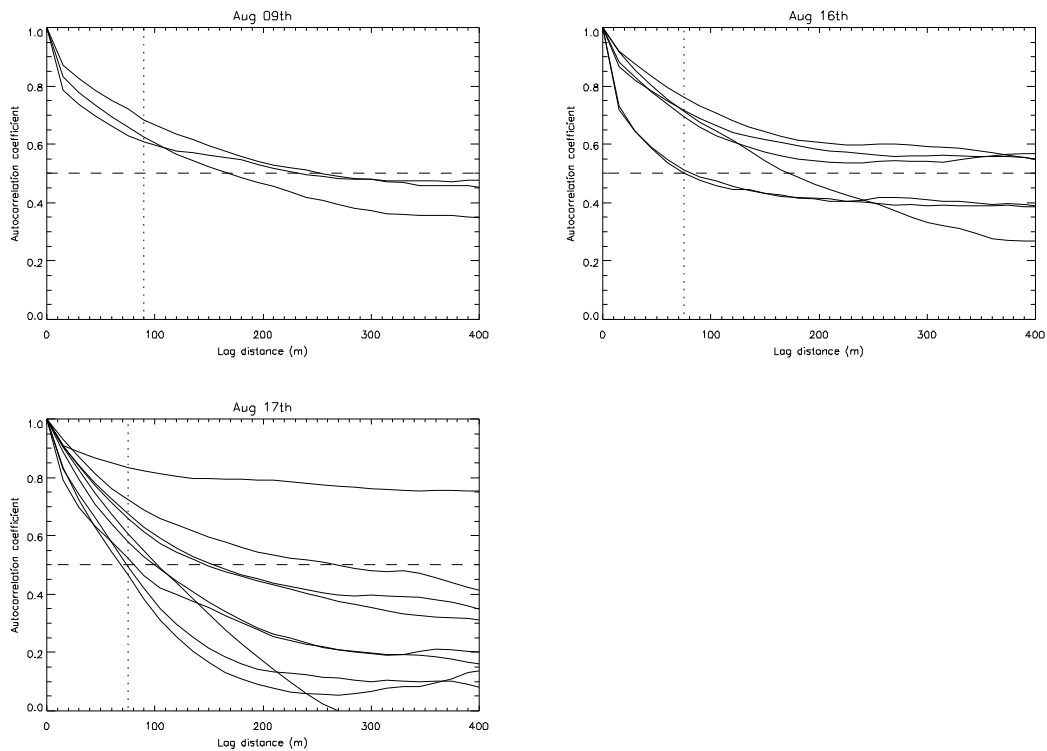


Fig 3.6 Autocorrelation coefficients calculated for WCR second gate reflectivities for the three flights. The solid lines are the autocorrelation coefficients as a function of distance along the flight track, assuming an aircraft speed of 100 m/s, for several straight and level flight legs. The horizontal dashed line represents 0.5 value of autocorrelation coefficient. The vertical dotted line indicates the distance between in-situ measurements and the radar second gate for each flight (90 m for Aug 09th, 75 m for Aug 16th and Aug 17th).

The autocorrelation coefficient of 2nd gate radar reflectivity decreases with the increasing distance (Fig 3.6). An autocorrelation value of 0.5 can be considered to define the maximum size of coherent features. The bad news is that Fig 3.6 suggests that both drizzle patches and echo-void areas are rather small in marine stratus, about 70 m to a few 100 m in diameter. The good news is that nearly all autocorrelation coefficients are larger than 0.5 at the distance between the aircraft and the radar second gate (dotted lines in Fig 3.6) for each flight. The spatial correlations between in-situ measurements and WCR second gate echoes therefore are expected to be reasonable, but not excellent. The 75-90 m displacement will certainly introduce some uncertainty.

3.5 Threshold reflectivity for drizzle based on WCR measurements

As mentioned above (Section 3.3), only events with more than two successive seconds of non-zero 2DC measurements are included for drizzle cases. Similarly, if there are at least two successive seconds with both zero 1DC and zero 2DC measurements, but non-zero FSSP measurements, a cloudy region with a diameter larger than 200m is considered to have no drizzle. That is, only ‘drizzle patches’ with an along-track diameter no smaller than 200m are considered, in order to reduce the error in the relationship between WCR reflectivity and in situ cloud probes, due to the relatively small size of drizzle and drizzle-free patches (Section 3.4). Under this circumstance, both the 2DC measurements and the radar second gate samples have a good chance to represent the same drizzle patch. For WCR second gate measurements, a reflectivity smaller than -36dBZ is considered to be noise. All noise values in the merged in situ/WCR time series are excluded as well.

The two series of WCR reflectivities, ‘with drizzle’ and ‘drizzle-free’, are studied at different cloud altitudes. We now try to find a threshold WCR reflectivity to discriminate drizzle-free from drizzly marine stratus. To do this, we use the two statistical methods discussed in Section 3.2. Drizzle threshold reflectivity values are estimated at nine layers at normalized cloud altitude ranging from 0.05 to 0.95. Since most side-looking radar beams are not precisely horizontal, an altitude correction of WCR reflectivity is done (Chapter 1.4). Some points of WCR reflectivity then may belong to a different cloud layer than that determined by the aircraft altitude.

3.5.1 WCR threshold reflectivity for drizzle for the Aug 09th flight

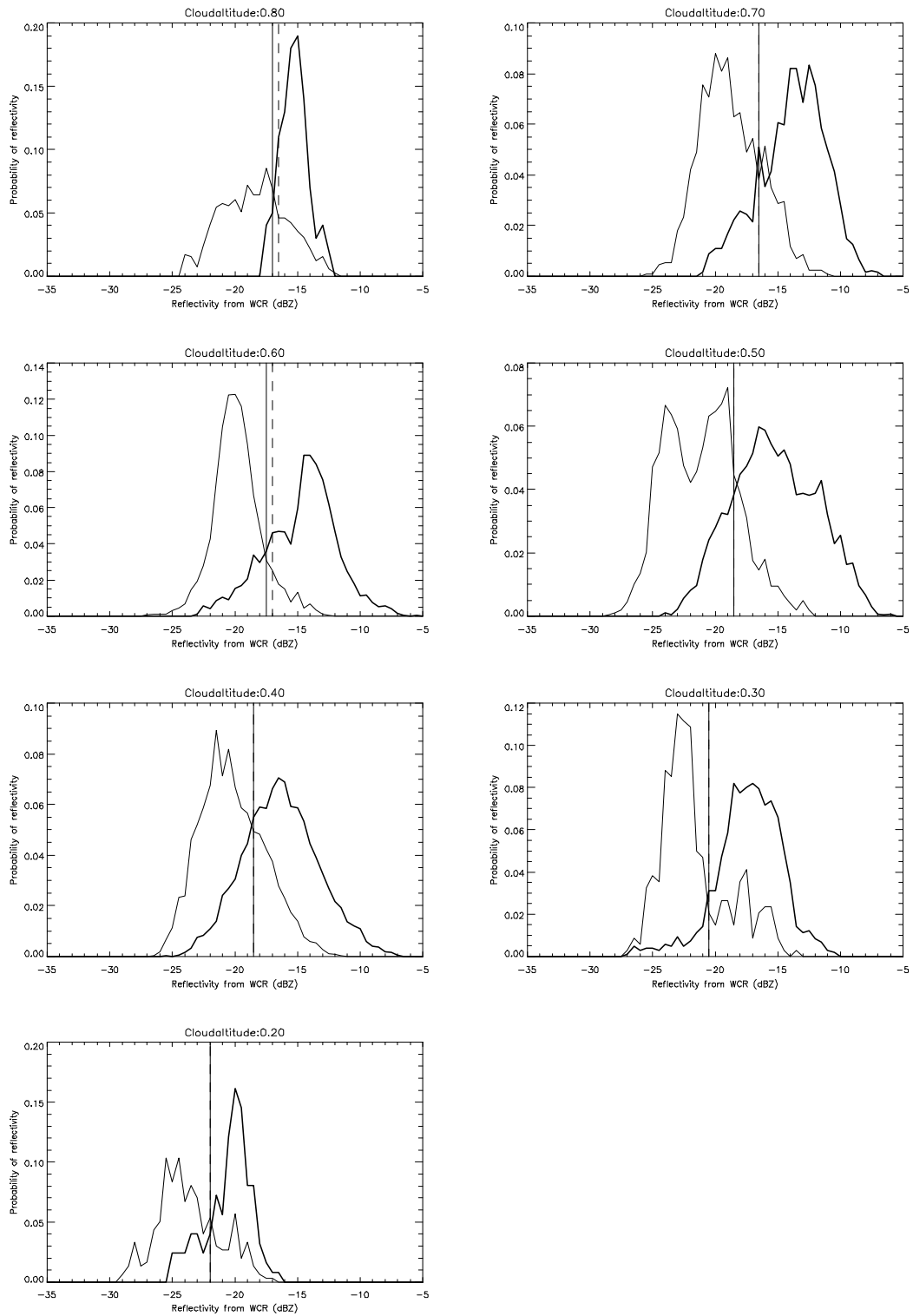
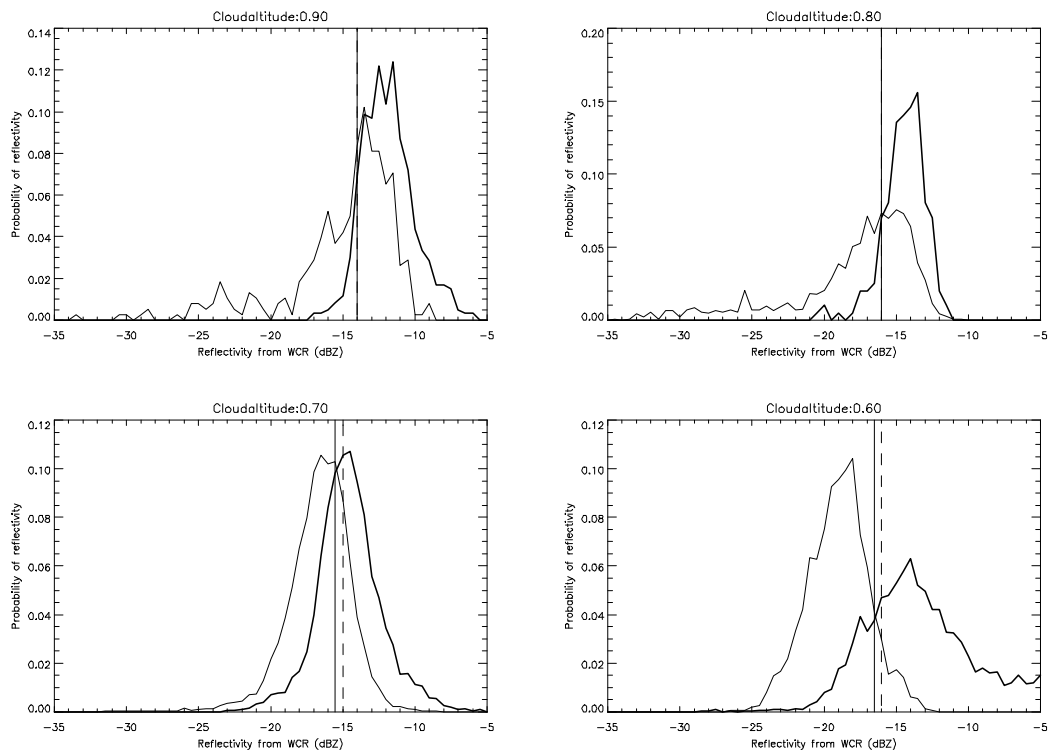


Fig 3.7 As Fig 3.1 but based on WCR 2nd gate measurements for the Aug 09th flight.

Table 3.5 Threshold reflectivity based on WCR measurements for the Aug 09th flight.

ϕ	Sample size (m)		Threshold Z with hit rate (dB)	Threshold Z with pdf crossover method (dB)	difference	mean
	Drizzle-free	Drizzle				
0.9						
0.8	300	2466	-17.0	-16.5	0.5	-16.75
0.7	4062	3855	-16.5	-16.5	0.0	-16.5
0.6	5676	11859	-17.5	-17.0	0.5	-17.25
0.5	8109	5979	-18.5	-18.5	0.0	-18.5
0.4	24867	8208	-18.5	-18.5	0.0	-18.5
0.3	3177	1020	-20.5	-20.5	0.0	-20.5
0.2	372	897	-22.0	-22.0	0.0	-22.0
0.1						

3.5.2 Threshold WCR reflectivity for drizzle for the Aug 16th flight



Identifying Drizzle Within Marine Stratus with W-Band Radar Reflectivity profiles

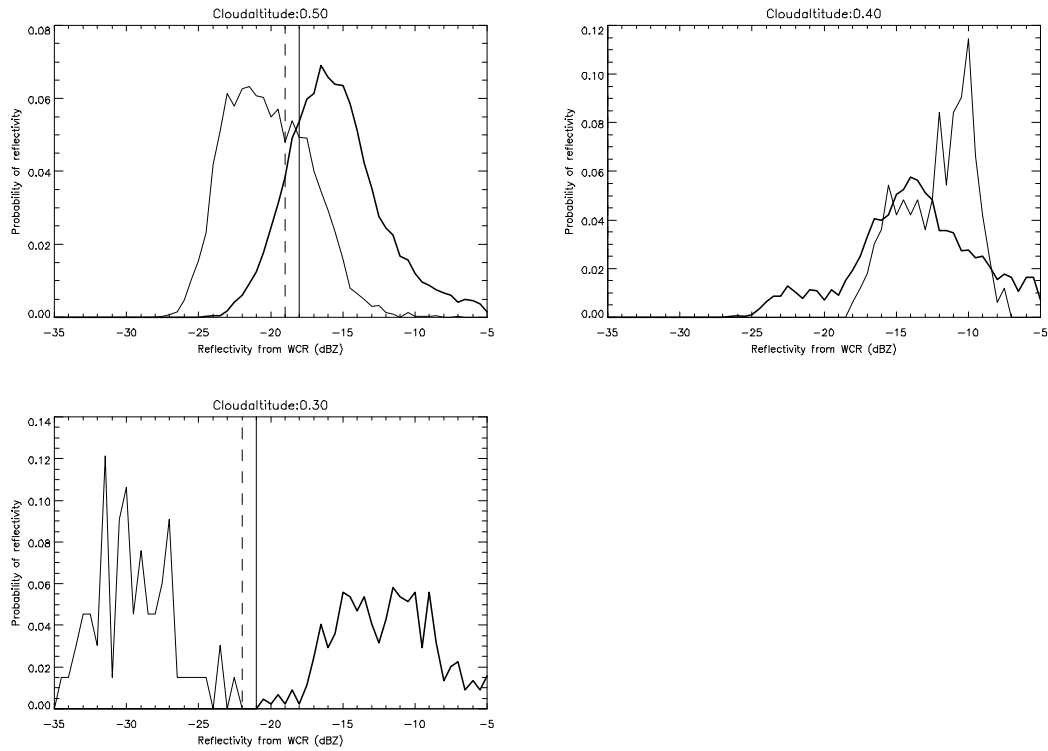


Fig 3.8 As Fig 3.1 but based on WCR 2nd gate measurements for the Aug 16th flight.

Table 3.6 As Table 3.5 but for the Aug 16th flight.

ϕ	Sample size (m)		Threshold Z with hit rate (dB)	Threshold Z with pdf crossover method (dB)	difference	mean
	Drizzle-free	Drizzle				
0.9	1794	1146	-14.0	-14.0	0.0	-14.0
0.8	597	4293	-16.0	-16.0	0.0	-16.0
0.7	9783	32928	-15.5	-15.0	0.5	-15.25
0.6	17031	4494	-16.5	-16.0	0.5	-16.25
0.5	23346	14814	-18.0	-19.0	1.0	-18.5
0.4						
0.3	1338	198	-21.0	-21.0	0.0	-21.0
0.2						
0.1						

3.5.3 Threshold WCR reflectivity for drizzle for the Aug 17th flight

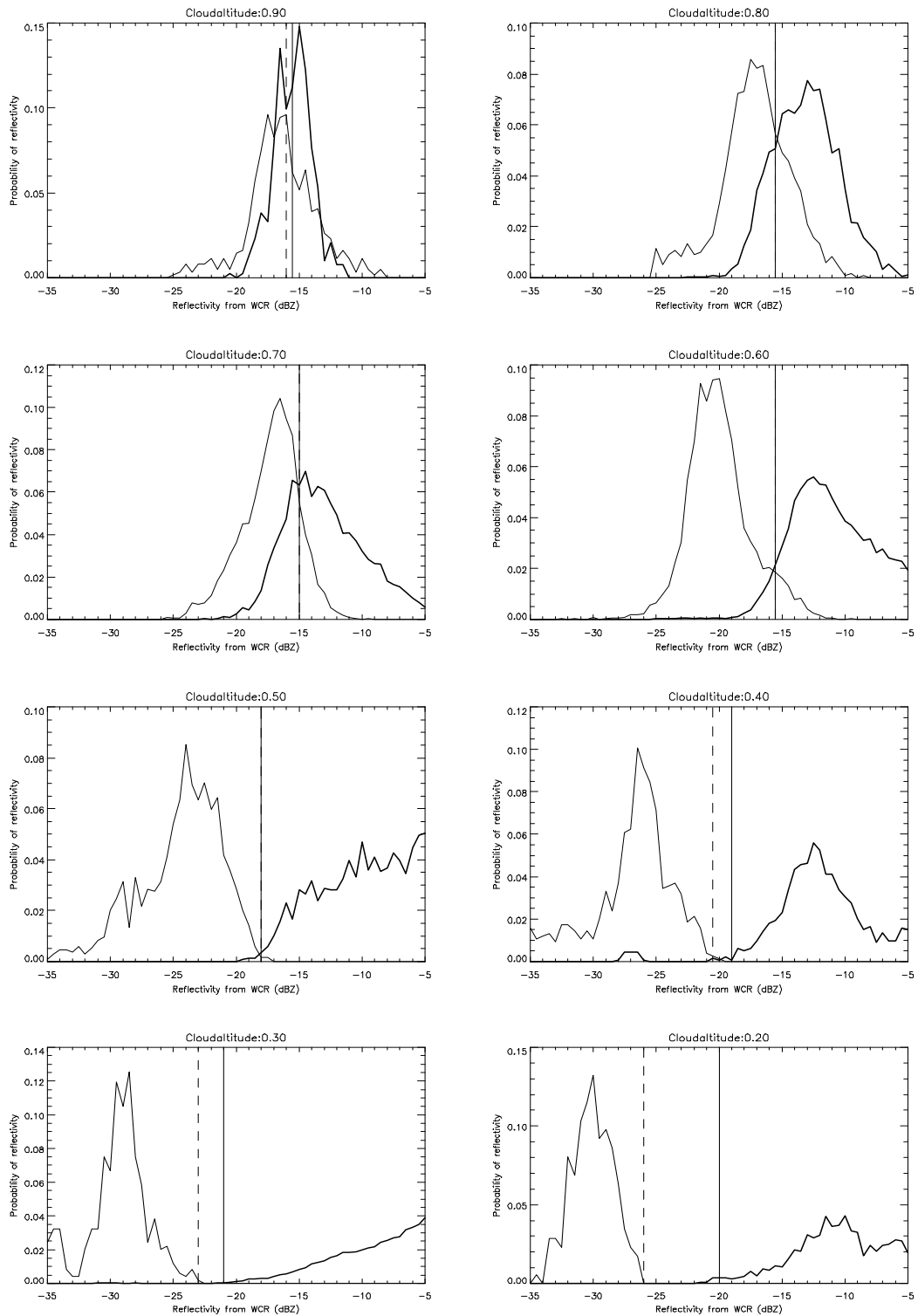


Fig 3.9 As Fig 3.1 but based on WCR 2nd gate measurements for the Aug 17th flight.

Table 3.7 As Table 3.5 but for the Aug 17th flight.

ϕ	Sample size (m)		Threshold Z with hit rate (dB)	Threshold Z with pdf crossover method (dB)	difference	mean
	Drizzle-free	Drizzle				
0.9	1176	1845	-16.0	-15.5	0.5	-15.75
0.8	10041	3603	-15.0	-15.0	0.0	-15.0
0.7	20025	10824	-15.0	-15.0	0.0	-15.0
0.6	65493	20166	-15.5	-15.5	0.0	-15.5
0.5	4164	4017	-18.0	-18.0	0.0	-18.0
0.4	4008	2265	-19.5	-19.5	0.0	-19.5
0.3	98130	1482	-21.0	-21.0	0.0	-21.0
0.2	4239	522	-22.0	-22.0	0.0	-22.0
0.1						

3.5.4 Discussion

In this section two statistical methods have been applied to WCR second gate measurements to obtain a threshold reflectivity for drizzle. The drizzle-free and drizzly pdfs of WCR reflectivity each have a distinct and well-separated peak. The separation is best for the flight encountering most large drizzle drops, Aug 17 (Fig 3.9) and worst for the flight with least or small drizzle drops, Aug 16 (Fig 3.8). The most likely reflectivity for drizzle-free cases always is smaller than that for drizzle cases. Again, as was observed with calculated reflectivity characteristics (Section 3.3), a larger separation between the two distribution peaks is present at the lower part of the cloud. The drizzle threshold reflectivity based on the hit rate is again within 1 dB to that based on the cross-over point between the two pdfs (Tables 3.5, 3.6, 3.7). This threshold increases with cloud altitude on all flights (Fig 3.10), as was the case for the calculated reflectivity (Fig 3.4). Fig 3.10 lends support to the existence of an unambiguous reflectivity threshold for drizzle, especially in the lower half of marine stratus.

For the Aug 16th flight, the two pdfs for the drizzle-free and drizzly series at the upper part of cloud (Fig 3.8) are not as separate as for the other two flights. This implies more uncertainty, possibly because the patches were smaller, or because, as discussed in Chapter 2, many drizzle droplets with diameter between 50 μ m to 100 μ m remained unsampled by the 1DC probe. These cases, probably with high WCR reflectivity values, were included in the drizzle-free data series on Aug 16th. The undersampling of these droplets, due to the poor performance of the 1DC probe, introduces large errors into the drizzle threshold reflectivity estimation. But even on Aug 16 the two pdfs are separated more clearly at lower levels, except for the cloud altitude of $\phi = 0.4$, where a threshold value cannot be determined because (Table 3.6) the drizzle-free pdf

has a wider distribution than the drizzle pdf. Although the IDC data quality was more questionable on Aug 16th, and the patches were relatively small on some flight legs (Fig 3.6), a positive trend of drizzle threshold with cloud altitude reveals itself (Fig 3.10), as on the two other flights.

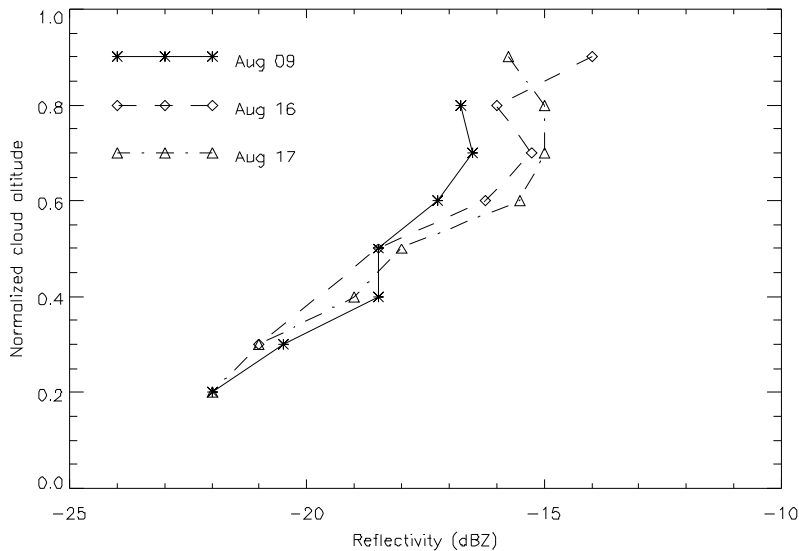


Fig 3.10 Threshold reflectivity for drizzle applied to WCR measurements.

In summary, similar threshold profiles are obtained using WCR reflectivity, for all three flights (Fig 3.10). The drizzle threshold reflectivity slope with cloud altitude is similar to that based on calculated reflectivity (Fig 3.4). The threshold is again most crisp in the lower half of the marine stratus, where the day-to-day variability is smallest.

3.6 Relation between calculated reflectivity and WCR reflectivity

Although the threshold reflectivity based on in-situ calculated reflectivities is much smaller than the threshold based on WCR measurements (Fig 3.11), the two profiles show a similar variation with cloud altitude.

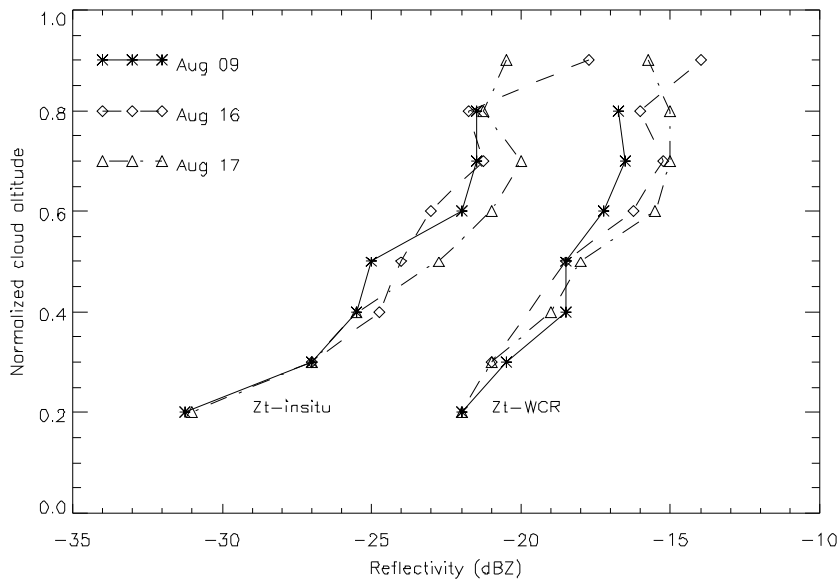


Fig 3.11 Threshold reflectivity profiles based on in-situ calculated reflectivities (left) and the profiles based on WCR measurements (right).

This phenomenon not only proves the existence of a threshold for drizzle, but also confirms that this threshold can be applied to WCR measurements. The question remains: which profile slope is better, the one based on WCR data, or the one based on in situ cloud probe data. Because of the distance between the aircraft and the radar second gate, an irrepresentative WCR reflectivity may be chosen for drizzle-free and drizzle cases. This kind of uncertainty doesn't exist in the selection of a threshold reflectivity based on reflectivities derived from in-situ measurements. Therefore we assume that the latter slope is correct. However the small sampling size, the poor performance of the 1DC probe, and the failure to include certain DSD bands (Chapter 2), all contrive to explain why the reflectivity derived from the observed DSD generally underestimates the true value.

Therefore we propose a best-guess threshold profile, which equals the average of the WCR threshold profile (Fig 3.10) and the one derived from in situ measurements (Fig 3.4) but the latter is increased by some value that is related to the difference between the WCR profile and the in-situ profile. Finding this increment value is the objective of this section.

The profiles of in-situ calculated reflectivities (Z-Insitu) and corresponding WCR reflectivities (Z-WCR) are compared for all three flights (Figs 3.12-3.14). This applies all WCR second-gate data, irrespective of their drizzle-free or drizzly status.

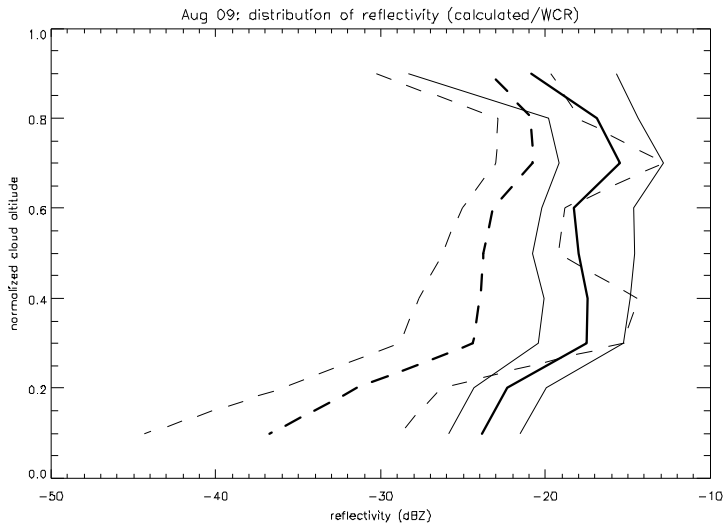


Fig 3.12 Profiles of in-situ calculated reflectivity (dashed) and WCR reflectivity (solid) for the Aug 09th flight. From left to right, three lines of each kind represent reflectivity values of the 20, 50, and 80 percentiles of the reflectivity distribution at each level.

Table 3.8 Median values of reflectivity calculated from probe data (Z-insitu) and WCR reflectivity (Z-WCR) for the Aug 09th flight.

ϕ	Z-insitu		Z-WCR		Difference (dBZ)
	Sample size (m)	Median values (dBZ)	Sample size (m)	Median values (dBZ)	
0.9	3750	-23.28	3633	-20.86	2.42
0.8	6500	-20.88	6897	-16.89	3.99
0.7	13980	-20.77	16461	-15.46	5.31
0.6	49360	-23.19	46548	-18.29	4.90
0.5	25120	-23.78	26733	-17.98	5.80
0.4	71150	-24.03	69378	-17.46	6.57
0.3	8670	-24.44	8631	-17.53	6.91
0.2	2480	-31.41	2682	-22.34	9.07
0.1	2510	-36.76	2541	-23.84	12.92

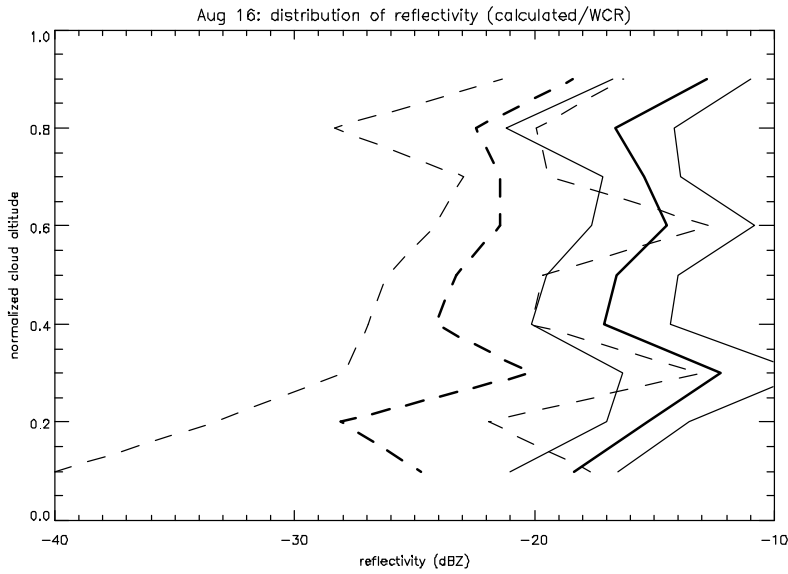


Fig 3.13 As Fig 3.12, but for the Aug 16th flight.

Table 3.9 As Table 3.8, but for the Aug 16th flight.

ϕ	Z-Insitu		Z-WCR		Difference (dBZ)
	Sample size (m)	Median values (dBZ)	Sample size (m)	Median values (dBZ)	
0.9	9020	-18.39	7803	-12.81	5.58
0.8	7600	-22.45	8103	-16.63	5.82
0.7	89980	-21.43	89394	-15.45	5.98
0.6	27680	-21.46	27465	-14.47	6.99
0.5	11300	-23.29	9306	-16.56	6.73
0.4	66830	-24.14	69444	-17.11	7.03
0.3	8280	-20.14	7722	-12.26	7.88
0.2	550	-28.07	477	-15.29	12.78
0.1	620	-24.74	528	-18.35	6.39

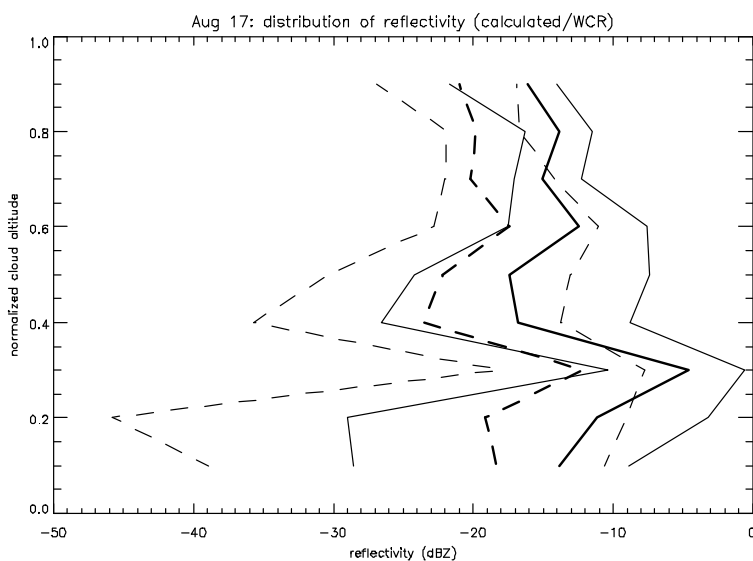


Fig 3.14 As Fig 3.12 but for the Aug 17th flight.

Table 3.10 As Table 3.8, but for the Aug 17th flight.

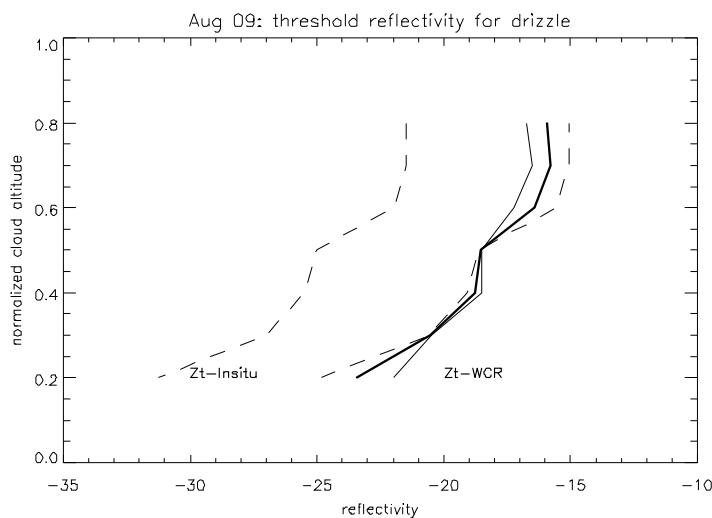
ϕ	Z-Insitu		Z-WCR		Difference (dBZ)
	Sample size (m)	Median values (dBZ)	Sample size (m)	Median values (dBZ)	
0.9	5240	-20.94	5715	-16.12	4.82
0.8	29730	-19.76	26295	-13.80	5.96
0.7	41690	-20.22	45315	-15.07	5.15
0.6	102920	-17.45	102483	-12.45	5.00
0.5	9970	-22.24	9171	-17.39	4.85
0.4	8750	-23.60	8367	-16.84	6.76
0.3	102720	-12.09	102777	-4.58	7.51
0.2	6240	-19.19	6420	-11.12	8.07
0.1	4800	-18.25	4890	-13.82	4.43

Numerical values between in-situ calculated and WCR reflectivities are studied on all three days. In-situ calculated reflectivities are obviously smaller than WCR echoes for all three flights. Fortunately, the median values (Figs 3.12-3.14) have a similar vertical variation. All the differences between the two median values for the three flights dwindle slightly from cloud base to cloud top (Tables 3.8-3.10) but following different slopes versus cloud altitude. No conclusive relationship between the difference profile and cloud altitude can be retrieved based on the measurements of these three flights. Multiple factors, such as spatial variance of cloud droplet spectrum, shortcomings of in-situ instruments, and variance of sample size can affect the difference. Therefore, *the mean difference at all levels for each flight*, 6.43 dBZ for Aug 09th,

7.24 dBZ for Aug 16th and 5.83 dBZ for Aug 17th is chosen to increase the threshold profile based on in-situ calculated reflectivity and then improve the threshold profile based on WCR reflectivity.

3.7 Threshold reflectivity applied to WCR measurements

Two independent profiles of threshold reflectivity for drizzle have been obtained, based on in-situ measurements and WCR echoes respectively. The two threshold profiles are similar, which is a good proof of the existence of threshold. We increase the Z_{insitu} threshold profile by the mean difference between Z_{WCR} and Z_{insitu} , discussed in Section 3.6. The increased Z_{insitu} threshold profile is centered on the WCR threshold profile. Since unavoidable errors exist in in-situ probing, the threshold profile based on in-situ measurements is not 100% exact either. The average values of the Z_{WCR} and the moved Z_{insitu} threshold profiles are considered to be the final threshold reflectivity for drizzle for each flight (Fig 3.15).



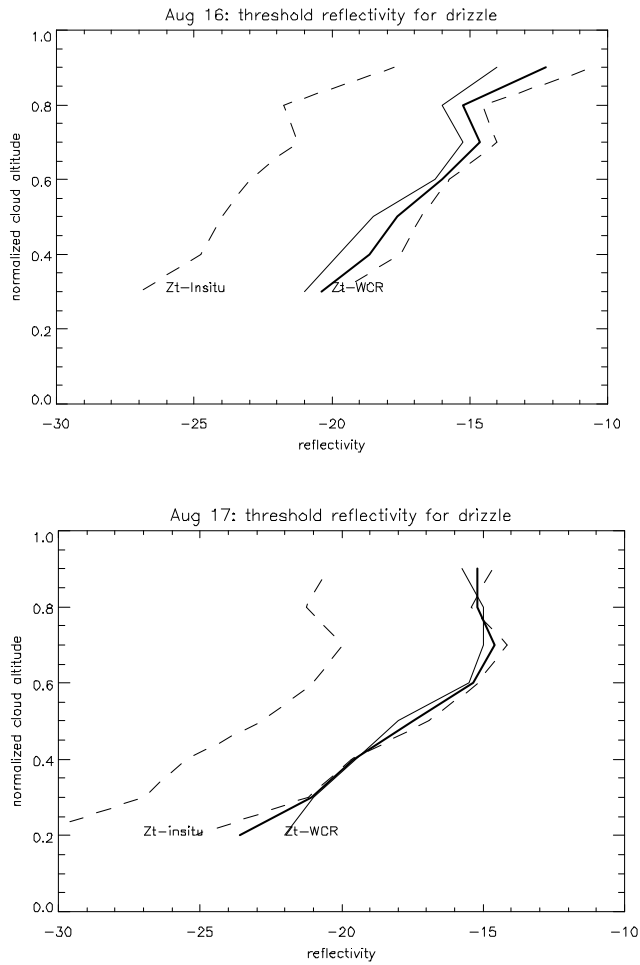


Fig 3.15 Profiles of threshold reflectivity for drizzle for three flights. The left dashed line is the threshold profile based on in-situ measurements. The right dashed line represents a new profile, which is the in-situ calculated threshold plus the mean difference between in-situ calculated and WCR reflectivities. The thin solid line is threshold profile based on WCR observations. The thick solid line represents average values of new calculated threshold profile and WCR threshold profile.

Table 3.11 Improved WCR threshold reflectivity (dBZ)

ϕ	Aug 09 th	Aug 16 th	Aug 17 th
0.9		-12.26	-15.21
0.8	-15.91	-15.26	-15.21
0.7	-15.78	-14.63	-14.59
0.6	-16.41	-16.01	-15.34
0.5	-18.53	-17.63	-17.46
0.4	-18.78	-18.63	-19.58
0.3	-20.53	-20.38	-21.08
0.2	-23.41		-23.58

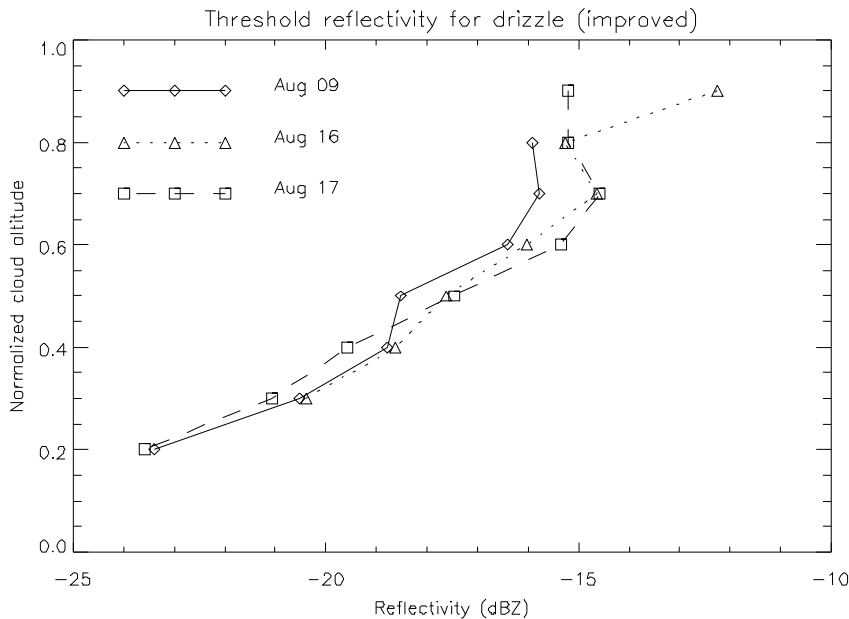


Fig 3.16 Threshold reflectivity profile for drizzle on Aug. 09th, Aug 16th and Aug 17th in CS99.

The mean values between moved in-situ calculated threshold and WCR threshold on all three days are summarized in Table 3.1 and Fig 3.16. Better consistency is obtained among the three improved threshold reflectivity profiles compared with those original threshold profiles based on in-situ measurements or WCR echoes (Fig 3.4, Fig. 3.10 and Fig. 3.16).

A final drizzle threshold reflectivity profile for the three flights is summarized in Table 3.11. This threshold profile can be applied to WCR data at any range gate, after attenuation correction, and reflectivities from other profiling radar, to determine the presence of drizzle in warm marine stratus.

One threshold at a normalized altitude of 0.9 on Aug 16th is far away from the data group (Fig 3.16). But no solid ground exists to reject this threshold value.

The least-squares method is used to regress the threshold curve versus normalized cloud altitude (Fig 3.17). A weight of 0.5 is applied to the anomalous threshold at 0.9 altitude on Aug 16th, while a weight of 1.0 applies to all other values.

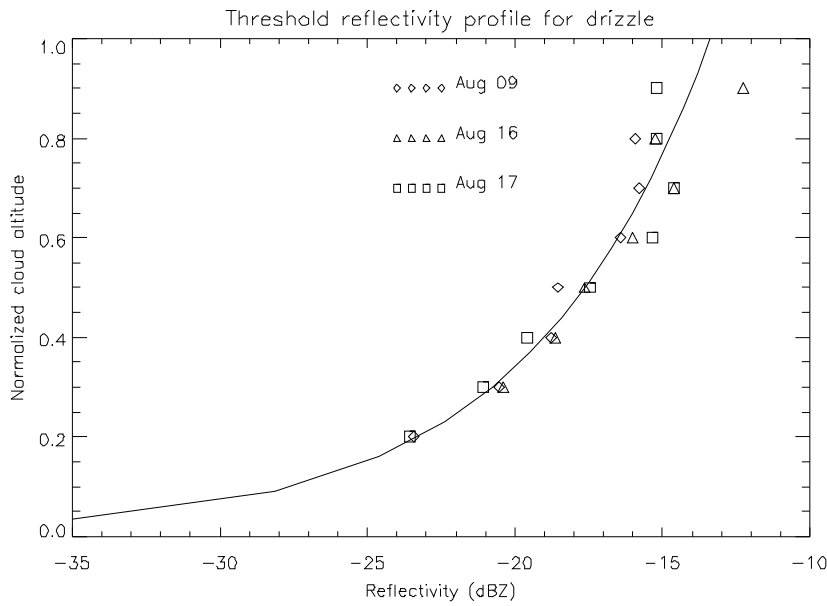


Fig 3.17 Regression threshold reflectivity profile for drizzle.

A regression curve is thus obtained for the improved threshold reflectivities of all three days:

$$Z_t (\text{mm}^6 \text{m}^{-3}) = 0.046\phi^{1.413} \quad (3.3)$$

where Z_t is the reflectivity factor, with the units of $(\text{mm}^6 \text{m}^{-3})$, and ϕ is the normalized cloud altitude.

The threshold reflectivity discriminating between drizzle cases and drizzle-free cases increases from cloud base to cloud top. This threshold profile can be explained by the distributions of cloud droplets and drizzle drops versus cloud altitude. The calculated reflectivity for drizzle-free cases increases with cloud altitude too (Fig. 3.11).

This equation is considered to be the final result of this study. It represents the threshold reflectivity discriminating between drizzle cases and drizzle-free cases versus normalized cloud altitude that can be applied to side-looking or profiling cloud radar measurements at any radar range after attenuation correction, to determine the presence of drizzle in warm marine stratus.

Chapter 4 Relationship between LWC and WCR reflectivity

4.1 Background

The radar-based investigation of microphysical characteristics of stratocumulus and stratus cloud has been a topic of research interest for many years (Chapter 1). Some studies use the Doppler velocity or Doppler spectrum. We will discuss several attempts to relate radar reflectivity (Z) with cloud physical parameters such as liquid water content (LWC), or effective radius (r_e). The radar reflectivity is proportional to the sixth moment to the cloud drop size, for droplets smaller than 300 micron, which behave as Raleigh scatterers for a W band radar. The accuracy of the relationship between radar reflectivity and cloud parameters depends on the knowledge of the DSD.

Both empirical and theoretical relationships between Z and LWC have been retrieved:

Atlas (1954) suggested a theoretical relationship between X-band radar reflectivity and LWC , based on DSD measurements in precipitating clouds, as the form of:

$$Z(mm^6 m^{-3}) = 0.048LWC^2 \quad (4.1)$$

where Z is radar reflectivity factor, and LWC has units of g/m^3 .

In 1987, Sauvageot and Omar proposed a relationship between a millimetric wavelength radar reflectivity factor and LWC based on instrumented aircraft measurements for non- or very weakly precipitating warm coastal cumulus and stratocumulus cloud.

$$Z(mm^6 m^{-3}) = 0.03LWC^{1.31} \quad (4.2)$$

where Z and LWC are defined as in equation 4.1. This relationship is valid for radar reflectivity values less than -15 dBZ. The authors assumed that when the radar reflectivity is larger than this value, the cloud includes drizzle-size drops.

Using the simulation results of a one-dimensional adiabatic cloud model, Sassen and Liao (1996) found that the total droplet number concentration (N_d) affects the relationship between the W-band radar reflectivity and LWC in stratus cloud:

$$Z(\text{mm}^6 \text{m}^{-3}) = \frac{3.6}{N_d} LWC^{1.8} \quad (4.3)$$

where Z and LWC are defined as in equation 4.1 and N_d is the total cloud droplet number in $\#/cm^3$. This equation agrees well with Eq. 4.1 and Eq. 4.2, assuming a typical number concentration $N_d = 100 \text{cm}^{-3}$.

Based on in-situ aircraft measurements of warm stratocumulus over the North Atlantic, Fox and Illingworth (1997) separated drizzle-free and drizzle cases by analyzing the Doppler velocity spectrum and contrived the following relationship between 3 mm radar reflectivity and LWC for drizzle-free cases:

$$Z(\text{mm}^6 \text{m}^{-3}) = 0.031 LWC^{1.56} \quad (4.4)$$

where Z and LWC are defined as in equation 4.1. The WCR does not measure the Doppler spectrum, and even if it was available, airborne Doppler spectra are much affected by aircraft motion. Therefore the ability to separate between falling drizzle and steady cloud droplets appears doubtful.

The latter three relationships between LWC and radar reflectivity are only valid to clouds without drizzle-size drops. In these studies, it was either assumed that no precipitation-size particles were present, or their presence was eliminated based on circumstantial radar evidence. In this study, a rigorously tested, height-dependent reflectivity value is used to isolate drizzle presence in marine stratus (Eq. 3.3). We now analyze the relationship between the W-band radar reflectivity and LWC drizzle-free marine stratus.

4.2 Relationship between LWC and WCR second gate reflectivity

No clear relationship between LWC and radar reflectivity exists in CS99 (Fig 4.1). Large radar reflectivity span is observed with little change of LWC. Even above -15 dBZ, the drizzle threshold proposed by Sauvageot and Omar (1987), a large range of LWC values is observed.

Identifying Drizzle Within Marine Stratus with W-Band Radar Reflectivity profiles

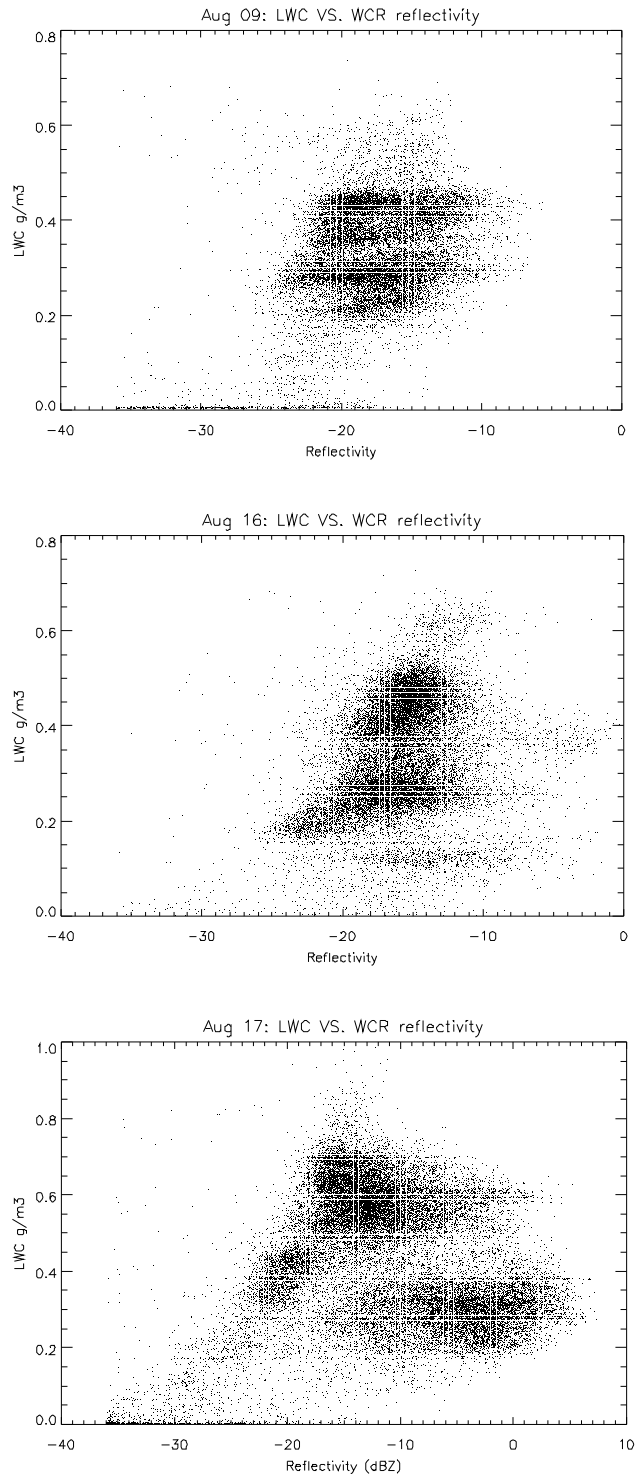
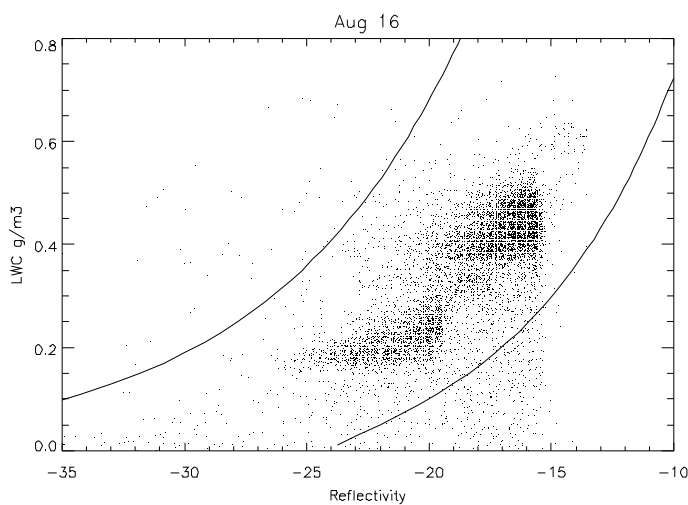
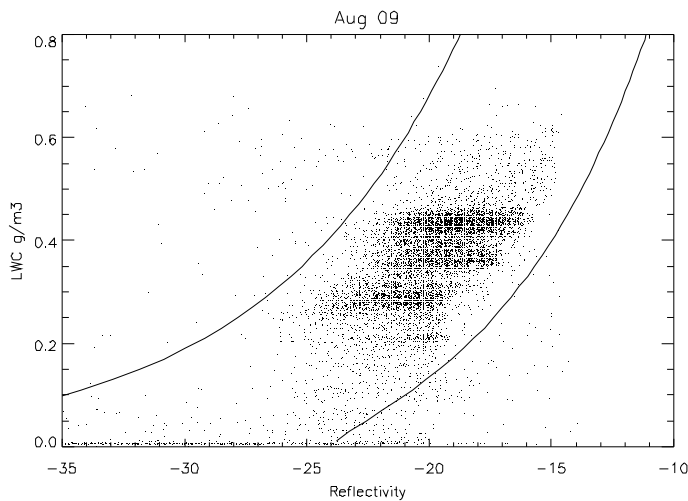


Fig. 4.1 In situ LWC versus WCR second gate reflectivity for all measurements, for the three flight days. The LWC is measured with the probe of PVM for Aug 09th and Aug 17th flights and probe of JW Hot-wire for the Aug 16th flight.

A scatterplot of LWC versus WCR reflectivity corresponding to drizzle-free marine stratus cases is shown for each flight in Fig 4.2. The threshold reflectivity method (Eq. 3.3) was used to exclude drizzle cases.

For drizzle-free cases, LWC and radar reflectivity form a much narrower distribution band compared to Fig 4.2. But still, some points are located a little far away, especially with low LWC value. This can be explained by errors due to probing and or due to the distance between aircraft and WCR second gate to the side.

Two boundary curves are used for each day to exclude the points far away from the dense band (Fig 4.2). These curves are equations of the type of $Z = aLWC^b$, where a and b are chosen arbitrarily for each day to include the bulk of the points, but not the outliers.



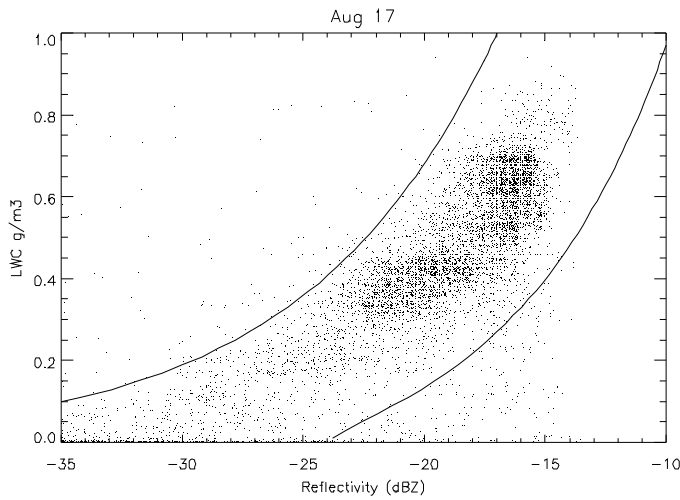
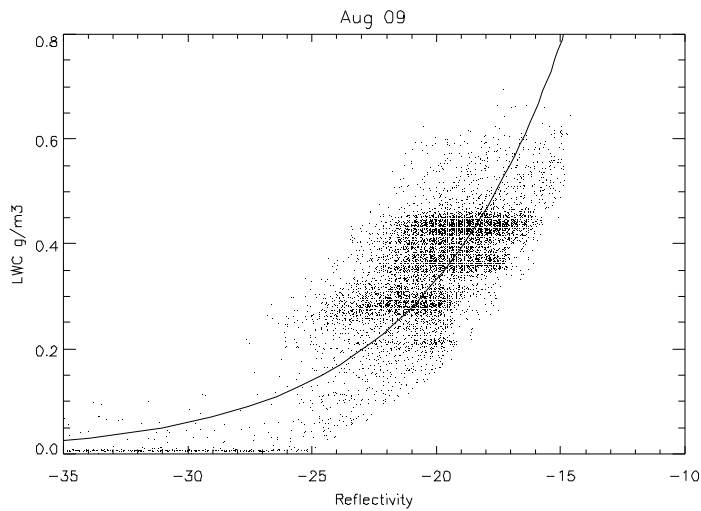


Fig. 4.2 LWC versus WCR reflectivity for drizzle-free cases. Solid curves represent the boundaries, which exclude points far away from dense band in further analyses.

An equation between radar reflectivity factor and LWC is regressed with the least-squares method:

$$Z(mm^{-6}m^3) = aLWC^b + c \quad (4.5)$$

where Z is the radar reflectivity factor; LWC has units of g/m^3 ; and a , b , and c are regression parameters. Their values are determined based on data points delimited by the two curves shown in Fig 4.2.



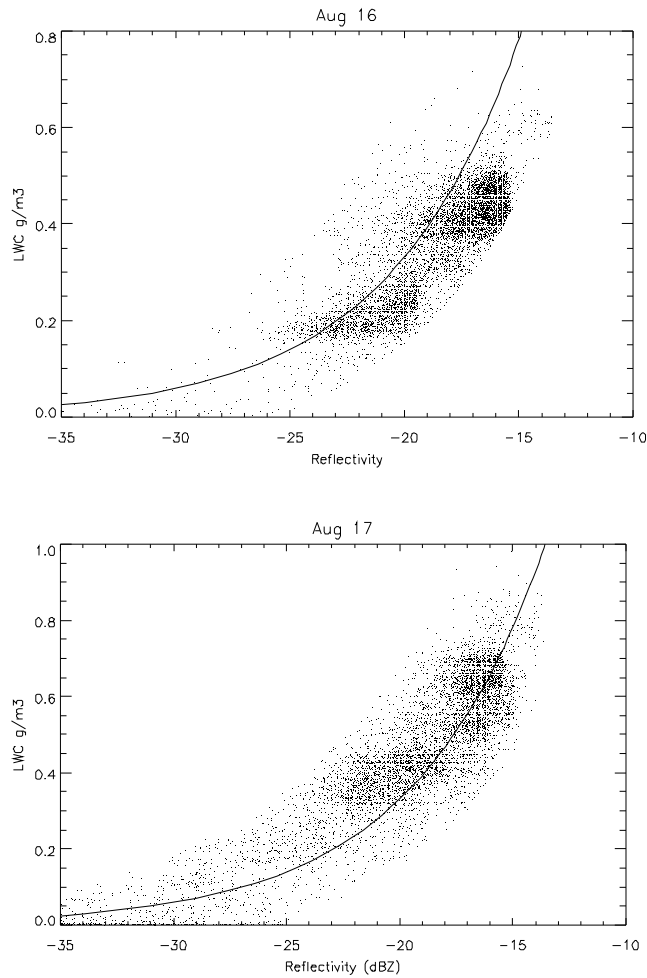


Fig. 4.3 As Fig 4.2, but the solid line is the regression curve based on the remaining points.

Table 4.1 Regression parameters for the equation $Z(mm^{-6}m^3) = aLWC^b + c$

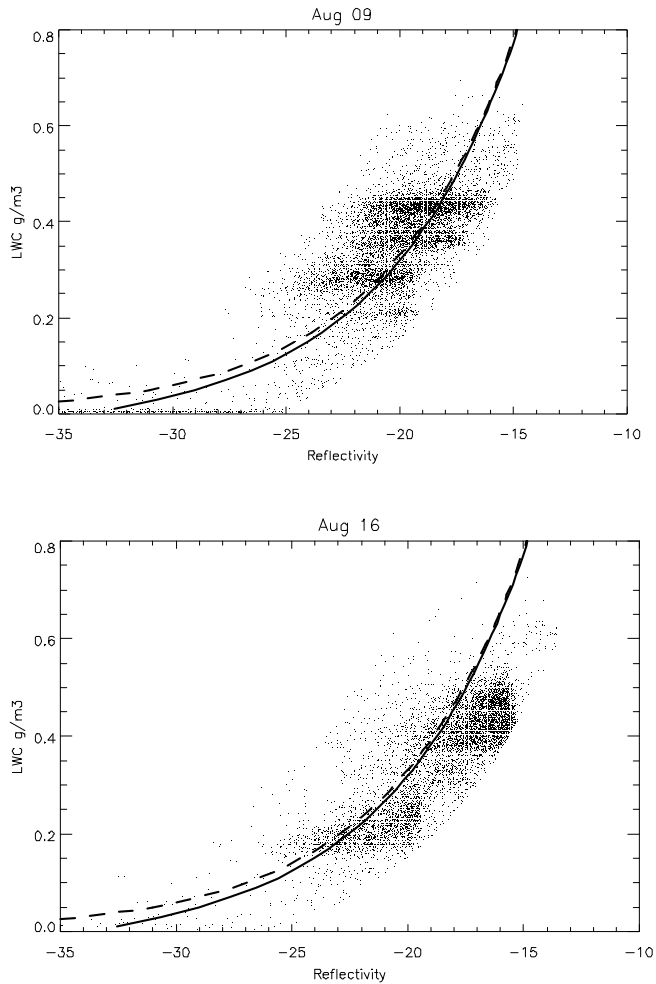
flight	a	b	c
Aug 09 th	0.040	1.332	0.00008
Aug 16 th	0.040	1.488	0.00197
Aug 17 th	0.055	1.200	-0.00067
Mean	0.044	1.34	0.00046

The mean values of a , b , and c are chosen to be the proposed regression parameters based on CS99 data. The following equation is then proposed to estimate LWC in drizzle-free marine stratus:

$$Z(mm^{-6}m^3) = 0.044LWC^{1.34} + 0.00046 \quad (4.6)$$

Unlike the relationships between LWC and radar reflectivity expressed by Eq. 4.2 (Sauvageot and Omar 1987), Eq. 4.3 (Sassen and Liao 1996), and Eq. 4.4 (Fox and Illingworth 1997), a third

extra parameter of c is included in Eq. 4.6. This parameter mainly affects the figure of regression curve at low LWC areas (Fig 4.4). The new relationship (Eq. 4.6) is superimposed on the scatterplot of the remaining in-situ measured LWC against radar reflectivity, and the effect of parameter c is studied for the three flights (Fig 4.4).



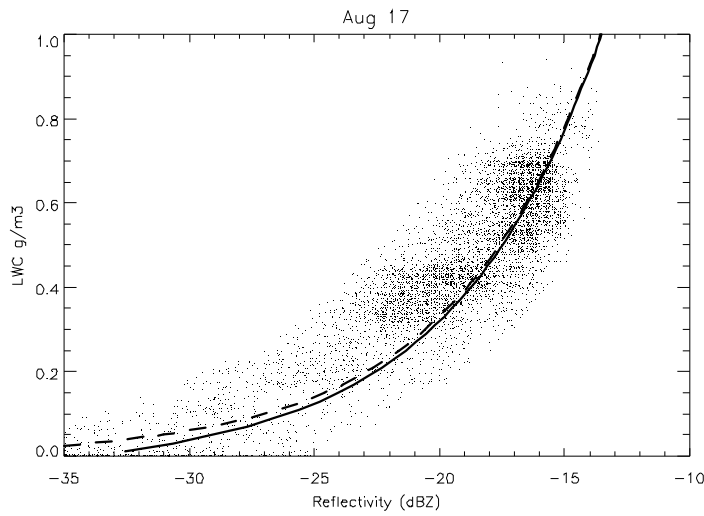


Fig. 4.4 The new relationship between LWC and radar reflectivity (Eq. 4.6 with the form as $Z(\text{mm}^{-6}\text{m}^3) = aLWC^b + c$). The solid line represents the equation of $Z(\text{mm}^{-6}\text{m}^3) = 0.044LWC^{1.34} + 0.00046$. And the dashed line is the simulation result when c equates zero.

Only when the LWC is smaller than 0.2 gm^{-3} is a clear difference observed between the two curves. The regression curve with $c=0$ is underestimated at low LWC areas (Fig4.4). This underestimation is so small that the parameter of c is negligible.

Based on above analyses, the equation $Z(\text{mm}^{-6}\text{m}^3) = 0.044LWC^{1.34}$ is suggested to represent the relationship between LWC and side-looking WCR second gate reflectivity for warm marine stratus (Fig. 4.5).

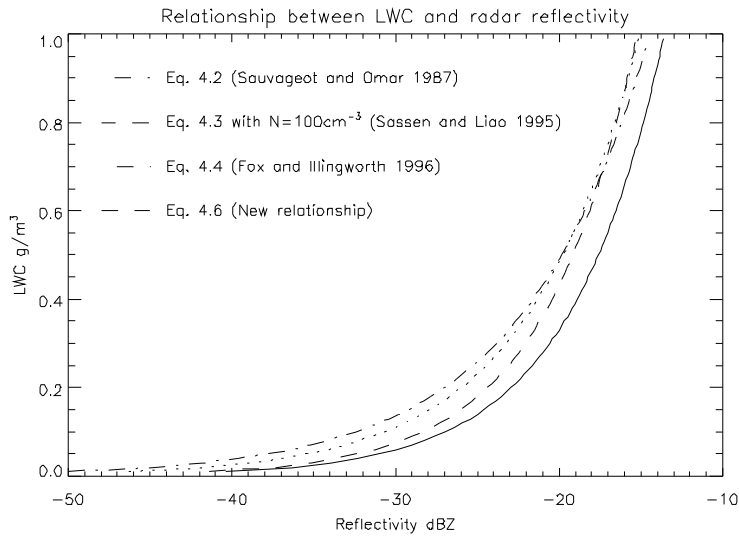


Fig. 4.5 Relationship between LWC and radar reflectivity. The solid line represents equation of $Z(mm^{-6}m^3) = 0.044LWC^{1.34}$ which is the proposed equation based on CS99 data.

The three equations produced similar curves (Fig. 4.5). Eq. 4.2 and Eq. 4.4 underestimate radar reflectivity for CS99 data.

Chapter 5 Discussion

Marine stratus clouds are ubiquitous over subtropical oceans, mainly near west coasts. With a much higher albedo (30~40%) compared to the ocean surface (<10%) these persistent clouds have a significant impact on the global radiation balance and the maintenance of the marine boundary layer. Both experimental and numerical methods have been used to examine and interpret the microphysical structure of marine stratus. Cloud radars, developed rather recently in the history of meteorological radars, offer a great opportunity to learn more about marine stratus clouds. The identification and explanation of cloud radar echoes in marine stratus has attracted much interest lately (Atlas 1954, Sauvageot and Omar 1987, Sassen and Liao 1996 and Fox and Illingworth 1997). One question of interest regards the ubiquity of drizzle in marine stratus, and the significance of this drizzle in stratus dynamics.

Most droplets in marine stratus behave as Rayleigh scatterers. Therefore, the radar reflectivity Z has a higher dependence on drop size than any other cloud parameter, e.g. LWC is proportional to the 3rd moment of the DSD (Eq. 2.6 and Eq. 2.7). Due to the sensitivity of Z to large drops, the existence of drizzle drops may introduce large error in the study of relationship between cloud parameters and radar reflectivity. In view of this point, the main purpose of this study is to develop a threshold reflectivity profile to identify drizzle patches in marine stratus.

In this study we defined a drizzle case based on 1DC and 2DC measurements. This definition has the advantage to be direct, but has the drawbacks that (1) the 1DC and 2DC sample sizes are rather small, requiring an airborne sample distance that often exceeds the size of a 'drizzle patch' in marine stratus; and (2) in situ measurements are displaced relative to radar data, by at least 75 m. In other words the radar may be measuring a different region than the aircraft. Fox and Illingworth (1997) defined drizzle with radar data (Doppler spectra). So the drizzle definition applies to the same cloud parcel for which reflectivity is measured. But Doppler spectra do not unambiguously discriminate drizzle presence.

The model approximated DSDs corresponding to drizzle-free and drizzly cases in marine stratus are studied first to obtain a theoretical investigation of the characteristics of radar reflectivity. The lognormal model has been used to simulate the DSD in marine stratus. Although much uncertainty exists in the retrieval of the lognormal spectra, the lognormal model still is a

good tool to diagnose the reflectivity characteristics within marine stratus. The lognormal DSDs confirm that the radar reflectivity for drizzle cases is always larger than that for drizzle-free cases, and that the median radii of both populations are height-dependent.

Two data sources are used to determine the threshold reflectivity profile for drizzle, reflectivity calculated with in-situ DSD measurements (assuming Raleigh scattering) and, reflectivity measured with WCR. The latter of course is preferred since it represents a large sampling volume, but its drawback is that it does not represent the same air where the drizzle presence is detected (at the aircraft), but rather some 75-90 m to the side. Because of the assumptions involved, a bulk statistical method is required, and two different statistical methods agree very well. The two threshold reflectivity profiles (one based in probe data, the other based on WCR data) display similar vertical variation. However they depart by about 6.5 dBZ, i.e. the in-situ calculated reflectivities are systematically smaller than WCR reflectivity on all three flights. We are not sure why this discrepancy exists, but we suspect that the cloud probes undersample the true DSD, mainly in the 1DC range (50-100 micron). It is surprising that this discrepancy is weak height-dependent, but the height-dependence pattern varies from flight to flight in marine stratus. Perhaps the discrepancy can be used to improve probe-based DSD estimations. In any event, we adjusted the probe-calculated reflectivity upward by about 6.5 dB.

As an example application of the threshold reflectivity profile for drizzle, the relationship between LWC and radar reflectivity for drizzle-free cases is studied. No relationship is evident in the scatterplot of LWC against radar reflectivity, when all data are considered. Excluding drizzle cases with the threshold reflectivity profile, a much narrower distribution remains in the LWC-Z plane, yielding a relationship between LWC and radar reflectivity, which is quite similar to the equations proposed by Sauvageot and Omar (1987), Sassen and Liao (1996), and Fox and Illingworth (1997).

Chapter 6 Conclusion

Cloud radar and cloud microphysical data on Aug. 09th, Aug. 16th, and Aug. 17th 1999 collected off the Oregon coast with the Wyoming King Air are analyzed to obtain a threshold radar reflectivity to discriminate between drizzle cases and drizzle-free cases in warm marine stratus. Here, drizzle is defined as having a diameter of at least 50 μm . Only those drizzle (drizzle free) cases are considered that have drizzle (no drizzle) for at least 2 seconds. Several results are reached:

- Drizzle-size drops are prevalent in coastal warm marine stratus, and their frequency varies significantly from day to day and on the mesoscale.
- Increasing radar reflectivity always corresponds to increasing drizzle probability in CS99 (Fig. 1.1).
- Rapid (1 Hz) in situ droplet sampling is rather incomplete, especially at the tail end of the DSD, therefore size-integrated quantities, such as LWC and especially radar reflectivity, which is proportional to the sixth moment of drop size, may be underestimated. This deficiency can be overcome by assuming the continuous lognormal DSD that best matches the instrument observations (FSSP for drizzle-free cases and FSSP, 1DC, and 2DC for drizzly stratus). Physical characteristics of radar reflectivity and LWC are diagnosed based on the best matching lognormal DSD within marine stratus.
- Differences exist between reflectivities (calculated assuming lognormal DSDs) for drizzle-free cases and drizzle cases (Fig. 2.14, Fig 2.15 and Fig. 2.16). These differences are dependent on the height within the stratus layer, whose base height and depth varies significantly from day to day. Therefore threshold values are estimated as a function of normalized cloud altitude ϕ .
- Two threshold reflectivity profiles for drizzle are obtained, using statistical methods. The two profiles are based both on calculated reflectivities with in-situ measuring DSD, and on side-looking WCR second gate reflectivities. The two profiles correspond very well, for both datasets, however the WCR-derived threshold profile is 5-8 dB higher than the probe-derived profile, although the slopes of the profiles are quite similar. Because the reflectivity derived from observed DSDs tends to underestimate true values, the probe-

derived threshold profile is incremented by a height-independent correction, to bring it closer to the WCR-derived profile. The final profile is simply the average between the displaced probe-derived profile and the WCR-derived profile.

- A regression equation $Z_r (mm^6 m^{-3}) = 0.046\phi^{1.413}$, based on the ‘final’ profile for three flights, is obtained to represent the dependence of threshold reflectivity for drizzle on normalized cloud altitude (Fig. 3.17). This equation can be applied to data from any radar at 95 GHz or lower frequency.
- After exclusion of drizzle cases based on the above regression, the following relationship between liquid water content (LWC) and radar reflectivity for drizzle-free cases is found: $Z(mm^{-6}m^3) = 0.044LWC^{1.34}$ (Fig. 4.4).

This work can be extended. In particular, the above relationships can be used to:

- Examine the relationships between radar reflectivity and other cloud physical parameters, such as liquid water path (LWP), for drizzle-free marine stratus.
- Apply the drizzle threshold value to profile and map drizzle in marine stratus using vertical or horizontal radar reflectivity data. These spatial structures should be revealing to marine stratus dynamics, as simulated in large-eddy simulations.

References

- * Ackerman, A. S., O.B. Toon and P. V. Hobbs, 1993: Dissipation of marine stratiform clouds and collapse of the marine boundary layer due to the depletion of cloud condensation nuclei by clouds. *Science*, **262**, 226-229.
- * Atlas, D., 1954: The estimation of cloud parameters by radar. *J. Meteor.*, **4**,309-317.
- * Babb, M. D., J. Verlinde, and B. A. Albrecht, 1999: Retrieval of cloud microphysical parameters from 94-GHz Radar Doppler power spectra, *J. Atmos. Oceanic Technol.*, **16**, 489-503.
- * Baumgardner, D., B. Baker, and K. Weaver, 1993: A Technique for the Measurement of Cloud Structure on Centimeter Scales. *J. Atmos. Oceanic Technol.*, **10**, 557-565.
- * Borovikov, A. M., 1961: *Cloud Physics*. Gidrometeoizdat, Leningrad, 336 pp.
- * Bretherton C. S., P. Austin and S. T. Siems, 1995: Cloudiness and Marine Boundary Layer Dynamics in the ASTEX Lagrangian Experiments Part II: Cloudiness, drizzle, surface fluxes, and entrainments. *J. Atmos. Sci.*, **52**, 2724-2735.
- * Clark, T. L., 1976: Use of Log-Normal Distributions for Numerical Calculations of condensation and Collection, *J. Atmos. Sci.* **33**, 810-821.
- * Clothiaux, E. E., M. A. Miller, B. A. Albrecht, T. P. Ackerman, J. Verlinde, D. M. Babb, R. M. Peters, W. J. Syrett, 1995: An Evaluation of a 94-GHz Radar for Remote Sensing of Cloud Properties. *J. Atmos. Oceanic Technol.* **12**, 201-229.
- * Davidson, K. L., C. W. Fairall,, P. J. Boyle, and G. E. Schacher, 1984: Verification of an Atmospheric Mixed-Layer Model for a Coastal Region, *J. Clim. Appl. Meteor.*, **23**, 617-636.
- * Fox, N. I., and A. J. Illingworth, 1997: The Potential of a Spaceborne Cloud Radar for the Detection of Stratocumulus Clouds. *J. Applied Meteorology*, **36**, 676-687.
- * Fox, N. I., and A. J. Illingworth 1997: The Retrieval of Stratocumulus Cloud Properties by Ground-Based Cloud Radar, *J. Applied meteorology*, **36**, 485-492.
- * Frisch, A.S., C.W. Fairall, and J.B. Snider 1995: Measurement of Stratus Cloud and Drizzle Parameters in ASTEX with K_a-Band Doppler Radar and a Microwave Radiometer. *J. Atmos. Sci.*, **52**, 2788-2799.
- * Frisch, S., M. Shupe, I. Djalalova, G. Feingold, and M. Poellot, 2002: The Retrieval of Stratus

- Cloud Droplet Effective Radius with Cloud Radars, *J. Atmos. Oceanic Technol.*, **19**, 835-842.
- * Galloway, J., A. Pazmany, J. Mead, R. E. McIntosh, D. Leon, J. French, S. Haimov, R. Kelly, G. Vali, 1999: Coincident In Situ and W-Band Radar Measurements of Drop Size Distribution in A Marine Stratus Cloud and Drizzle. *J. Atmos. Oceanic Technol.* **16**, 504-517.
 - * Gerber, H., 1996: Microphysics of Maine Stratocumulus Cloud with Two Drizzle Modes. *J. Atmos. Sci.*, **53**, 1649-1662.
 - * Hudson, J. G., and Yum S. S., 1997: Droplet Spectral Broadening in Marine Stratus. *J. Atmos. Sci.*, **54**, 2642-2654.
 - * Houze, R. A., 1993: *Cloud Dynamics*. San Diego: Academic Press.
 - * Kerstein, A. R., 1988: Linear Eddy modeling of Turbulent Scalar Transport and Mixing. *Comb. Sci. Technol.*, **60**, 391-421.
 - * Kerstein, A. R., 1991: Linear-eddy Modeling of Turbulent Transport. Part 6: Microstructure of Diffusive Scalar Mixing Fields. *J. Fluid Mech.*, 231, 361-394.
 - * Kollias, P., B. A. Albrecht, and F. Marks, 2002: Why Mie? Accurate Observations of Vertical Air Velocities and Raindrops Using a Cloud Radar, *Bull. Amer. Meteor. Soc.*, **83**, 1471-1483.
 - * Krasnov A. O., and Russchenberg W. J. H., 2002: The Relation between the Radar to Lidar Ratio and the effective Radius of Droplets in Water Clouds: An Analysis of Statistical Models and Observed Drop Size Distributions. *11th conference on Cloud Physics*, P1.7.
 - * Krueger, S. K., 1993, Linear Eddy Modeling of Entrainment and Mixing in Stratus Clouds. *J. Atmos. Sci.*, **50**, 3078-3090.
 - * Löhnert U., S. Crewell. and C. Simmer 2001: Profiling Cloud Liquid Water by combining Active and Passive Microwave Measurements with Cloud Model Statistics, *J. Atmos. Oceanic Technol.*, **18**, 1354-1366.
 - * Lhermitte, R., 1987: A 94-GHz Doppler Radar for Cloud Observations. *J. Atmos. Ocean. Technol.*, **4**, 36-48.
 - * Miles, N. L., J. Verlinde, and E. E. Clothiaux, 2000: Cloud Droplet Size Distributions in Low-Level Stratiform Cloud. *J. Atmos. Sci.*, **57**, 295-311.
 - * Moeng, CH., D. H. Lenschow, and D. A. Randall, 1995: Numerical Investigations of the Roles of Radiative and Evaporative Feedbacks in Stratocumulus Entrainment and Breakup. *J. Atmos. Sci.*, **52**, 2869-2883
 - * Randall, D. A., J. A. Coakley, Jr. D.H. Lenschow, C. W. Fairall, and R. A. Kropfli, 1984:

- Outlook for Research on Subtropical Marine Stratiform Clouds. *Bull. Amer. Meteor. Soc.*, **65**, 1290-1301.
- *Sassen, K. and L. Liao, 1996: Estimation of Cloud Content by W-Band Radar, *J. Appl. Meteor.*, **35**, 932-938.
- * Sauvageot, H. and J. Omar, 1987: Radar Reflectivity of Cumulus Clouds, *J. Atmos. Oceanic Technol.*, **4**, 264-272.
- * Stevens, B., W. R. Cotton, G. Feingold, and C.-H. Moeng, 1998: Large-Eddy Simulations of Strongly Precipitating, Shallow, Stratocumulus-topped Boundary Layers. *J. Atmos. Sci.*, **55**, 3616-3638.
- * Vali, G., R. D. Kelly, J. French, S. Haimov, D. Leon, R. E. McIntoshh, and A. Pazmany, 1998: Finescale Structure and Microphysics of Coastal Stratus. *J. Atmos. Sci.*, **55**, 3540-3564.
- * Warner, J., 1969: The Microstructure of Cumulus Cloud. Part I: General Features of the Droplet Spectrum, *J. Atmos. Sci.*, **26**, 1049-1059.
- * White, A. B., C. W. Fairall, and D. W. Thomson, 1991: Radar Observations of Humidity Variability in and above the Marine Atmospheric Boundary Layer, *J. Atmos. Oceanic Technol.*, **8**, 639-658.
- * Wyant, M. C., C. S. Bretherton, H. A. Rand, and D. E. Stevens, 1997: Numerical Simulations and a Conceptual Model of the Stratocumulus to Trade Cumulus Transition. *J. Atmos. Sci.*, **54**, 168-192.